ADELAIDE UNIVERSITY
School of Earth and Environmental Sciences

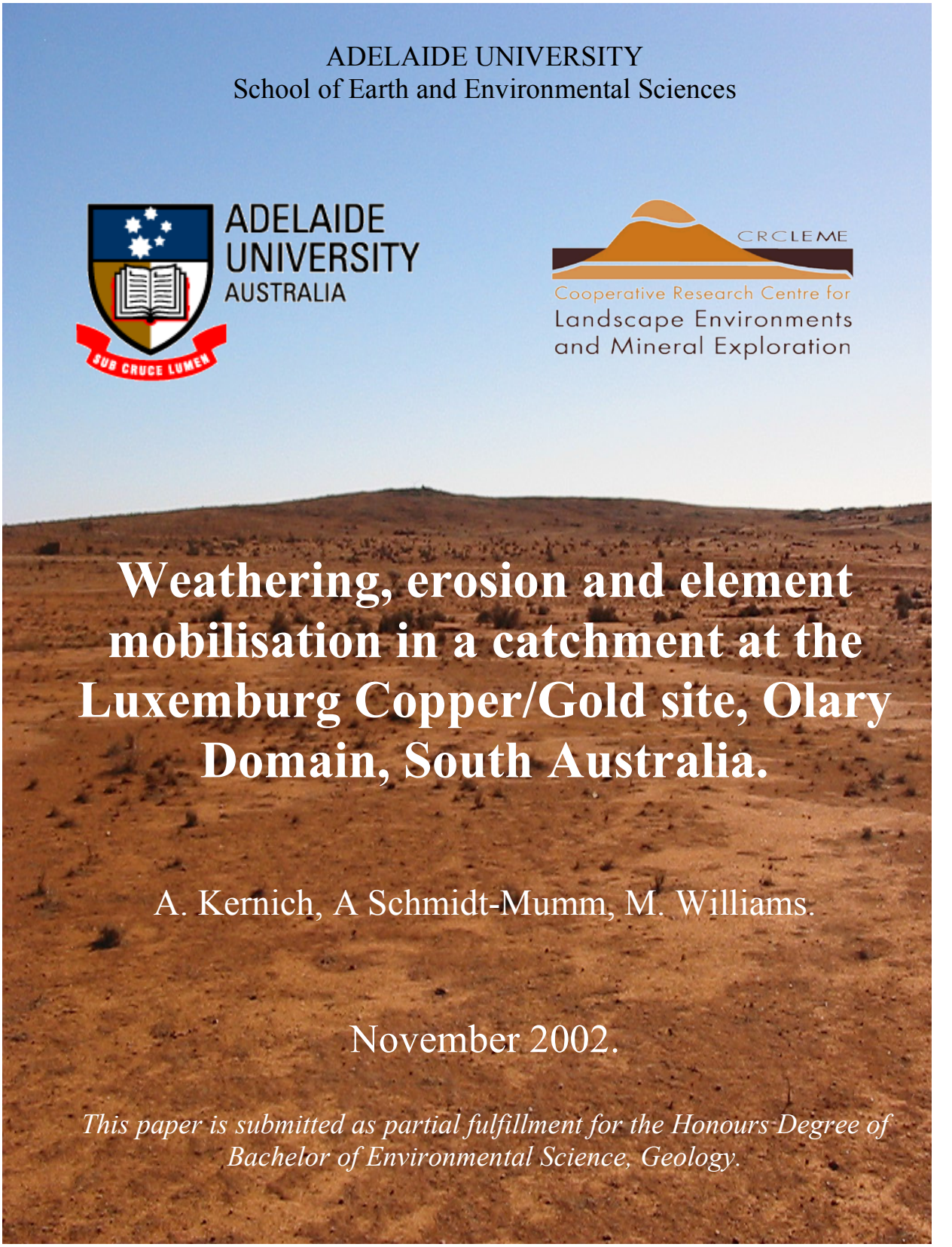

Weathering, erosion and element mobilisation in a catchment at the Luxemburg Copper/Gold site, Olary Domain, South Australia.

A. Kernich, A Schmidt-Mumm, M. Williams.

November 2002.

This paper is submitted as partial fulfillment for the Honours Degree of Bachelor of Environmental Science, Geology.

Table of Contents

Weathering, erosion and element mobilisation in a catchment at the Luxemburg Copper/Gold site,

Olary Domain, South Australia.

A. L. Kernich, A Schmidt-Mumm, M. Williams.
School of Earth and Environmental Sciences, University of Adelaide.

Abstract

The Olary Domain, Curnamona Province has significant economic importance as a target for base metal and gold exploration. A veneer of Cainozoic or younger regolith occurs over large areas of the Olary Domain, which complicates mineral exploration. The study area is located within a small catchment at the old Luxemburg Cu/Au mining site in the mid North of South Australia in the Southern area of the Olary Domain. This investigation focuses on relating physical and chemical weathering processes present between basement amphibolite, granites and gneisses and a local waterway, including parameters such as bedrock geochemistry, regolith profile interpretation, channel morphology, and landscape evolution. Mapping the extent and character of the regolith in the Luxemburg area in a detailed Regolith Landform Map was also a large feature of this study.

Results from the Regolith Landform Map allow inferences on the present day surface dispersion pathways. Geochemical investigations of the regolith profile within the catchment indicate a considerable fingerprint from the underlying amphibolite, specifically shown by Fe, Ti, Ni, Cr, V and Sc values. The elemental signature of the surface regolith reflects the underlying parent regolith units. Geochemical patterns within the ephemeral channel can be related to source geology, streambed morphology and landscape position. Harker plots and grain size analysis indicate that the channel sediment is chemically immature and La/Sc plots against Ti, Zr and Th illustrate that the amphibolite body primarily controls its elemental signature.

The geochemistry of the underlying moderately weathered bedrock can be seen and deciphered in an area of iron rich, relatively thin regolith. Bedrock signatures are also evident within the chemistry of bulk samples from the local ephemeral channel deposits. Recent mining activity within the area does not seem to have influenced the results of this study.

Keywords: Amphibolite geochemistry, Curnamona Province, element mobilisation, geochemical exploration, Olary Domain, regolith.

---

1. Introduction

Outcrops of bedrock are sparse in the Olary Domain and occur as isolated inliers within Neoproterozoic Adeladian sedimentary rocks, Tertiary to recent sediments, and in-situ regolith (Preiss and Conor 2001). Regolith in the Curnamona Province is further characterised by the dominance of relatively thin fluvial, alluvial and aeolian sediments that span the Tertiary to Recent, and isolated occurrences of Tertiary land surfaces that have been protected by hardpan covers.

The extent and complex nature of regolith over the Olary Domain complicates exploration techniques and has been the focus of extensive recent study aimed at increasing the success of regolith sampling as a tool for mineral exploration. (Lawrie, 2000; Eggleton 2001; Pain et al. 2001; Rutherford and Cohen, 2002).

This study is focused on determining whether underlying bedrock signatures can be adequately identified through the geochemistry of this thin and geologically young regolith. The study area is located within a small catchment at the old Luxemburg Copper-Gold gold mine site on Tikalina station, roughly 30 km from Olary in South Australia's Mid North East

(Figure 1). Annual rainfall and air temperature data for the Yunta region indicates that the study site has a semi-arid environment. (Bureau of Meteorology web site, 24/3/02)

Historically, Luxemburg began operating as a small mine consisting of adits and costeans shortly after the 1887 discovery of auriferous quartz veins (Campana and King 1958). Further discoveries continued during the late 1800s and early 1900s. A crushing plant was constructed in 1915 to extract copper and gold but operations ceased shortly after due to insufficient available water. In 1969, Sundowner Minerals discovered the Luxemburg East prospect using geophysical methods, although this prospect was not of economic importance.

Recent detailed studies of the area include that of Ellershaw (2001) and Stephen (2001), which concentrated on the characteristics of mineralisation, geological field relationships and geophysical investigations over the amphibolite body at Luxemburg.

2. Geological Setting

Regional Geology

The Olary Domain, South Australia, is part of the Proterozoic Curnamona Province that extends across central eastern South Australia and western New South Wales and includes the Broken Hill Domain. The Olary Domain geology is comprised largely of Palaeoproterozoic sedimentary and volcanic and intrusive rocks of the Willyama Supergroup that have been regionally metamorphosed to varying extents. Significant volumes of Mesoproterozoic granitoids and scattered mafic sills and dykes have intruded these rocks (Robinson et al., 1998).

The Willyama Supergroup, the dominant rock type in the Olary Domain has had numerous shows of poly-metallic mineralisation most commonly comprising Cu and Au or U, but in places also Th, REE, Co, Zn, Pb and Ba (Conor, 2001). These prospects include Radium

Hill (U, REE), Portia (Cu, Au and Mo), White Dam (Cu and Au), Kalkaroo (Cu, Au and Mo), and Ram Dam (Zn and Pb) along with many other small un-named shows.

Campana and King (1958), Clarke et al. (1986), and most recently Conor (2000a) have undertaken studies correlating the stratigraphy of the Olary Domain to the Broken Hill Domain. Significant differences between domains exist, the most notable being the complete absence or attenuated presence of the Broken Hill stratigraphic Group in the Olary Domain, which hosts the Broken Hill mineralisation in New South Wales.

Regional Cenozoic Sediments

Regional sedimentary units within the Olary Domain merge from Cretaceous Marree subgroup sediments to Recent soil, stream and fan deposits and are roughly grouped into three main phases of deposition (Alley, 1998, Lawie, 2001).

The first phase spans the Cretaceous to Mid Tertiary. It consists of the Marree subgroup which shows generally carbonaceous, finely laminated, fine-grained clastics and silty to sandy shales (Callen, 1990) and the Eyre Formation, (Early to Mid Tertiary), which consists of mineralogically mature fluvio-lacustrine sediments and cover sands. The second phase, from the Mid to late Tertiary, consists of immature fine clastics, olive to grey coloured sandy clays and silts with distinct channel facies and extensive shallow lake sequences of the Etadunna and Namba Formations (Alley 1998). Pleistocene to Recent sediments make up the third phase of deposition and consist primarily of red-brown to yellow-brown oxidised alluvial, fluvial and aeolian sediment accumulations (Williams, 1994b; Alley, 1998; Fanning and Holdaway, 2001). Deposits range from channel and floodplain styles deeper in the sequence to more recent overbank, stream and floodplain deposits with some incorporation of aeolian material within these alluvial-colluvial sediments (Lawie, 2001).

Detailed site Geology

Outcrop in the Luxemburg catchment is limited to Neoproterozoic Willyama granites and gneisses, locally occurring pegmatite and quartz veins and an amphibolite body (Ellershaw; 2001; Stephen, 2001). Outcrops of Adelaidian sedimentary rocks unconformably overlying the Willyama basement occur to the south but are not present in the study area (Stephen, 2001).

Granitic rocks in the area show I and S type affinities and have been tentatively identified by Stephen (2001) as belonging to Basso and Bimbowrie suites of the Willyama Supergroup, respectively. Granitic and gneissic outcrops are hosted by Wiperaminga Subgroup, which make up the basal unit of the lower Curnamona group (Connor, 2001). A diagram showing the rock relationships can be seen in Figure 2, adapted from Connor (2000a).

Quartz reefs of centimetre to metre scale thickness and varying in length occur throughout the study area but are primarily centred around the amphibolite body in the catchment valley. Pegmatite veins of centimetre scale thickness and metre scale length commonly occur within the granites and gneisses in the study area.

The amphibolite body's relationship to the surrounding geology is only tentatively understood and the timing of emplacement is unknown. It is thought to be an intrusive body that has undergone some deformation and significant hydrothermal alteration in the form of metasomatism and chlorite alteration (Ellershaw, 2001; Stephen, 2001). There are a number of other mafic intrusives in the region including the Woman in White and Radium Hill amphibolites that may relate to this body but as yet there is no correlation.

Identifiable regolith cover within the Luxemburg catchment consists of weathered in-situ bedrock, discontinuous units of red-brown to yellow-brown Quaternary soils, stream, and fan deposits with laminated and powdery regolith carbonate accumulations. An ephemeral stream channel is located in the centre of the valley, which is currently incising into the regolith cover and bedrock of the valley floor. Hill slopes are dominated by weathered

bedrock exposures and a colluvial mantle of bedrock derived pebble to boulder sized fragments. Minor accumulations of red-brown aeolian silts and clays are evident throughout the regolith in the area.

The noticeable effects of mining activity within the study area vary from ruined buildings, old roads and paths, strewn metal and ceramic rubbish to direct mining impacts including tunnels, adits, costeans and waste heaps. These human imprints are considerable in size and are broadly distributed throughout the study area (Stephen, 2001).

3 Sampling Methods

Regolith Landform mapping

Regolith Landform mapping was undertaken to achieve an overall perspective of the regolith in the study area. Field mapping was based on the Cooperative Research Centre for Landscape Environments and Mineral Exploration (CRC LEME) protocol with specific guidance from Dr Steve Hill, University of Canberra, and Ms Kylie Foster, Geoscience Australia. The final map shown in the appendix, was digitised into a GIS format using the program ArcView 3.1.

Sampling strategy

Sample types and locations are shown in Figure 3.

Amphibolite and granite grab samples were collected from outcrop and waste heaps within the study area. Regolith and channel samples were collected from the bed and banks of the ephemeral channel and from the adjacent valley sides. Regolith cores were taken to refusal depth using an Atlas Copco motor drill hammer on Nordmeyer drill rods and coring units.

Field observations, relationships and sketches of the regolith profile outcropping in the creek banks were recorded in field notes.

The longitudinal profile of the channel (Figure 11a.) was produced from measurements using a compass and clinometer at set locations along the ephemeral channel for a distance close to two kilometres. CSIRO laboratories Adelaide undertook particle size analysis on channel sediment and regolith profile samples (table 1).

Analytical preparation and analysis techniques

Preparation of thin sections for rock petrography was carried out by Pontifex and Associates Pty Ltd, Adelaide. Mineralogy and petrography was determined using a Nikon Optiphot2-POL. Polarising Microscope and an Olympus CH X40 magnification reflective microscope. For mineralogical identification, channel sediments were sifted to a 125-250um size fraction and run through a Frantz Isodynamic Magnetic Separator with a side slope of 20 degrees and varying field strengths to separate mineral species. Sediments were then identified using an Olympus CH X40 magnification reflective microscope on loose grain samples.

X-ray Fluorescence Spectroscopy (XRF), was undertaken using a Philips PW 1480 X-ray Fluorescence Spectrometer with a dual-anode (Sc-Mo) X-ray tube operating at 40kV, 75mA. The major element results are expressed as weight percent oxides on a 'dry form' basis, with the two iron cations being combined and shown as Fe_2O_3 total. The samples were first dried overnight in an Oven at 100 degrees Celsius and then milled to a fine sand-silt size using a tungsten-carbine mill.

Samples were analysed by AMDEL laboratories, Adelaide, for economic metal content using an aqua-regia digest on bulk stream sediments of around 300gms weight. Metal concentrations were determined by Inductively Coupled Plasma Mass Spectroscopy (ICP-MS). The samples were first dried by AMDEL at approximately 100 degrees Celsius then milled to a nominal 90% passing fraction of 106um. ICP-MS Detection limits ranged from 1ppb to 0.1ppm dependant on the element (tables 4a and b).

4 Results:

Regolith Landform Map

The Regolith Landform map over the Luxemburg mine-site area, point sample locations and accompanying descriptions are shown in the appendix.

Landforms in the study area are dominated by erosional rises and plains with considerable bedrock exposure to the West of the study area. Alluvial processes prevail in the channel with colluvial sheet wash processes dominating the expansive depositional plains and slopes on the Eastern side of the study area (refer to Regolith Landform Map in appendix). Bedrock exposures within the mapped area produce colluvial slopes that laterally merge with alluvial and colluvial plains on the valley floor and out to the East.

The map indicates:

1) Areas of bedrock exposure within the Luxemburg valley and surrounding area.

2) Significant regional colluvial surface material movement on slopes and plains, especially dominant within the valley under detailed study.

3) The pervasive nature of carbonate throughout the study area on lower slopes and plains

4) Minor but uniform amounts of surface aeolian red brown well sorted unconsolidated silts and clays.

Regolith profile descriptions

Regolith cover in the study site uniformly comprises red brown, silt and clay rich fluvial, alluvial and aeolian sediments with unconsolidated surface clay and sand or quartz pebble lag. Depth to moderately weathered bedrock in the catchment valley averages between 1-3 metres. The occurrence of regolith carbonate accumulations and their form varies with location.

Three distinct regolith units are identifiable throughout the catchment area. Profile diagrams and accompanying descriptions are present in Figures 5a-c.

The basal "Pedal unit" has a well-developed soil structure and consists of multiple gravelly lenses within a red brown clay matrix. Minor surface carbonate accumulations occur at depth. The "Massive unit" is dominated by sand size particles (Figure 6) that show a similar mineralogy and texture to that of the pedal unit (Figures 5a-c.).

Grain size analysis results displayed in table 1 indicate that the Post European Material (PEM), which abruptly overlies the Massive unit, dominantly comprises fine sand and clay with 13.5% silt and minor coarse sand. Units were analysed for carbonate content expressed as calcium carbonate with the two upper units displaying equal amounts of 0.1% and the lower Pedal unit having a substantially higher value of 0.33% (table 1).

As shown in Figure 6, clay content is relatively high in the PEM unit, decreases within the massive unit and increases to a maximum with depth. The silt fraction continuously decreases with depth through a range of 10% with a surface maximum of 13.5%. The fine sand fraction decreases with depth also to a minimum of 20.5%, with the two upper units displaying similar values. Coarse sand follows a similarly inverse pattern to that of the clay content with the minimum at the surface, maximum within the Massive unit and a slight decrease within the Pedal unit.

Amphibolite chemical character

The amphibole arrangement of $(Al,Si)_4O_{11}$ tetrahedra chains allows for a large variety of cations to be incorporated or substituted into the structure. Four basic subdivisions of amphiboles are distinguished by the dominant cation within the mineral lattice. These are: calcic – Ca, alkali – Na, sodic-calcic - Ca/Na and iron-magnesium-manganese -(Fe, Mg, Mn)

amphiboles (Deer, et al. 1992). X-Ray Fluorescence data (table 3) suggests that the amphibolite body shows a tentative calcic character.

A Chrondrite normalised elemental plot for lithologies present at Luxemburg can be seen in Figure 4. The amphibolite samples in this figure illustrate enhanced levels of Titanium, Manganese, Nickel as well as the trace elements Chromium, Scandium and Vanadium.

Six amphibolite rock samples were analysed for this study and their elemental composition was somewhat variable as seen in the plot "Amphibolite major oxides v SiO_2" (Figure 7), illustrating the relationship of silica to other major oxides in the amphibolite. Iron and calcium have generally negative trends with increasing silica content while aluminium shows the strongest positive correlation to silica with a regression coefficient (R^2) of 0.88. General positive relationships occur for titanium (R^2=0.48) and manganese (R^2=0.54) with magnesium, sodium and potassium demonstrating variability.

Bedrock Geochemistry

Chrondrite normalised Spidergram Plots for the lithologies and channel sediments present within the Luxemburg area are shown in Figure 4.

Rock types show similar patterns in the incompatible elements from rubidium up to strontium, with the granites displaying higher concentrations of thorium. The amphibolite then presents a relatively shallow decreasing trend compared to the much steeper, lower and more variable trend of the Basso and Bimbowrie data. The granites both have significant peaks at Zr and Y, which further separates their patterns from that of the amphibolite.

The Basso and Bimbowrie granites are distinctly separate from the Luxemburg amphibolite and also display chemical differences that separate the two lithologies (Benton, 1994). Figures 8a and 8b show strong and discrete grouping of major oxides occurring between the different rock types. The plot of Na_2O and K_2O against Aluminium (Figure 8a) illustrates the low Al concentration within the amphibolite but also the separation of potassium and

sodium levels in the Basso compared to the Bimbowrie granite. Figure 8b highlights the elevated levels of calcium and magnesium present within the amphibolite and the lower levels of calcium within the Basso compared to the Bimbowrie granite.

Figure 9, adapted from Hallberg (1983), shows the lithologies represented in fields for major rock types defined by their Ti/Zr ratio. All samples plot entirely within their expected zones, with no overlap between the sample groups. This further supports the significant geochemical differentiation seen between these granitic suites and the amphibolite body.

The elements titanium, manganese, nickel, zinc, copper and the trace elements chromium, vanadium and scandium are thought to represent primarily the amphibolite signature within the regolith and channel sediments. These elements are enriched in the amphibolite (Figure 4), and are indicative of mafic rock types (Hallberg, 1984; Berkman, 1999; Anupam and Rajamani et al., 2000). Silica, aluminium, sodium, potassium and the trace elements zirconium, thorium and yttrium are believed to be indicator elements for granitic influences on the regolith and channel sediment chemistry (Nesbitt 1979; Aubert et al. 2001;).

Regolith Profile Geochemistry

Graphs displaying the variation of selected element concentrations to depth from regolith drill cores are seen in Figures 10a-f.

Elements thought to be particularly influenced by mining activities include copper, nickel and zinc and their concentration with depth in the regolith profiles are shown with dashed trend lines. Figure 10a, representing elements typically enriched in amphibolite, shows similar patterns with depth for all element concentrations.

A large gravel lens identifiable in drill core exists at a depth of around 120cm, with concentrations of elements thought representative of amphibolite decreasing at the same depth. Positive influences on Si, Al, Na, K, Zr, Y and Th in Figure 10c are seen at the same depth, which is taken to indicate an increase in granite-derived material. Elements selected

to indicate felsic content within the regolith decrease substantially with depth in the profile observed in Figure 10c. Potassium has by far the steepest decline that becomes apparent at depths greater than where amphibolite clasts were first recognized. Figures 10b, 10d and 10f indicate element concentrations with depth from drill hole number 3.

Sampling density in drill hole 3 was reduced to individual specimens for each profile unit. Sampling of this style was conducted to see if the general trends from drill hole 2 could be established with minimal data. Patterns within 10b and 10d are difficult to ascertain, with a slight relationship with depth noticeable in 10f.

Figure 10e shows magnesium oxide concentrations are higher than calcium within the weathered amphibolite zone and Pedal unit, but are transposed within the Massive unit. The general increase in both oxide concentrations seen in Figure 10e is also represented in Figure 10f from drill core 3.

Current channel morphology

The Luxemburg channel exhibits a U-shaped form with steep sides and a flat bed. The main channel in the valley has a number of substantial tributaries that convolute approximately 200m from the head of the primary channel. The drainage area is confined to hills and rises immediately surrounding the valley floor. The channel is currently incising into regolith cover on the valley to form vertical banks with a maximum depth of 1.7m and width of 2.3m, before opening out onto a gradually sloping alluvial fan.

The channel longitudinal profile (Figure 11a.) illustrates the gradient of the primary channel and displays a typical concave curve (Morisawa, 1968) with minor deviations. The graph displays five sharp decreases in elevation that separates the concave curve into six rough zones (marked on Figure 11a). The first zone displays a linear decrease in elevation up to approximately 300m. The second section from 300 to 600 decreases in slope slightly but is relatively horizontal with distance. The third and fourth zones (from 600-900 and 900-1200

meters respectively) show similar decreasing trends separated by a sharp drop in slope at approximately 900m. A sharp decease in slope marks the start of the fifth section which flattens out until another sharp decrease at approximately 1400 meters.

Channelised flow opens onto an alluvial plain at around 1400 metres and the slope generally decreases until the last location at 1976m.

Channel sediment description

Channel sediments show a dominant coarse sand size fraction (table 1) that primarily comprises quartz, feldspar, with amphibolite and granitic composite clasts and significant opaque heavy mineral concentrations in the sand to silt sized fractions. Mineralogical investigations of the 125-250um fraction under microscope identified significant sub-angular feldspars, quartz and magnetic opaque minerals. Considerable concentrations of hornblende, muscovite, actinolite, chlorite, biotite, tremolite and sphene are also present in sediment samples along the entire length of the drainage-way investigated. The sediment also had minor amounts of carbonate nodules and coated grains and were distinctly lacking in garnet, zircon, kyanite or andalusite. All grains analysed showed textural immaturity, and had significant surface iron staining.

Grain size analysis of channel sediments from three locations (Figure 11b.) illustrates the pattern of variation with distance along the channel. Clay and silt content within the channel is minimal and varies little between each sample site analysed. The silt content is negligible in that it varies from a maximum of 2.3% at the location closest to the head of the channel to a constant 1.5% at the middle and furthest sample sites. Clay content is greatest with distance, but varies little with the minimum amount recorded at the central sampling site. Fine sand has its lowest value at the location near to the head of the channel and increases to a maximum at the middle site and a slightly lower value at the furthest location.

Channel sediment chemistry

Strong linear relationships are observed for all major oxides excluding magnesium and calcium in Harker plots of the channel sediments (Figures 18a-j). Magnesium and calcium show a linear relationship (Figure 12a) which is independent of silica, aluminium or iron content within the channel (Figures 12a-c). Figures 13a and b also illustrate the near perfect linear relationship between vanadium, chromium and iron content in the channel sediment. The sediments further show a relatively linear relationship between the chemically mobile elements potassium, sodium, aluminium and iron (Figures, 14a, 14b and 14c). A plot of (Cr+V)/Fe with distance along the channel shows a relatively static relationship independent of distance (Figure 17). Figure 4 "Whole Rock and Channel Sample Spidergram Plot" indicates that the channel samples strongly resemble a broad but similar pattern to that of the amphibolite. The pattern has notable but mild positive deviations from that of the amphibolite for the elements lanthanum, cerium, yttrium and vanadium. Similar negative deviations are seen for scandium, manganese and nickel.

Channel sediments fall within the Intermediate and Mafic zones of a Zr/Ti plot shown in Figure 9, with zirconium showing similar range and values to that of the amphibolite rock samples. Strong groupings are observed for the amphibolite and channel samples compared to those of the granites in plots of Sc/La against Titanium, Zirconium and Vanadium (Figures 15a, b and c). Sediment samples for plots 15b and c fall noticably closer to the amphibolite samples than granite, while in Figure 15a there is more of a separation between granite, channel and amphibolite sample groups.

Economic metal concentrations of copper, gold, zinc, lead uranium and cobalt are plotted against distance for the channel sediments in Figures 16a and b. All elements show similar patterns with distance except for gold, which is of extremely low concentrations. Element concentration patterns seen within Figures 16a and b and 17 can be correlated with the zones identified within the longitudinal profile of Luxemburg Channel (Figure 11a).

Sharp decreases in slope occur at roughly 400, 600, 900, 1200 and 1400 meters which are locations on Figures 16a, b and 17 where the elemental concentrations plotted generally increase.

5 Discussion

Regolith profile interpretations

The basal unit within the profile, the Pedal unit consists of a well-developed soil formed on alluvium. Abrupt boundaries exist between units, which illustrates significant periods of erosion between depositional episodes. The profile diagrams (Figures 5a-c) indicate several episodes of hill slope instability, fluvial and alluvial sediment deposition and soil development. These characteristics indicate that the regolith units are time transgressive, but also discontinuous.

A sharp erosional break between the Pedal and the Massive units recognisable throughout the study area implies that some of the Massive unit is formed from the reworking of the upper horizons within the Pedal unit. Clay content within the Massive unit is low which further suggests its formation from the stripping of the former A horizon within the Pedal unit. The Post European Material is believed to have formed within the last 200 years from extensive erosion across the landscape and comprises reworked Pedal and hillslope material with an aeolian component. It therefore is plausible that the elemental composition of the

PEM reflects the underlying regolith units as observed in the geochemistry of the profiles (Figures 10a-10d).

Similarities between regolith profile descriptions can be drawn between this study and those of Williams (1994a) and Fanning and Holdaway (2001). Stratigraphic sections within Williams (1994a), from central western New South Wales illustrate episodes of alluvial sand and aeolian dust accumulation and soil development and are dated between 14 500 and 1 840 years. Fanning and Holdaway (2001) worked on dating regolith profiles within the Sturt National Park in north-western NSW. Units with similar descriptions to those present at Luxemburg have ages (determined by radiocarbon and Optically Stimulated Luminescence techniques) of between 40 000 years, for the equivalent of the Pedal unit and 200 years for similar Post European Material. It is therefore probable that the profiles present within the Luxemburg catchment are Quaternary in age and relate to the climate fluctuations and aridity within the last 150 000 years.

The late Quaternary environment in the interior and southern extent of Australia is well documented and can be seen in Figure 19. adapted from Thomas (1989).

Current incision into the regolith profiles by the drainage channel within the Luxemburg catchment reflects the combination of changes in land use, rainfall amount and seasonality (Morisawa, 1968; Williams, 1994b). These changes are probably as recent as the European influence on the vegetation cover in this old mining and pastoral area, but may also be influenced by the gradual increase in aridity over the last 5 000 years (Figure 19).

Bedrock Geochemical Relationships

Although Si, Fe, Al, Mg, Ca, and Na are a considerable constituent of amphibolite (Deer et al., 1992.) Fe, Mg and Ca can be highly mobile within the weathering environment (Nesbitt 1979; Van der Weijden and Van der Weijden 1995; Anupam and Rajamani et al, 2000). Si,

Al and Na are abundant within all the rock types in the study area and therefore are of little use as discriminators between the mafic amphibolite and felsic granitoids.

Ti and Zr are considered essentially immobile within the weathering environment and along with Cr have been widely used for the geochemical discrimination of mafic and felsic rock types (Berkman 1999; Cullers 1988; Hallberg, 1983).

The Luxemburg amphibolite displays high concentrations of Ti and the relatively immobile elements Cr, V, Ni and Sc. The Basso and Bimbowrie granites, although distinct from each other show common enrichment patterns in zirconium, yttrium, and thorium. These chemical distinctions are used to help differentiate the chemical signatures seen within the regolith of the study area.

Geochemical Nature of the Regolith Profiles

The Regolith Landform Map indicates that both drill cores are positioned on the same regolith landform unit, indicating similar profile characteristics. The central location of drill hole 2 in the Luxemburg catchment suggests that the mining impact could be significant, and its presence is recorded in Figure 5b, although this is not visible in the geochemical data. Drill hole 3 was located further to the southeast where the channel became focused between two hill slopes before opening out onto an alluvial plain.

Amphibolite indicator elements within drill hole 2 show strong increasing trends with depth that become significant at depths greater than 125cm. Figure 10b illustrates decreases of granite indicator elements with depth in the profile of drill hole 2. K, Na and Al which are highly fractionated within the source rocks (Figure 8a) and mobile within the weathering environment (Nesbitt, 1992.), show the greatest variations with depth. Si, Zr, Y and Th also show decreases with depth but their trends are milder than those of the relatively mobile elements. Although the higher concentrations of mobile elements indicate an amphibolite

influence on the regolith profile, the trace elements Zr, Y and Th, also reflect mafic sources at depth.

Relationships between elements within the dataset from drill hole 3 are hard to establish, with low-density sampling not repeating the general trends observed in drill hole 2. The role of carbonate in controlling Mg and Ca oxide concentrations in regolith profiles is unknown, although the strong relationship between Ca and Mg concentrations with depth seen in the core from drill hole 2, along with regolith profile descriptions (Figure 10e) suggest that carbonate is pervasive at that location.

Channel sediment maturity and transport mechanisms

The strong linear relationships between all the major rock forming minerals and SiO_2 (excluding Mg and Ca) indicate two attributes. The first is chemical immaturity of sediment, and the second is an insignificant contribution of clay minerals as these two factors would both lead to deviations from the linear relationships seen. The minimal content of clay and silt sized particles within channel sediment is supported by grain size analysis results shown in table 1 and Figure 11b. Chemical immaturity of sediment is also supported by petrographic descriptions and plots of relatively mobile elements K and Na against Al (Figure 14b) showing moderate linear trends. The strong correlations between these elements and the iron content within the channel (Figure 14c) also suggest that the samples are mineralogically immature. Harker plots of channel surface sediment samples and samples from deeper within the profile show that the channel deposits' elemental chemistry deviates little from linear relationships with depth.

Significant proportions of heavy minerals are present within the channel sediment, which strongly influences the elemental chemistry represented by Figures 13a, 13b and 17. Figure 17 illustrates that the absolute concentrations of Cr, V and Fe vary substantially with distance

along the channel. Their relative concentrations, expressed as Cr+V/Fe, are more steady with distance along the channel. This implies that the elements within the heavy minerals have not substantially fractionated with distance, further supporting little weathering of the heavy mineral fraction.

Teutsch et al. (1999) found that rainfall levels in environments similar to the study area did not significantly influence metal concentrations (including iron) within soil profiles. This suggests that the concentrations of metals seen within the Luxemburg channel can be directly related to physical transport mechanisms.

Similarities between the patterns of economic and heavy mineral concentration levels shown in Figures 16a, 16b and 17 are observed. Comparisons can be made between the Longitudinal Profile of Luxemburg Channel and locations of element concentrations. This indicates that the elemental concentrations within the channel are primarily controlled by physical dispersion mechanisms that can be directly related to channel morphology and landscape position.

Channel sediment provenance

The sinuosity and channel morphology is important for the movement and distribution of bed load, as is the competence of a waterway. The competence defines the size of the particles carried in the bed load and can change greatly with time as well as position within the channel (Morisawa, 1968). This is especially true of an ephemeral waterway that has seasonal and sporadic flow as is present in this study.

The stream sediment composition and character, determined from petrological work, all suggest a local provenance. The mineral composition, along with the lack of garnet, zircon, kyanite or andalusite supports local provenance from the amphibolite and surrounding granites in the valley system. It is thought that Willyama rocks which host the granitic and gneissic intrusives have significant zircon and garnet and appreciable andalusite and kyanite

concentrations (Conor 2001). The lack of these minerals within the channel sediment and regolith profiles correlates with field observations of only minor outcrops of the host sequence within the valley system.

Rare-earth elements (REE) are among the most immobile elements during low-grade metamorphism, hydrothermal alteration and weathering (Rollinson, 1993). In sediments, the principal control on the concentration of REE is the provenance as they are insoluble and are present in very low concentrations in meteoric water (Fleet, 1984). Scandium is enriched in the amphibolite samples and its concentrations within sediments are controlled by ferromagnesian minerals which are relatively stable in the weathering environment (Cullers, 1988).

Thorium is believed to be present in primary mineral phases such as sphene (Cullers 1988) and apatite, shown by its linear correlation with P_2O_3 illustrated in Figure 14a. Characteristic element discriminators for mafic and felsic rocks, Ti and Zr are highly immobile in the weathering environment (Hutton, 1977; Hallberg, 1984; Nesbitt and Wilson, 1992). Plots of La/Sc against Ti, Zr and Th imply that the primary elemental signature of the channel sediments is derived from the amphibolite.

Studies by Aubert et al. (2001) and Cullers et al. (1987) found that REE source rock patterns are most representative in the silt-sized fraction of clastic sediments. This relationship is therefore especially strong considering that analysis was undertaken on bulk samples of the channel sediment.

The presence of heavy minerals may have an erratic effect on REE concentrations within individual samples (Rollinson, 1993). Groupings of channel sediment data are tight within Figures 15a, b, and c and this would suggest that there is little erratic influence on REE concentrations.

Carbonate behaviour

Carbonate silt, nodules and coated rock fragments were observed within the channel sediment and through grain size analysis. MgO and CaO show non-linear relationships with SiO_2, Al_2O_3 or Fe_2O_3T in channel sediments. This could be explained by their relative chemical mobility within the weathering environment. There is a positive linear relationship in stream sediments between Ca and Mg that is not present within the parent rock types. These relationships are interpreted as showing the pervasive carbonate that occurs within the study area.

Some of the carbonate has probably been reworked and redeposited many times from initial sources that could include both bedrock and aeolian components. Carbonate accumulations predominantly occur within topographic hollows and on the valley floor, independent of bedrock geology (refer to regolith landform map and legend descriptions), which supports the cycling and re-deposition of this material within the environment. The extent and nature of carbonate within the regolith is probably dependant on three variable factors: bedrock geochemistry, aeolian contributions and landscape position.

6. Conclusions and recommendations

The Regolith Landform Map indicates that the dominant current dispersion patterns within the study area are controlled by colluvial and alluvial processes. The regolith profiles, landscape character and climate would suggest that these processes have been episodically active in the past. Recent human activities including mining and pastoral occupation of the area have altered the present dispersion mechanisms, especially within the valley floor, evident by the incision of the channel into past regolith cover.

Field observations, mineral compositions of channel sediment along with Previous studies, indicate that outcrop of Willyama host rock is minimal in the catchment, and the felsic influence from the surrounding granites and gneisses can be related to Basso and Bimbowrie geochemistry (Benton, 1994, and Stephen, 2001). Whole rock elemental chemistry demonstrates that the amphibolite is chemically distinct enough to trace within the regolith cover of the catchment.

The amphibolite geochemical signature can be deciphered with increasing in certainty at depth, in this thin regolith cover of probable Quaternary age. Sampling techniques used imply that initial dense geochemical sampling of the profile is required to distinguish elemental trends, and that reducing sampling density may not be viable for obtaining meaningful results. Effects from mining and pastoral activity do not seem to greatly influence the chemistry of the regolith. The amphibolite geochemical fingerprint is still visible in chemically immature bulk samples of channel sediment showing strong heavy mineral geochemical relationships.

Further work

The aeolian and carbonate effects on the geochemistry observed in the regolith samples of this study are largely unknown. Carbonate content was minimal in the regolith profile samples analysed in table 1, but was variable and locally extensive (refer to Regolith Landform Map Point Sample Descriptions in the appendix). Further work separating the extent of the aeolian component and the sources and nature of carbonate within the regolith profile would help to quantify geochemical signatures observed in this study. Sediment dating of regolith units may also give better insights into the geochemistry observed and the history of landscape evolution within this region. The small number and low sampling density of regolith drill cores should be noted to suggest that the results are not entirely conclusive.

7. Acknowledgments

I owe my family so much for their constant support, interest, concern, understanding and care during this eventful year, thankyou. Additional gratitude is felt for my sister who was there when I needed it most, your understanding and hospitality is so greatly appreciated.

I acknowledge and greatly appreciate the financial support and academic opportunities and guidance made available to me through my association with CRC LEME.

I would sincerely like to thank Aaron and Hash for their support, guidance, friendship and assistance throughout this year, especially during field work. Thanks is well overdue to Karen and Dan for their field work support, which is not forgotten, and thanks also goes out to Andy, Tiger, Four, and Grunter for their first-rate hospitality and friendship – Ibbly Dibbly.

Thanks must also go to my supervisors Andreas and Martin for their guidance and support throughout this year, and the wonderful support from staff within the department.

To the honours people who have made this year the best of my life, how will I ever cope without you? I honestly don't know.

8. Appendices

Regolith Landform Map, Luxemburg Mine Site Olary Domain, South Australia.

Regolith Landform Map, Luxemburg Mine Site
Olary Domain, South Australia

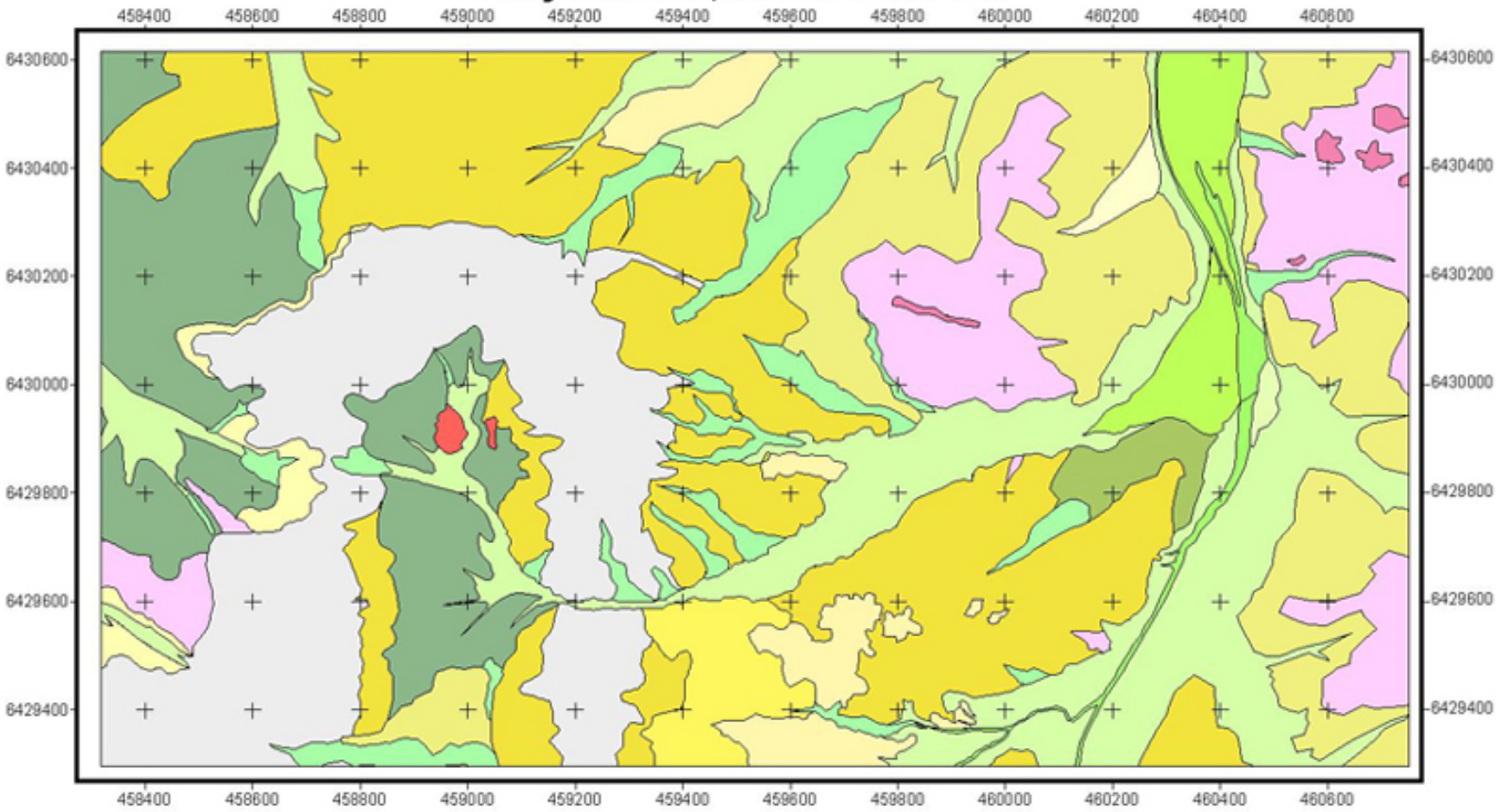

N

0 100 200 300 Meters

Legend

- AOap
- Aap
- Aca
- Aed
- Afs
- CHap
- CHer1
- CHer2
- CHer3
- CHer4
- Cer
- Cpd1
- Cpd2
- SSel
- SSer2
- SSer3

Mapped and Compiled By
Kernich, A and Brown, A
2002

Regolith Landform Map Unit descriptions

Alluvial sediments

AOap – Unconsolidated red brown clays and silts with predominantly sand to cobble sized quartz, granite lithic fragments, opaque minerals and feldspar grains. Surface shows heavy mineral and quartz sand to pebble sized grains in sheet wash banding with a considerable magnetic fraction within a channel overbank deposit. Densely colonised by Black Blue Bush and Native Tobacco with minor Bassia and Bathurst Burr.

Aap - Red brown to yellow brown, poorly sorted, moderately consolidated, clay to silt with spatially variable sub angular to sub-rounded sand to cobble sized clasts predominantly comprising of quartz with minor granitic, amphibolite, feldspar, muscovite and opaque clasts. Significant surface iron staining and moderate proportion of carbonate coated clasts and carbonate fragments.
Locally variable surface lag of sand to pebble sized clasts predominantly comprising of coarse sand sized fraction. Minor variable meter scale channels, surface incision, gullying, rilling and contour banding on a dissected alluvial plain. Colonised by very open chenopod shrub land with heavily grazed Bassia, Black Blue Bush, Bathurst Burr and Sida.

ACa - Angular to sub rounded, crudely bedded, fine to coarse sands and gravels, arranged in fining upward sequences predominately consisting of quartz, with magnetic opaque minerals in finer fractions and minor granite and amphibolite lithic clasts in coarse fraction Surface materials consist of coarse sand to pebble size quartz clasts and minor exposures of weathered bedrock and red brown fine silts and clays within a converging ephemeral channel displaying active incision. Locally specific colonies of Native Tobacco, Bassia and Bathurst Burr.

Aed - Red brown unconsolidated silt and clays, with angular to sub angular quartzose and lithic sands to small pebbles, and occasional granitic cobbles occur within depressions displaying minor channelling on moderate slopes. Surface lag predominately sand sized quartz and granitic material, sparsely vegetated with Sida.

Afs - Slightly consolidated apedal red brown silt and fine sand, with sand to boulder sized clasts comprising of quartz, feldspar and opaque minerals with granitic and amphibolite clasts in sand and above size fractions. Surface features include palaeo-channel lags defined by coarse pebbles and boulders, sheet flow banding and minor gullying present on alluvial fan deposits. Colonised by a variably sparse to moderately dense chenopod shrubland, with Black Blue Bush, Bathurst Burr and Bassia.

Colluvial Sediments

CHap - Fine sandy silts and yellow brown clays, with coarse sand to cobble sized quartz, feldspar and granitic clasts and minor carbonate nodules and powder. Alluvial plain, with colluvial sheet flow, wind etching and minor mud flaking on surface. Colonised by a very open chenopod shrubland with Black Blue Bush, and Bathurst Burr, and very minor Rosewood and Native Tobacco.

CHer1- poorly sorted, apedal, yellow/brown clay-silt, with moderate powdery carbonate. Sand to boulder sized granitic lithic fragments with quartz feldspars and opaque magnetic minerals, with minor carbonate nodules. Sheet flow on erosional rise with minor channelised flow. Extremely sparse chenopod shrubland with Pearly Blue Bush and minor Black Blue Bush

CHer2- Apedal yellow brown clay to silt, with sub angular to angular coarse sand to gravel sized quartz, feldspar and opaques. Coarse sand to boulder sized granite and amphibolite fragments and moderate to locally major powdery carbonate, carbonate nodules and coated fragments. Minor granite, pegmatite and quartz vein outcrops with localised iron and copper staining. Surface dominated by pebble to boulder sized quartz, lithic fragments and opaque minerals on a shallow to moderately sloping erosional rise, with minor channelised flow. Colonised by very open chenopod shrubland with Pearly Blue Bush, Black Blue Bush and Bassia, with Bathurst Burr in channels.

CHer3 - Silt to predominantly boulder sized milky and white quartz clasts with poorly sorted, unconsolidated yellow brown silts and clays. Minor silt sized powdery carbonate and boulder to course sand sized highly weathered granite and amphibolite clasts and opaque minerals. All grains exhibit moderate to heavy iron staining. Surface dominated by dense cobble to boulder sized quartz lag with strong sheet flow banding on a shallow erosional rise. No vegetation present.

CHer4 - Yellow brown massive, apedal carbonate rich clays to silts with sand to cobble sized quartz, nodular carbonate and minor granite lithic fragments, sand to pebble sized feldspar, mica and opaque clasts. Surface dominated by slightly consolidated yellow brown silts and clays, powdery carbonate and sand to cobble sized grains on a shallow erosional rise. Colonised by very open to open chenopod shrubland with dominant Pearly Blue Bush with Black Blue Bush and Bassia.

Cer- Red brown silt to clay with fine sand to pebble sized quartz, feldspar and sand sized magnetic fraction and minor micas with scattered boulder sized quartz and granitic fragments. Surface features include localised concentrations of sand sized magnetic fractions, quartz and felspar on a low erosional rise. Colonised predominantly by very open Sida, with Cottontails and Bathurst Burr.

Cpd1- Red brown silt to course sand sized very angular poorly sorted quartz with sand to pebble sized angular lithic fragments and opaque mineral clasts showing significant iron staining and minor carbonate coating. Surface shows concentrations of unconsolidated sand to pebble sized fractions on a sloping dissected depositional plain with minor small scale guttering and incision. Vegetation cover is a highly disturbed, very open remnant chenopod shrubland with Black Blue Bush, and localised Sida and Bassia.

Cpd2 - Yellow brown clay to silt with silt to boulder sized quartz, granite lithic fragments and sand to pebble sized carbonate, angular feldspars and opaques all with abundant iron staining. Very minor centralised channel flow and erosion of surface fines. Quartz and heavy mineral surface banding defined by sand to pebble sized fraction on a gently sloping depositional plain. Colonised by open chenopod shrubland with Black Blue Bush, Bassia and minor Bathurst Burr.

Saprolith

SSel- Slightly to moderately weathered massive, coarse grained, albitic granitic bedrock with minor pegmatite and quartz veins and local occurrences of foliated medium grained gneissic outcrops. Quartz veins are milky to rose coloured and show box-work structures after primary sulphide weathering. Surface shows bedrock exposures with significant iron staining and joint weathering with sand to boulder sized angular to sub angular minerals and composite grains from granite weathering. Minor well sorted unconsolidated red brown silt/clay on surface and in joints on an undulating low hill. Colonised by extremely open chenopod shrubland, with mature Black Blue Bush and Pearly Blue Bush, Sida and Bassia.

SSer1- Slightly to moderately weathered massive, coarse grained, albitic granitic bedrock with minor pegmatite and quartz veins and local occurrences of foliated medium grained gneissic outcrops. Quartz veins are milky and rose coloured and show box-work structures after primary sulphide weathering. Surface shows bedrock exposures with significant iron staining and joint weathering with sand to boulder sized angular to sub angular minerals and composite grains from granite weathering. Minor well sorted unconsolidated red brown silt/clay on surface and in joints on an erosional rise. Colonised by open chenopod shrubland, with mature Black Blue Bush and Pearly Blue Bush, Sida and Bassia.

SSer2- Metre scale, slightly weathered, massive quartz veins within granitic bedrock, displaying centimetre scale joint weathering and moderate iron staining on surface. Exposures have minor well sorted red brown unconsolidated silts and clays on surface and produce angular boulder to pebble sized quartz lag down slope. The landform is an erosional rise with no vegetation present.

SSer3- Outcropping moderately weathered coarse grained amphibolite with significant mineral etching, joint weathering and iron staining on surface. Surface materials consist of pebble to boulder sized amphibolite fragments and minor red brown silts and clays on a small erosional colonised by very sparse Sida, with extremely sparse Black Blue Bush.

REGOLITH
AO: Overbank Deposit
AC: Channel Deposits
A: Alluvial Sediments
CH: Sheet Flow Deposit
C: Colluvial Sediments
SS: Slightly Weathered Bedrock/Saprock

LANDFORM
a: alluvial landforms
ap: alluvial plain
pd: depositional plain
ed: drainage depression
er: erosional rises
el: low hills
fs: sheet-flood fan

Point sample locations – Regolith Landform Map, Luxemburg Mine Site Olary Domain, South Australia.

Point Sample Locations - Regolith Landform Map, Luxemburg Mine Site
Olary Domain, South Australia

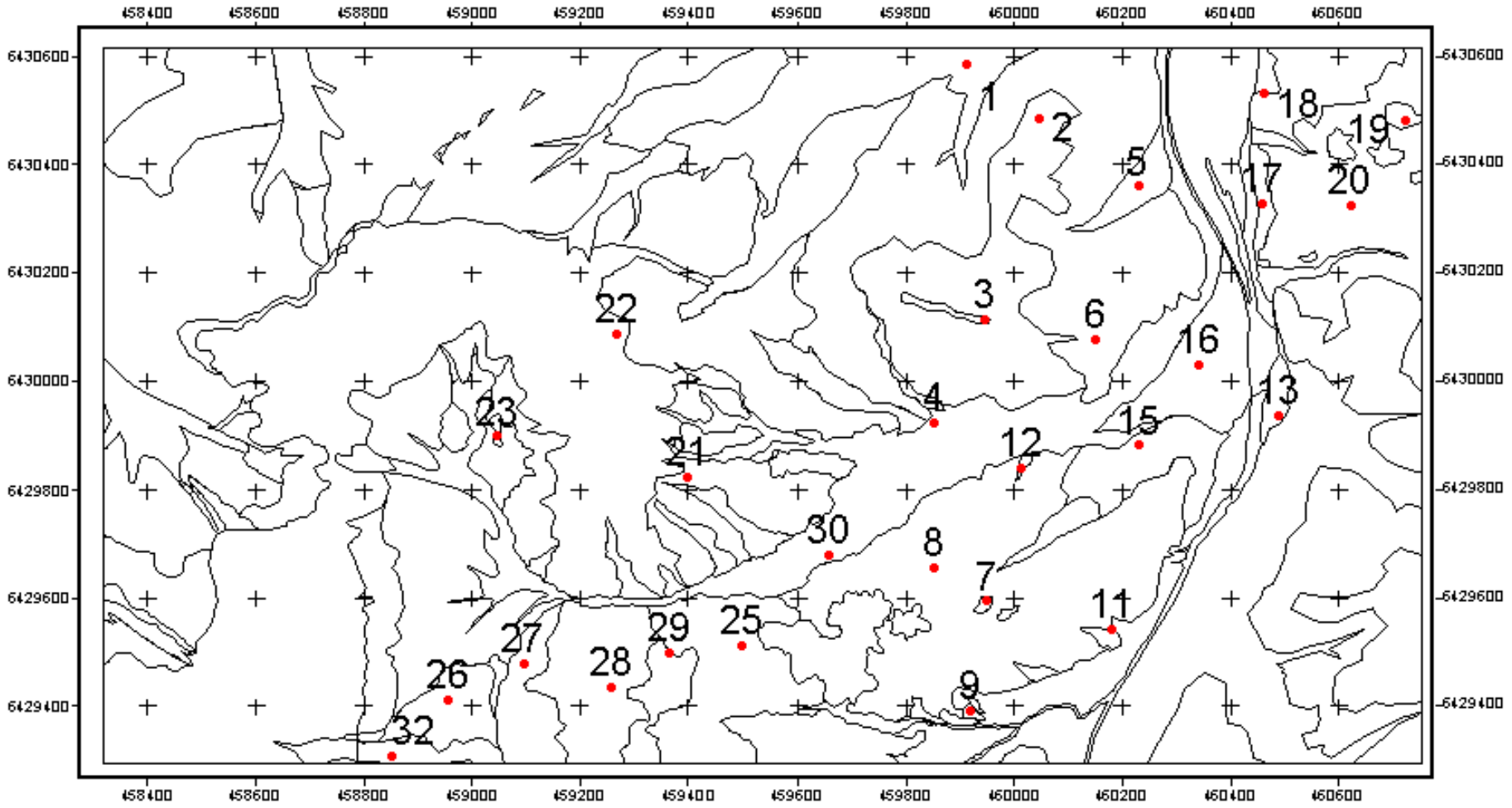

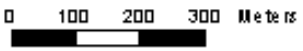

Mapped and Compiled By
Kernich, A and Brown, A
2002

Point sample location descriptions, Regolith Landform Map.

These descriptions were defined using the method of sorting, roundness and size classification adopted by Geoscience Australia. Where possible, the descriptions were based on definitions outlined in the RTMAP Regolith Database Filed Book and Users Guide of Pain et al. (2000).
For map locations, refer to "Point sample locations, Regolith Landform Map, Luxemburg Mine Site Olary Domain, South Australia".

1) Regolith: Fine, poorly sorted, a pedal red/brown silt and clay with course sands to pebbles comprising of quartz, composite lithic fragments feldspars and opaques in order of dominance. Slight crust on surface as defined by finer material.

Landform: Dissected Alluvial Plain with minor Alluvial Channels (ap).
Surface: Slight cover of predominantly coarse sand to pebble size quartz but also lithic granitic fragments, feldspars, plagioclase, micas and opaques. No larger sized feldspars above small pebble size. Sheet wash lag present as defined by alternating banding arrangement of surface sands to pebbles, and patches of consolidated surface silts and fines.
Minor: Alluvial channel deposits in meter scale, shallow alluvial channels. Minor wind etching as defined by lineation on surface of consolidated fines and the presence of well sorted silt to sand sized small mounds at western side of some vegetation.
Vegetation: Open chenopod shrub land with dominant Black Blue Bush and Bassia with minor Bathurst Burr.

2) Regolith: Slight to moderately weathered bedrock comprising of medium to course grained granite with a significant course micas(muscovite and minor biotite) and meter scale quartz veining. Granite and quartz forming granule to bolder sized fragments. Granite heavily iron stained with substantial lichen cover on surface. Joint fractures opened up to cm scale and significant mineral etching present.
Landform: Moderate undulating Erosional Rise (er).
Surface: Weathered bedrock and fragments from cobble to bolder sized the latter dominant. Minor fine sand to gravel sized angular fragments comprising of weathered granitic minerals, quartz, feldspars with minor opaques and micas.
Minor: Fine well sorted red silt/clay with slight powder carbonate present in the silt fraction.. Marginal build up of well-sorted silts on western side of vegetation and boulders.
Vegetation: Open Chenopod shrub land, dominated by Pearly Blue Bush.

3) Regolith: Meter scale slightly weathered quartz vein within granitic bedrock. Joints opened up to cm scale and moderate iron staining present on surface. Minor lichen and algae also present on surface. Bedrock producing principally angular boulder to pebble sized quartz lag further down slope.
Landform: Erosional Rise (er).
Surface: Slightly weathered quartz bedrock and bedrock fragments.
Minor: Well-sorted fine silts and clays with some lithic fragments of quartz from silt to bolder size, algal/lichen sheet present also on silt dominant surfaces.
Vegetation: Very open, heavily grazed chenopod shrub land with Pearly Blue Bush identifiable.

4) Regolith: Massive, a pedal yellow/brown fine silts and clays with angular coarse sands through to small pebbles of quartz, feldspars, opaques and lithic fragments. Opaque magnetic fraction present within course sand to granular fraction.

Landform: Alluvial plain (ap).

Vegetation: Extremely sparse chenopod shrub land with minor Bassia, Black Blue Bush, and Bathurst Burr present in channels.

Surface: Clay/mud cracks on surface in some areas, etching by wind also present as defined by lineation in consolidated surface silts. Well-sorted silts and clays built up on eastern side of vegetation. Slight intermittent lag of predominantly quartz with minor opaques and feldspars present, in course sand to granule-sized fraction.
Minor: Alluvial sediments in one meter scale channels. Minor sheet flow banding of surface clasts present. Dense vehicle and sheep tracks present.

5) Regolith: Yellow/brown fine sandy silt to clay with course sands to cobbles of lithic fragments, feldspars and quartz. Quartz up to cobble size with lithic fragments and feldspars up to pebble size. Carbonate also present in hard nodular form from granules to pebble size and fine powdery from in silt sized fraction.

Landform: Alluvial plain (ap).

Surface: Colluvial sheet flow present as defined by surface grain banding and minor wind etching also present in some areas.

Minor: Mud flaking present on some areas that have consolidated silty surfaces.

Vegetation: Very open chenopod shrub land with Black Blue Bush and Bassia dominant and minor Native Tobacco and Rosewood trees.

6) Regolith: Yellow/brown sand silt and clay, massive, poorly sorted a pedal. Rock fragments from course sands to bolder size comprising of quartz and albitic lithic fragments. Sand to cobble sized significantly magnetic opaque fragments, and significant carbonate present from silt to cobble size nodular and powdery forms.

Landform: Erosional Rise (er).

Surface: Minor lichen/algal cover on surface silts and clays and lithic clasts. Varying degrees of mineral etching and substantial iron staining on surface of lithic clasts.

Minor: Minor deflation of surface fines in patches and build up of well-sorted sands to clays around the eastern side of vegetation.

Vegetation: Extremely sparse Pearly Blue Bush, mostly deceased.

7)Regolith: Yellow/brown poorly sorted clay to silt. Silt to bolder sized quartz fragments present, highly weathered lithic fragments coarse sand to bolder sized with iron staining present. Predominantly magnetic opaque fraction cobble to course sand sized. White to rosy coloured, heavily iron stained quartz, from silt to cobble sized. Some minor nodular and laminated carbonate fragments, roughly pebble in size.

Landform: Erosional Rise (er).

Surface: Poorly sorted quartz dominant lag from coarse sands to large pebbles. Lithic fragments of feldspars, plagioclase, opaques both magnetic and non-magnetic in granule to pebble size. Small pebble to large pebble sized composite clasts. All surface clasts highly iron stained.

Minor: Sheet flow banding predominant as defined by alignment of surface material with minor deflation patches also.

Vegetation: Not present.

8) Regolith: Yellow/brown clay to fine silt up to coarse sands, poorly sorted with significant powdery carbonate content in the clay to silt fraction. Sub-angular to angular quartz present from predominantly sand sized to bolder size. Cobble to silt sized carbonates present in nodular and powdery form. Carbonate coated nodules and lithic fragments present in above silt sized fraction. Minor coarse sand to cobble sized lithic fragments, feldspars and magnetic and non-magnetic opaques.

Landform: Erosional Rise (er).

Surface: Algal/lichen mats commonly distributed on surface. Aeolian deflation of some fines as defined by surface layer of consolidated silts and minor build up of well sorted silts to sands around bases of vegetation.

Minor: Meter scale outcrops of moderately and slightly weathered granitic bedrock.

Vegetation: Varyingly open chenopod shrub land, dominated by Pearly Blue Bush with minor Black Blue Bush, Bassia and Rosewood trees.

9) Regolith: Orange/brown poorly sorted clay to silt. Silt to bolder sized quartz fragments and coarse sand to bolder sized highly weathered lithic fragments with substantial surface iron staining present. Minor predominantly magnetic cobble to course sand size opaque fraction present. Significant white to rosy coloured, silt to cobble sized heavily iron stained quartz. Some minor nodular and laminated predominantly pebble sized carbonate fragments.
Landform: Erosional Rise (er).
Surface: Semi sorted dense 1-2cm sized quartz lag dominant.
Vegetation: Not present.

11) Regolith: Slightly weathered granite bedrock and meter scale quartz veins.
Landform: Erosional Rise (er).
Vegetation: Open chenopod shrub land dominated by Bassia and pearly Blue Bush.

12) Regolith: Slightly weathered granitic bedrock extending to the local channel where hard layered carbonates are overlying in outcrop. Course grained, foliated, albitic granite with high percentage of quartz, feldspars and plagioclase with minor muscovite and biotite.
Landform: Erosional Rise (er).
Surface: Significant iron staining and joint weathering on bedrock exposure. Sand to pebble sized angular to sub-angular minerals and composite grains from weathering of granite with feldspars, quartz, and micas recognizable.
Minor: Well sorted, unconsolidated red/brown clays and silts on surface and within joint cracks.

Vegetation: Open chenopod shrub land dominated by Pearly and Black Blue Bush.

13) Regolith: Extremely unconsolidated red/brown clays and silts with a dominant silt sized fraction. Sand to bolder sized sub-rounded to angular quartz, feldspars and opaque clasts and granule to boulder sized composite lithic fragments. High percent of opaques both magnetic and non-magnetic in sand to course sand fraction.
Landform: Channel Overbank deposits (a).
Surface: Sheet flow banding as defined by surface material and sand to pebble sized grains mainly composed of magnetic opaques.
Vegetation: Moderately closed chenopod shrub land dominated by Black Blue Bush with minor Bassia and Bathurst Burr and Native Tobacco Bush on the edges of channels.

15) Regolith: Yellow/brown, poorly sorted, massive, a pedal clay to silt. Silt to boulder sized angular quartz, course sand to boulder sized sub-angular highly feldspatic lithic fragments, and sand to pebble sized angular feldspars and dominantly magnetic opaques. Minor powder carbonate present in silt to sand fraction. Abundant iron staining on surface of clasts.
Landform: Depositional Plain (pd).
Surface: Sheet flow banding dominant as defined by alignment of surface clasts, particularly opaques and quartz in the sand to pebble sized fraction. Multiple cross cutting animal tracks present.
Minor: Some aeolian deflation of surface fines present as defined by small depressions with consolidated silt to clay sized surfaces and minor build up of well sorted sands to silts at the base of vegetation..
Vegetation: Very open chenopod shrub land dominated by Black Blue Bush and Bassia with minor Bathurst Burr.

16) Regolith: Spatially ranging from alluvial channel and fan deposits. Alluvial channels have clay to boulder sized clasts with a dominant sand sized fraction. Fan deposits have clay to boulder sized clasts with a dominant red/brown silt and fine sand sized fraction. Channel deposits contain abundant lithic fragments from pebble to predominantly boulder in size. Majority of channel clasts are granitic with minor amphibolite and quartz fragments present. Clasts range in grade from moderately weathered to only slightly weathered, angular to sub-rounded. Some pebble to

sand sized nodular carbonate fraction in both channel and fan deposits. Fan deposits are a pedal and slightly consolidated.
Landform: Fan deposit system with at least three distinct palaeo-channels (fs).
Surface: Palaeo-channel lag defined by courser pebbles and boulders indicating past channels and minor gulling present within fan deposits to the sides.
Vegetation: Variable moderately dense to sparse chenopod shrub land with Black Blue Bush, Bassia, Bathurst Burr in fan deposits and Native Tobacco in channels.

17) Regolith: Poorly sorted red/brown clay to fine silt with coarse sand to cobble sized granitic lithic fragments, quartz and feldspar minerals. Minor carbonate nodules present ranging from course sand to pebble sized.
Landform: Erosional Rise (er).
Surface: Sheet wash dominant process as defined by alignment of surface material and clasts in 'stick dam' structures.
Minor: Sparse, very shallow and open alluvial depressions.
Vegetation: Sparse chenopod shrub land with heavily grazed Pearly Blue Bush the only species noted.

18) Regolith: Yellow/brown, a pedal clay to fine silts. Silt to boulder angular to sub-rounded quartz dominant mineral with the sand fraction and cobble to boulder being predominant sizes. Very minor nodular carbonate present in coarse sand to granule size and some very minor granitic lithic clasts.
Landform: Erosional Rise (er).
Surface: Boulder to pebble sized quartz clast lag.
Vegetation: Extremely sparse chenopod shrub land with Black Blue Bush and Bassia.

19) Regolith: Slightly weathered massive milky quartz bedrock. Open joints orientated in a NW-SE direction and significant iron staining present on surface.
Landform: Erosional Rise (er).
Surface: Bedrock exposures and angular quartz clasts ranging from course sands to gravels.
Minor: Thin cover of fine grained, well sorted, unconsolidated red/brown silts and clays.
Vegetation: Very open chenopod shrub land with Pearly Blue Bush some small patches of unidentifiable grasses.

20) Regolith: Slightly to moderately weathered granitic bedrock. Coarse to medium grained albitic granite with quartz, feldspars and plagioclase dominant minerals with minor muscovite and hornblende. Mineral etching and significant iron staining present on surface. Very open joints and fracture plains. Some bedrock friable with foot and hands although the majority is not.

Landform: Erosional Rise (er)
Surface: Sand to granular size mineral and lithic fragments from granitic weathering with quartz, feldspars, plagioclase and micas identifiable. Minor coverage of algae and lichen on surface of weathered bedrock and silt/clay surfaces
Minor: Well sorted, unconsolidated red/brown clays and silts throughout with mounds up to 10cm in height around bases of some vegetation.
Vegetation: Moderately dense chenopod shrub land with Pearly Blue Bush.

21) Regolith: Yellow/brown massive, a pedal clays to fine silts with sand to boulder sized clasts throughout. Silt to boulder sized sub-angular to angular milky, rosy and clear quartz fragments with surface etching and iron staining. Silt to small boulder sized sub-angular, massive, dominantly magnetic opaque fraction with surface iron staining. Sand to pebble sized angular to sub-angular feldspars and minor plagioclase with heavy iron staining on surface. Coarse sand to granule sized muscovite preset in minor amounts. Granule to boulder sized sun-angular to sub-rounded composite granitic lithic fragments with heavy mineral etching and iron staining on surface. Very minor percent of nodular carbonate present in sand to granule sized fraction.
Landform: Undulating erosional rise with some very minor open, shallow channel depressions (er).

Surface: Dominated by pebble to boulder-sized quartz with minor (~15%) opaques. Lichen on some clasts and minor sheet flow banding patterns present as defined by surface grain alignment and sorting. Highly disturbed from post settlement excavation and traffic.
Minor: Minor sporadic outcrops of moderately to slightly weathered granitic and quartzose bedrock.
Vegetation: Very sparse chenopod shrub land dominated by Black and Pearly Blue Bush and minor Bassia and Sida.

22) Regolith: Slightly to moderately weathered granitic and gneissic bedrock and quartz veins. Granites albitic, coarse grained and massive with a high percent of quartz, feldspars and plagioclase with minor muscovite and opaques. Some areas are foliated and others have very coarse muscovite minerals present (pegmatites?) Gneissic exposures have a higher concentration of the darker minerals. Quartz is predominantly milky and rosy in colour and is weathering to form sand to boulder-sized fragments on the surface.
Landform: Undulating erosional low hill (el).
Surface: Granites show considerable mineral etching, joint opening and iron staining. Numerous Lichen varieties present on rock surface and on coarse sands to pebbles sized clasts from granite, gneissic and quartz weathering. Sheet flow predominant as defined by alignment of surface clasts.
Minor: Well sorted, unconsolidated, thin layer of yellow/brown clays and fine silts on surface and in between joint cracks and fractures.
Vegetation: Sparse chenopod shrub land dominated by well established Black and Pearly Blue Bush. Minor Sida, Bassia and a single rosewood tree present.

23) Regolith: Moderately weathered very coarse-grained amphibolite with identifiable amphibole, actinolite and chlorite present in fibrous, radial alignments.
Landform: Erosional Rise (er).
Surface: Very open joint plains and significant surface coverage by numerous types of lichen. Iron staining present and significant mineral etching.
Minor: Poorly sorted red/brown clays and silts to coarse sands. Amphibolite mineral clasts in coarse sand to boulder sized fraction with minor pebble to small boulders of quartz and granitic composite clasts.
Vegetation: Very open chenopod shrub land with Sida dominant and minor 'bunnyears' and Black Blue Bush.

25) Regolith: Yellow/brown, poorly sorted, a pedal silt to clay with significant amounts of subangular to angular sand to boulder sized quartz. Minor coarse sand to pebble sized granitic clasts, muscovite and feldspar grains. Significant carbonate present in silt fraction as powder carbonate form and some nodular form present in coarse sands to gravel sized fraction.
Landform: Subdued Erosional Rise (er).
Surface: Build up of well-sorted red/brown clays to sands around vegetated areas, and deflation hollows in meter scale patches with surface lag. Lag varies from cobble sized quartz clast lag to pebble sized nodular carbonate dominated lag in patches. All clasts are heavily iron stained and variable minor to severe mineral etching present on lithic clasts. Carbonate dominated lag also has considerable algae cover on clast surfaces.
Minor: Wind etching and sheet flow process active as defined by alignment of surface fines and lag.
Vegetation: Sparse to open chenopod shrub land with Black and Pearly Blue Bush dominant and minor Bassia.

26) Regolith: Orange/brown, poorly sorted, a pedal silt to clay with sand to cobble sized quartz, lithic fragments and minor opaques and felds. Course sand to pebble sized nodular carbonate abundant and significant powder carbonate in silt fraction present. Lithic clasts comprise of both granitic type composite clasts and amphibolite type composite clasts. High percent of quartz present in course sand to gravel size fraction. All minerals and clasts heavily iron stained and some amphibolite and minor occurrences of granitic clasts with laminar carbonate coating on surface.
Landform: Subdued Erosional Rise (er).

Surface: Sheet flow predominant as defined by alignment of surface material and finer lag particles. Pebble sized lag on surface comprised predominantly of nodular carbonate and quartz with minor amphibolite and granitic clasts. Some algae and lichen present on silt/clay and clast surfaces.
Minor: Minor build up of well-sorted red/brown clays to sands around bases of vegetation, and deflation hollows in meter scale patches in some areas defined by consolidated surface fines.
Vegetation: Very open chenopod shrub land with Black and Pearly Blue Bush.

27) Regolith: Yellow/brown, poorly sorted, a pedal silt to clay with sand to boulder sized lithic fragments, quartz and minor opaques and feldspar. Minor carbonate present in nodular and powder forms to pebble sized fraction. Granitic, amphibolite and quartz clasts range in size from course sands to boulders <15cm in diameter with a dominant size range from cobble to boulder.
Landform: Erosional Rise. (er)
Surface: Lag of predominantly cobble sized amphibolite and granitic clasts ranging to boulder sized with minor quartz in the same size fraction present. All heavily iron stained and some minor lichen present on surface of clasts and clay/silt surfaces. Sheet flow dominant process as defined by alignment of surface material and finer lag particles.
Vegetation: Extremely sparse chenopod shrub land with Bassia and Black Blue Bush present.

28) Regolith: Slightly to moderately weathered albitic granitic bedrock. Grain size ranges from medium to very course with some foliation present in areas and other areas of heavily jointed and extremely course muscovite growth. Meter to inch scale quartz veining also present.
Landform: Erosional Low Hill. (el)
Surface: Severe mineral etching and lichen cover of up to 90% on some granite, varying to only slightly etched and no lichen cover in other areas. Moderate iron staining throughout.
Minor: Red/brown, well sorted fine silts to clays with poorly sorted sand to pebble sized lithic fragments and granitic minerals from granite weathering including quartz, feldspar, plagioclase and muscovite.
Vegetation: Very sparse and overgrazed chenopod shrub land with "Bunny ears", Sida, Black Blue Bush, Bassia and unknown tree and bush species.

29) Regolith: Orange/brown, poorly sorted, a pedal silt to clay with sand to cobble sized granitic fragments and quartz with minor opaques and feldspar.
Landform: Erosional Rise (er).
Surface: Major disturbance on/near surface from workings and audits. Surface clasts are dominantly sub angular to angular cobble to small boulder sized and have moderate iron staining and mineral etching. Waste piles and clasts from workings and audits are dense.
Vegetation: Extremely sparse chenopod shrub land with Black Blue Bush present.

30) Regolith: Red/brown, poorly sorted moderately consolidated, a pedal, silt to clay. Significant amount of subangular to angular sand to cobble sized quartz. Minor coarse sand to pebble sized granitic and amphibolite clasts, muscovite and feldspar grains.
Landform: Alluvial plain with minor current alluvial channels (ap).

Surface: Small scale rilling to meter scale incision orientated towards present channels. Patchy minor surface lag of predominantly coarse sand up to boulder sized quartz, amphibolite and granitic clasts.
Vegetation: Overgrazed open chenopod shrub land with Black Blue Bush, and Bathurst Bur present in channel ways and incisions.

32) Regolith: Red/brown, poorly sorted moderately consolidated, a pedal, fine silt to clay. Minor amounts of sand to boulder sized quartz and coarse sand to pebble sized lithic clasts.
Landform: Erosional Rise (er).
Surface: Variable channel to sheet wash flow within the area.
Vegetation: Moderately open chenopod shrub land dominated by Sida, Black Blue Bush and Bathurst Bur.

9. References

Alley, N.F., 1998. Cainozoic stratigraphy, palaeoenvironments and geological evolution of the Lake Eyre Basin. Palaeogeography, Palaeoclimatology, Palaeoecology, 144, 239-263.

Anupam, S., and Rajamani, V., 2000. Major Element, REE, and Other Trace Element Behaviour in Amphibolite Weathering under Semiarid Conditions in Southern India. The Journal of Geology, 108, 487-496.

Aubert, D., Stille, P., and Probst, A., 2001. REE fractionation during granite weathering and removal by waters and suspended loads: Sr and Nd isotopic evidence. Geochimica et Cosmochimica Acta, 65(3), 387-406.

Benton, R.Y., 1994. A Petrological, Geological and Isotopic Investigation of Granitoids from the Olary Province of South Australia – Implications for Proterozoic Crustal Growth. Honours thesis, University of Adelaide.

Berkman, D., 1999. Fiddling with numbers. Australian Laboratory Services, Minerals Division – News, 8(1),

Bowler, J.M., and Wasson, R.J., 1984. Glacial age environments of inland Australia. In: J.C. Vogel (Editor), Late Cainozoic palaeoclimates of the southern hemisphere. Balkema, Rotterdam, pp.183-208.

Callen, R.A., and Tedford, R.H. 1976. New Late Cainozoic rock units and depositional environments, Lake Frome area, South Australia. Transactions of the Royal Society of South Australia, 100, 125-168.

Callen, R.A., 1990. Explanatory notes for the Curnamona 1:250 000 geological map. Geological Survey of South Australia, Adelaide, South Australia.

Campana, B. and King, D., 1958. Regional geology and mineral resources of the Olary Province. Geological Survey of South Australia, Bulletin 34, 133.

Clarke, G.W., Burg, J.P., Wilson, C.J.L., 1986. Stratigraphic and structural constraints of the Proterozoic tectonic history of the Olary Block, South Australia. Precambrian Research, 34, 107-137.

Climatic data for the Yunta region, Bureau of Meteorology web site, visited 24/3/02. www.bom.gov.au

Conor, C., 2001. Curnamona Province Team Field Guide Book. Part 1 Olary Domain. Primary Industries and Resources South Australia, Adelaide, South Australia.

Conor, C.H.H. 2000a. Definition of major sedimentary and igneous units of the Olary Domain, Curnamona Province. MESA Journal 19, 51-56.

Conor, C.H.H., 2000b. Towards a formal lithostratigraphy for the Olary Domain, Curnamona Province, South Australia. In: Peljo, M. (Eitor), Broken Hill Exploration Initiative: abstracts of papers presented at the May 2000, conference in Broken Hill. AGSO Record, 2000/10, 23-26.

Constable, S.A., 1999. Geological mapping and the geochemical and petrological characterisation of the 'Woman-in-White' amphibolite and associated felsic rocks. Honours thesis, University of Adelaide.

Cullers, R.L., Barrett,T., Carlson,R., and Robinson B., 1987, Rare-earth element and mineralogic changes in Honocene soil and stream sediment: a case study in the Wet Mountains, Colorado, U.S.A., Chemical Geology, 63, 275-297.

Cullers, R.L., Basu, A. and Suttner, L.J., 1988. Geochemical signature of provenance in sand-size material in soils and stream sediments near the Tobacco Root Batholith, Montana, U.S.A. Chemical Geology, 70(4), 335-348.

Deer, W.A., Howie, R.A. and Zussman J., 1992. An introduction to the rock forming minerals – second edition. Longman Group, UK.

Eggleton, R.A. (Editor), 2001. The Regolith Glossary – Surficial Geology, Soils and Landscapes. Cooperative Research Centre for Landscape Evolution and Mineral Exploration, National Capital Printing, Canberra.

Ellershaw, A., 2001. Fluid inclusion, petrographic and sulphur isotope investigations into Luxemburg mineral deposits, Curnamona Province, South Australia. Honours thesis, University of Adelaide.

Fanning, P.C., and Holdaway, S.J., 2001. Temporal limits to the archaeological record in arid western New South Wales Australia: Lessons from OSL and radiocarbon dating of hearths and sediments. In: Jones, M., and Sheppard, P. (Editors), Australasian Connections and New Directions: Proceedings of the 7th Australasian Research in Anthropology and Linguistics, 5, p85-104.

Fleet, A.J., 1984, Aqueous and Sedimentary geochemistry of the rare earth elements. In: Henderson, P. (Editor), Rare earth element geochemistry. Elsevier, p343-373.

Hallberg, J.A., 1984. A Geochemical Aid to Igneous Rock Type Identification in Deeply Weathered Terrain. Journal of Geochemical Exploration, 20, 1-8.

Hutton, J.T., 1977. Titanium and zirconium minerals. In: J.B. Dixon and S.B. Weed (Editors), Minerals in Soil Environments. Soil Science Society. America, Madison, Wis., 673-688).

Hill, S., (presenter), 2002. Regolith Mapping Workshop Olary Domain, Luxemburg, South Australia. Cooperative Research Centre for Landscape, Environments and Mineral Exploration report.

Kershaw, A.P., 1978. Record of last interglacial cycle from northeastern Queensland. Nature, 272, 159-161.

Lawie, D., 2001. Exploration Geochemistry and Regolith over the Northern part of the Olary Domain, South Australia. Post Doctorate thesis, University of New England.

Morisawa, M., 1968. Streams - their dynamics and morphology. Earth and Planetary Science Series, McGraw-Hill Inc, New York.

Nesbitt H.W., 1979. Mobility and fractionation of rare earth elements during weathering of a granodiorite. Nature. 279, 206-210.

Nesbitt, H.W., and Wilson, R.E., 1992. Recent chemical weathering of basalts. American Journal of Science. 292, 740-777.

Pain, C., Chan, R., Craig, M., Gibson, D., Ursem, P. and Wilford, J., 2000. RTMAP Regolith Database Field Book and Users Guide (2nd E), CRC LEME Report 138, Canberra.

Pain, C., Graig, M., Gibson, D.L. and Wilford J., 2001. Regolith Landform Mapping: An Australian Approach. In: Bobrowsky, P., Geoenvironmental Mapping, Method, Theory and Practice. A.A. Balkema, Swets and Zeitlinger, Netherlands, 29-56.

Preiss, W.V. and Conor, C.H.H., 2001. Origin and nomenclature of the Willyama Inlier, Curnamona Province. MESA Journal, 21, 47-49.

Robinson, R.S., Preiss W.V., Crooks, A.F., Hill, P.W.and Sheard M.J. 1998. Review of the Proterozoic geology and mineral potential of the Curnamona Province in South Australia. AGSO Journal of Australian Geology and Geophysics, 17(3), 169-182.

Rollinson, H.R., 1993. Using Geochemical Data: evaluation, presentation, interpretation. Longman Group UK Limited.

Rutherford. N., Cohen, D., 2002. New Approaches to Detecting Geochemical Anomalies. SMEDG-AIG Symposium 2002 “Exploration in the Shadow of the Headframe”, Shore School, NSW.

Stephen, T.D., 2001. Insights into mineralisation of the Luxemburg Mine Area, Olary, South Australia, from geological mapping, strain and microstructural analysis, and geophysics. Honours thesis, University of Adelaide.

Teutsch, N., Erel, Y., Halicz, L. and Chadwick, O.A., 1999. The influence of rainfall on metal concentrations and behavior in the soil. Geochimica er Cosmochimica Acta, 63(22), 3499-3511.

Thomas, D.S.G., 1989. Extensions of the arid realm. In:Thomas, D.S.G., (Editor), Arid Zone Geomorphology, Belhaven Press, London.

Van der Weijden C. H., van der Weijden R. D., 1995. Mobility of major, minor and some redox-sensitive trace elements and rare-earth elements during weathering of four granitoids in central Portugal. Chemical Geology, 125, 149-167.

Williams M.A.J., 1994a. Some implications of past climatic changes in Australia. Transactions of the Royal Society of South Australia, 118(1), 17-25.

Williams M.A.J., 1994b. Cenozoic climatic changes in deserts: A synthesis. In: Abrahams, D., and Parsons, A., (Editors), Geomorphology of Desert Environments. Chapman and Hall, New York, 644-670.

Wood, D.A., Tarney, J., Varet, J., Saunders, A.D., Bougault, H., Joron, J.L., Treuil, M., Cann, J.R., 1979. Geochemistry of basalts drilled in the North Atlantic by IPOD Leg 49: implications for mantle heterogeneity. Earth and Planetary Science Letters, 42, 77-97.

10. Tables

Grain size analysis results

Sample ID Particle size as %	PEM (LO2 AK 53)	Massive Unit (LO2 AK 54)	Pedal Unit (LO2 AK 55)	2031-02ave	2031-5.5ave	2031-09ave
CO3 as CaCO3	0.10	0.10	0.33	0.02	0.29	0.18
Clay	33.43	9.09	40.09	6.53	5.63	6.69
Silt	13.48	9.32	4.38	2.26	1.54	1.54
Fine Sand	44.73	43.55	20.49	18.56	23.53	21.87
Coarse Sand	4.89	35.01	29.23	71.45	67.77	67.66
Total	96.53	96.97	94.19	98.80	98.47	97.76

Table 1.

Drill Core Samples		Drillhole 2									Drillhole 3		
		2031-2-33	2031-2-34	2031-2-35	2031-2-37	2031-2-38	2031-2-39	2031-2-41	2031-2-42	2031-2-43	2031-3-45	2031-3-46	2031-3-48
	Depth (cm)	0-25	25-84	84-105	105-120	120-141	141-160	160-183	183-214	214-225	0-33	33-106	106-166
	Ave depth	12.5	54.5	94.5	112.5	130.5	150.5	171.5	198.5	219.5	16.5	69.5	136
XRF	ELEMENT												
	Major wt%												
	SiO2	64.21	62.40	60.25	67.47	59.53	58.01	52.03	47.91	44.69	74.47	68.27	63.94
	Al2O3	12.88	13.64	12.76	11.67	10.93	10.02	7.23	5.50	4.54	10.91	12.73	12.79
	Fe2O3T	6.63	8.08	9.03	7.02	11.03	12.47	16.03	15.13	16.49	3.58	6.10	6.62
	MnO	0.06	0.07	0.08	0.07	0.10	0.11	0.16	0.18	0.20	0.04	0.06	0.06
	MgO	2.42	3.70	4.61	3.19	5.93	7.00	10.08	13.98	15.34	1.81	1.92	2.39
	CaO	3.55	2.57	3.78	2.28	4.27	4.66	7.32	10.80	12.54	1.54	1.52	3.56
	Na2O	2.25	2.12	2.01	2.61	2.41	2.09	1.45	1.10	1.07	3.53	1.66	2.22
	K2O	1.99	1.76	1.55	1.75	1.32	1.16	0.69	0.32	0.10	1.52	1.93	1.99
	TiO2	0.74	0.87	0.94	0.85	1.16	1.29	1.93	1.53	1.69	0.44	0.67	0.73
	P2O5	0.08	0.08	0.08	0.11	0.07	0.07	0.08	0.09	0.10	0.07	0.07	0.08
	SO3	0.06	0.02	0.04	0.00	0.01	0.01	0.01	0.02	0.01	0.00	0.02	0.06
	LOI	5.13	4.14	4.51	2.60	2.86	2.64	2.54	3.18	3.03	1.57	4.45	5.05
	Total	99.99	99.45	99.65	99.62	99.63	99.53	99.56	99.74	99.81	99.47	99.40	99.48
	Trace (ppm)												
	Zr	226.0	177.7	166.5	210.0	162.0	183.3	135.6	99.6	79.6	130.1	176.3	190.8
	Nb	21.7	16.9	17.5	18.7	27.2	28.3	31.7	22.1	21.6	12.6	13.1	15.1
	Y	32.1	27.7	23.7	29.4	22.4	30.7	24.0	14.3	11.8	21.6	30.4	36.4
	Sr	122.8	160.0	191.7	124.2	166.9	171.4	266.0	287.1	319.9	95.8	113.9	142.7
	Rb	88.3	80.7	71.8	77.7	64.6	62.4	36.2	18.4	5.4	53.0	88.9	91.4
	U	2.3	1.1	1.8	2.3	2.4	1.2	2.6	0.3	0.7	2.0	1.7	2.1
	Th	15.2	12.8	12.6	13.4	11.8	13.5	8.2	8.8	6.8	10.9	15.2	16.9
	Pb	14.7	14.1	22.6	14.4	10.7	16.2	12.1	5.4	1.0	7.7	11.6	12.7
	Ga	16.5	19.9	20.1	15.8	17.4	15.6	13.6	11.8	11.1	14.1	17.4	18.0
	Cu	49	57	51	47	58	73	72	92	120	21	41	40
	Zn	58	66	69	55	70	75	93	108	107	29	57	55
	Ni	90	99	123	85	173	222	319	489	513	48	44	55
	Ba	301	267	451	281	258	215	203	121	33	246	290	379
	Sc	14.6	17.4	16.9	14.1	20.0	21.7	26.4	33.5	40.3	7.8	13.6	14.3
	Co	50	36	43	51	50	56	73	91	98	61	25	33
	V	120	139	148	116	177	193	272	206	259	58	110	106
	Ce	87	81	69	81	76	87	70	65	55	62	80	87
	Nd	34	33	29	32	27	35	32	26	22	25	35	35
	La	42	38	33	39	32	42	30	30	25	27	39	40
	Cr	341	342	468	330	690	842	1153	1380	1787	177	145	201

Table 2.

Whole Rock Samples		LUXEMBURG AMPHIBOLITE						BASSO GRANITES (from Benton, 1994)						BIMBOWRIE GRANITES (from Benton, 1994)						
XRF	ELEMENT			2031	2031	2031	2031						Basso	Bimbowrie	Bimbowrie	Bimbowrie	Bimbowrie	Bimbowrie	Bimbowrie	Bimbowrie
	Major wt%	2031-2001	2031-2002	-R010	-R017	-AB005	-AB006	Basso017	Basso026	Basso079	Basso087	Basso091	ZA001206	-054	-055	-009	-012	-015	-040	-103
	SiO2	38.61	48.60	41.94	42.97	44.06	44.60	78.14	77.29	76.96	77.37	77.12	76.00	72.22	71.22	72.64	71.66	75.34	72.23	73.29
	Al2O3	4.88	7.39	5.43	6.60	6.47	6.38	11.77	11.67	11.51	11.94	11.83	11.10	14.95	15.00	14.68	15.10	14.02	14.90	14.46
	Fe2O3T	17.87	14.96	20.89	16.80	15.87	16.89	1.43	3.51	2.14	2.15	2.25	2.30	1.74	2.29	1.98	2.01	0.98	1.59	1.48
	MnO	0.40	0.22	0.40	0.23	0.20	0.28	0.01	0.00	0.01	0.01	0.00	0.00	0.01	0.01	0.02	0.01	0.01	0.02	0.01
	MgO	11.15	10.94	12.31	13.12	13.73	12.71	1.15	0.41	1.72	0.92	1.14	1.35	0.45	0.62	0.42	0.54	0.27	0.46	0.32
	CaO	16.72	10.74	12.02	10.26	12.83	12.87	0.11	0.06	0.08	0.11	0.08	0.08	0.50	0.56	0.50	0.57	0.35	0.60	0.31
	Na2O	0.60	0.80	0.75	0.39	0.86	1.04	6.04	6.59	5.26	6.60	6.23	5.90	3.68	4.70	3.51	3.55	3.96	4.35	3.57
	K2O	0.40	1.15	0.57	3.51	0.92	0.44	0.91	0.24	1.74	0.46	0.77	0.92	5.26	4.14	4.90	5.17	4.18	5.01	5.07
	TiO2	1.70	2.25	2.08	2.34	2.35	2.49	0.19	0.18	0.18	0.18	0.18	0.31	0.25	0.38	0.23	0.38	0.11	0.23	0.15
	P2O5	0.13	0.17	0.11	0.16	0.17	0.15	0.01	0.01	0.01	0.01	0.01	0.02	0.18	0.13	0.23	0.16	0.19	0.17	0.14
	SO3	0.45	0.36	0.04	0.11	0.03	0.16	0.01	0.01	0.00	0.00	0.00		0.00	0.00	0.00	0.00	0.00	0.00	0.00
	LOI	6.79	1.48	2.14	2.71	2.08	1.73	0.23	0.16	0.29	0.26	0.25	0.45	0.75	0.76	0.83	0.81	0.68	0.47	0.78
	Total	99.69	99.05	98.67	99.21	99.58	99.73	99.97	100.11	99.88	99.99	99.85		99.99	99.81	99.93	99.95	100.08	100.02	99.57
	Trace (ppm)																			
	Zr	99.60	135.20	103.60	192.10	143.30	191.70	337.60	379.80	432.20	523.70	468.30	630.00	167.30	256.80	158.00	220.90	71.20	139.90	89.10
	Nb	23.60	40.10	28.80	54.10	54.90	53.50	83.10	80.30	93.10	86.7	86.90	75.00	17.70	18.00	24.20	32.50	18.90	19.30	22.10
	Y	35.40	21.30	20.40	17.90	16.40	16.70	115.40	90.10	196.60	251.90	178.50	140.00	26.20	85.50	28.60	21.60	12.60	26.20	35.50
	Sr	251.80	82.80	97.50	120.50	199.20	107.80	18.52	22.50	12.30	13.40	14.80	20.00	37.93	47.54	35.07	33.68	26.46	56.26	24.10
	Rb	27.80	72.50	41.90	207.90	55.60	14.80	126.43	32.27	171.00	36.00	57.20	110.00	369.12	263.89	444.31	397.80	339.19	406.71	285.00
	U	4.30	2.90	2.60	2.80	0.20	3.50	11.20	15.2	10.70	3.90	7.20	7.50	6.80	10.50	16.90	17.20	6.50	21.60	3.90
	Th	6.80	9.80	7.00	14.00	9.30	15.30	37.40	41.8	39.30	44.40	43.00	40.00	46.10	73.40	40.90	88.90	19.60	46.60	27.50
	Pb	1.60	0.80	3.90	1.90	3.10	1.40	5.70	9.2	6.70	5.40	8.30	4.00	31.80	28.90	26.10	25.50	21.70	33.10	13.90
	Ga	14.10	15.50	12.00	15.60	9.40	13.00	28.50	27.60	27.30	31.60	29.20	35.00	20.40	19.50	23.60	21.20	19.00	20.70	20.70
	Cu	1094.00	1813.00	741.00	14.00	196.00	19.00	0.00	5.00	0.00	6.00	1.00	0.00	4.00	8.00	6.00	1.00	8.00	5.00	7.00
	Zn	106.00	140.00	147.00	181.00	109.00	137.00	5.00	9.00	12.00	2.00	8.00	60.00	40.00	38.00	47.00	36.00	19.00	53.00	12.00
	Ni	389.00	297.00	491.00	467.00	445.00	403.00	1.00	0.00	12.00	0.00	3.00	30.00	1.00	4.00	0.00	0.00	0.00	10.00	0.00
	Ba	63.00	110.00	136.00	282.00	103.00	32.00	321.00	329.00	39.00	25.00	42.00	70.00	279.00	367.00	212.00	25.00	270.00	299.00	201.00
	Sc	32.90	31.70	61.60	32.20	33.90	47.60	4.80	3.40	4.60	4.40	5.00	5.00	2.90	5.50	3.90	9.50	4.90	3.50	4.20
	Co	58.00	72.00	63.00	78.00	84.00	93.00	46.10	44.00	40.40	86.80	53.90	50.00	76.00	44.90	95.20	44.70	39.90	74.30	110.10
	V	212.00	340.00	318.00	371.00	322.00	355.00	22.60	25.10	19.40	3.70	3.00	20.00	18.30	29.90	18.70	2.30	22.20	18.90	8.00
	Ce	52.00	120.00	31.00	106.00	80.00	113.00	153.00	162.00	66.00	132.00	155.00	115.00	85.00	296.00	76.00	188.00	112.00	116.00	46.00
	Nd	17.00	43.00	22.00	37.00	34.00	48.00	43.64	43.64	43.64	43.64	102.00	135.00	30.00	76.00	21.60	107.00	57.00	59.00	24.00
	La	24.00	59.00	15.00	57.00	35.00	63.00	72.00	68.00	26.00	57.00	67.00	40.00	21.00	68.00	19.00	85.00	48.00	68.00	22.00
	Cr	1377.00	1023.00	4295.00	1390.00	1181.00	1020.00	2.00	2.00	4.00	1.00	5.00	0.00	7.00	8.00	7.00	1.00	3.00	46.00	1.00

Table 3.

Stream Samples		SURFACE													
	ELEMENT														
XRF	*Major wt%*	2031-01S	2031-02S	2031-03S	2031-04S	2031-3.5U	2031-05S	2031-5.5U	2031-06S	2031-6.33U	2031-6.66U	2031-07S	2031-7.5U	2031-08S	2031-9U
	SiO2	64.69	70.38	67.74	70.23	64.17	60.94	70.95	70.43	70.14	67.34	41.53	72.52	72.29	70.80
	Al2O3	11.30	12.32	12.61	11.58	10.55	10.30	11.56	11.68	10.90	11.26	6.64	11.45	11.43	10.62
	Fe2O3T	8.56	4.82	5.63	4.39	12.47	16.85	5.20	5.74	7.17	8.86	38.78	4.28	4.02	7.23
	MnO	0.08	0.06	0.06	0.05	0.08	0.08	0.05	0.05	0.05	0.07	0.16	0.04	0.04	0.05
	MgO	3.85	2.73	3.10	3.13	2.58	2.07	2.04	2.11	1.97	2.32	2.47	1.93	2.11	1.98
	CaO	3.08	2.16	2.35	2.89	2.37	1.97	1.85	1.97	2.01	2.22	2.32	1.97	2.19	1.76
	Na2O	3.22	3.89	2.72	4.20	3.70	3.57	3.92	3.91	3.77	3.76	2.04	3.91	4.04	3.46
	K2O	1.48	1.71	1.81	1.44	1.36	1.35	1.52	1.61	1.54	1.57	0.91	1.68	1.62	1.61
	TiO2	1.05	0.56	0.66	0.53	1.02	1.12	0.55	0.61	0.63	0.77	2.32	0.48	0.43	0.63
	P2O5	0.08	0.08	0.07	0.08	0.09	0.09	0.07	0.07	0.08	0.08	0.12	0.07	0.07	0.07
	SO3	0.02	0.01	0.01	0.01	0.01	0.01	0.00	0.00	0.01	0.00	0.00	0.00	0.01	0.00
	LOI	2.14	1.54	2.98	1.18	1.21	1.29	1.46	1.41	1.28	1.28	0.67	1.36	1.31	1.25
	Total	99.56	100.26	99.76	99.56	99.74	99.64	99.17	99.60	99.56	99.53	97.95	99.70	99.57	99.46
	Trace														
	Zr	194.30	136.80	151.40	109.20	148.10	131.20	136.10	162.40	120.30	135.10	147.10	129.00	109.50	125.70
	Nb	25.90	13.50	13.40	14.90	23.20	24.10	14.00	15.00	16.40	18.70	52.00	13.20	11.80	17.20
	Y	26.45	16.50	22.30	21.30	55.80	58.00	31.40	31.30	37.50	43.10	178.50	23.70	22.60	35.40
	Sr	155.65	129.60	134.20	120.90	113.00	107.40	104.20	106.80	104.60	112.10	97.90	108.00	107.50	104.70
	Rb	66.75	60.40	69.70	48.60	50.90	52.00	53.70	55.20	55.60	57.40	42.00	57.10	53.30	56.20
	U	2.05	1.60	2.10	1.50	3.40	1.70	2.50	1.30	2.70	1.10	5.80	1.10	2.00	1.00
	Th	12.85	9.30	11.70	8.30	17.10	20.70	12.80	12.20	17.70	18.80	49.90	10.10	10.20	13.80
	Pb	10.40	9.00	8.20	6.80	7.50	5.90	9.90	8.50	6.80	7.80	13.70	7.10	4.70	7.60
	Ga	14.40	15.30	15.60	13.40	15.40	16.90	15.50	14.10	13.50	16.50	15.80	15.20	13.10	14.80
	Cu	66.00	25.00	54.00	28.00	28.00	42.00	24.00	24.00	26.00	26.00	52.00	20.00	22.00	22.00
	Zn	56.00	32.00	44.00	27.00	35.00	34.00	27.00	26.00	26.00	29.00	64.00	23.00	21.00	25.00
	Ni	93.50	71.00	80.00	75.00	97.00	113.00	53.00	60.00	60.00	74.00	225.00	47.00	52.00	61.00
	Ba	292.50	293.00	310.00	263.00	256.00	274.00	257.00	305.00	269.00	278.00	228.00	291.00	278.00	261.00
	Sc	17.05	12.50	14.20	13.20	11.20	11.70	8.50	9.70	8.60	9.80	15.80	8.30	8.90	8.40
	Co	35.00	33.00	32.00	33.00	38.00	36.00	54.00	39.00	45.00	54.00	60.00	44.00	31.00	54.00
	V	144.50	82.00	96.00	77.00	161.00	210.00	83.00	86.00	101.00	131.00	609.00	64.00	65.00	102.00
	Ce	87.50	72.00	71.00	65.00	105.00	132.00	73.00	71.00	106.00	91.00	324.00	58.00	69.00	78.00
	Nd	36.00	29.00	31.00	28.00	46.00	60.00	32.00	31.00	46.00	40.00	146.00	27.00	30.00	36.00
	La	42.50	34.00	34.00	30.00	50.00	64.00	33.00	35.00	52.00	44.00	169.00	29.00	32.00	37.00
	Cr	380.00	243.00	266.00	301.00	693.00	908.00	281.00	319.00	361.00	510.00	2419.00	216.00	235.00	363.00
IC-PMS															
detection limit															
1.00	Au*	3.00	1.00	5.00	2.00	<1	<1	<1	2.00	<1	<1	<1	<1	<1	<1
0.05	Ag	<0.05	<0.05	<0.05	<0.05	<0.05	0.20	<0.05	<0.05	<0.05	<0.05	<0.05	<0.05	<0.05	<0.05
0.50	As	1.5	1	1.5	1	1	1	1	1	1	1	2	0.5	0.5	1
0.10	Bi	0.2	0.1	0.2	<0.1	0.2	0.2	0.1	0.1	0.2	0.2	0.3	<0.1	0.1	0.1
0.10	Cd	<0.1	<0.1	<0.1	<0.1	<0.1	<0.1	<0.1	<0.1	<0.1	<0.1	<0.1	<0.1	<0.1	<0.1
0.20	Co	18	10.5	13	9	16.5	19.5	9	9.5	9	11.5	32.5	7.5	7	8.5
0.20	Cu	39.5	16.5	33.5	17	18.5	18.5	15.5	15	18.5	15	21	14.5	13	15
0.10	Mo	0.3	0.3	0.3	0.3	0.5	0.5	0.3	0.3	0.3	0.3	0.9	0.2	0.3	0.3
1.00	Ni	30	32	40	28	62	80	29	31	32	35	125	24	26	26
0.20	Pb	4.4	3.3	4.2	2.6	3.3	3.6	2.7	2.7	2.3	2.5	4.8	2.3	2.2	2.4
0.10	Sb	<0.1	<0.1	<0.1	<0.1	<0.1	<0.1	<0.1	<0.1	<0.1	<0.1	<0.1	<0.1	<0.1	<0.1
0.50	Se	<0.5	<0.5	<0.5	<0.5	<0.5	<0.5	<0.5	<0.5	<0.5	<0.5	0.5	<0.5	<0.5	<0.5
0.10	Te	<0.1	<0.1	<0.1	<0.1	<0.1	<0.1	<0.1	<0.1	<0.1	<0.1	<0.1	<0.1	<0.1	<0.1
0.02	U	0.82	0.71	0.53	0.55	0.82	0.89	0.63	0.59	0.6	0.66	1.5	0.57	0.6	0.7
0.50	Zn	22	16.5	21.5	13	14.5	17.5	14	12	11	11.5	20.5	11.5	10	11.5

Table 4a. **(all trace and IC-PMS concentrations measured in parts per million excluding Au which is measured in parts per billion)*

Stream Samples		LOWER												
ELEMENT														
Major wt%	2031-01M	2031-02M	2031-03M	2031-04M	2031-3.5L	2031-05M	2031-5.5L	2031-06M	2031-6.33L	2031-6.66L	2031-07M	2031-7.5L	2031-08M	2031-9L
SiO2	64.68	70.53	66.20	66.74	48.72	57.63	70.30	71.01	61.65	69.33	57.57	67.13	66.13	72.68
Al2O3	11.84	12.20	11.23	11.18	8.07	9.38	11.86	12.10	10.07	11.37	9.19	10.12	10.48	10.92
Fe2O3T	7.78	4.58	7.69	9.37	29.84	20.75	5.65	4.67	14.73	7.74	21.05	9.08	10.36	6.22
MnO	0.08	0.05	0.07	0.06	0.13	0.10	0.04	0.04	0.09	0.05	0.10	0.08	0.07	0.04
MgO	3.87	2.48	3.21	2.45	2.80	2.44	1.94	1.96	2.93	1.99	2.38	3.27	2.79	1.19
CaO	3.12	2.12	3.34	2.26	2.42	2.17	1.91	1.91	2.81	1.79	2.22	2.99	2.69	1.22
Na2O	3.14	3.99	3.45	3.87	2.75	3.14	4.15	4.13	3.44	3.78	3.10	3.49	3.42	3.49
K2O	1.53	1.60	1.53	1.43	1.02	1.22	1.64	1.65	1.33	1.60	1.28	1.41	1.47	1.79
TiO2	0.91	0.50	0.76	0.72	1.84	1.32	0.51	0.48	1.17	0.65	1.37	0.88	1.00	0.61
P2O5	0.09	0.09	0.08	0.08	0.10	0.10	0.07	0.07	0.09	0.08	0.09	0.08	0.08	0.07
SO3	0.02	0.02	0.02	0.02	0.00	0.01	0.01	0.01	0.01	0.00	0.01	0.00	0.01	0.00
LOI	2.59	1.55	2.20	0.68	1.57	1.03	1.41	1.48	1.02	1.28	0.94	1.13	1.27	1.15
Total	99.65	99.70	99.76	98.37	99.74	99.29	99.50	99.51	99.34	99.66	99.26	99.65	99.78	99.36
Trace														
Zr	176.10	131.10	127.30	114.50	142.70	149.30	126.40	117.60	137.50	127.20	126.90	119.30	137.50	148.60
Nb	22.30	13.40	18.90	17.20	43.90	27.90	13.40	12.80	26.70	15.10	30.00	21.60	24.10	16.70
Y	22.30	18.90	22.90	31.60	127.40	64.10	26.60	24.50	70.20	33.30	73.20	36.90	37.80	37.30
Sr	157.90	134.80	144.80	115.60	105.60	108.30	107.70	110.00	122.80	102.80	105.70	116.70	114.30	96.30
Rb	70.00	56.50	56.80	50.10	42.40	49.90	56.40	55.80	49.20	57.30	50.40	49.80	52.70	61.20
U	2.30	1.30	1.60	1.20	2.90	1.50	0.80	1.50	1.10	1.10	2.60	2.20	2.40	2.50
Th	13.70	10.20	11.60	11.20	36.70	23.10	11.30	11.80	20.40	15.00	26.70	14.60	13.30	14.20
Pb	12.60	7.30	8.00	6.30	14.80	9.90	7.70	7.00	9.00	6.00	10.00	6.30	7.00	6.90
Ga	13.20	15.40	13.90	14.40	20.50	15.60	15.30	14.30	14.70	14.00	14.40	14.60	15.40	14.40
Cu	66.00	26.00	35.00	32.00	51.00	46.00	23.00	22.00	33.00	25.00	36.50	27.00	30.00	21.00
Zn	55.00	31.00	36.00	30.00	58.00	43.00	26.00	23.00	40.00	30.00	39.50	33.00	31.00	24.00
Ni	97.00	68.00	96.00	88.00	186.00	138.00	54.00	53.00	116.00	63.00	133.50	94.00	88.00	36.00
Ba	290.00	285.00	284.00	268.00	238.00	269.00	264.00	296.00	262.00	272.00	260.50	247.00	283.00	287.00
Sc	17.50	11.60	13.10	11.90	13.90	12.70	8.70	9.70	12.40	9.20	12.30	12.40	12.60	6.60
Co	32.00	32.00	32.00	29.00	58.00	39.00	55.00	31.00	50.00	38.00	42.50	54.00	35.00	36.00
V	135.00	76.00	110.00	120.00	486.00	264.00	86.00	71.00	218.00	112.00	280.00	133.00	137.00	84.00
Ce	88.00	72.00	73.00	89.00	239.00	151.00	71.00	68.00	135.00	84.00	175.00	84.00	90.00	77.00
Nd	36.00	28.00	33.00	40.00	106.00	67.00	30.00	30.00	58.00	36.00	81.50	39.00	42.00	35.00
La	45.00	34.00	37.00	43.00	116.00	74.00	34.00	33.00	63.00	40.00	87.50	39.00	45.00	40.00
Cr	360.00	243.00	434.00	470.00	1860.00	1090.00	305.00	257.00	976.00	416.00	1185.00	544.00	534.00	256.00
Au*	2.00	3.00	2.00	1.00	2.00	2.00	<1	1.00	<1	<1	<1	2.00	1.00	<1
Ag	<0.05	<0.05	<0.05	<0.05	<0.05	0.05	<0.05	<0.05	<0.05	<0.05	0.10	<0.05	<0.05	<0.05
As	2	1	0.5	1.5	1	1	1	1	1.5	1	1.5	1	1	1
Bi	0.2	0.1	0.1	0.2	0.2	0.2	<0.1	<0.1	0.2	0.1	0.2	0.2	0.2	0.1
Cd	<0.1	<0.1	<0.1	<0.1	<0.1	<0.1	<0.1	<0.1	<0.1	<0.1	<0.1	<0.1	<0.1	<0.1
Co	14	8.5	11.5	18.5	29	21	9	8	17	11.5	26	18.5	13.5	7.5
Cu	40	16	18.5	24.5	22.5	18	13	14.5	17	15.5	20.5	18.5	16.5	12
Mo	0.3	0.3	0.3	0.4	0.9	0.6	0.3	0.3	0.4	0.3	0.7	0.5	0.4	0.3
Ni	34	29	44	67	110	88	30	26	64	37	120	48	46	23
Pb	4.8	2.8	3.4	3.3	4.4	3.9	2.5	2.5	3	2.8	4.5	3	3.2	2.5
Sb	<0.1	<0.1	<0.1	<0.1	<0.1	<0.1	<0.1	<0.1	<0.1	<0.1	<0.1	<0.1	<0.1	<0.1
Se	<0.5	<0.5	<0.5	<0.5	<0.5	<0.5	<0.5	<0.5	<0.5	<0.5	<0.5	<0.5	<0.5	<0.5
Te	<0.1	<0.1	<0.1	<0.1	<0.1	<0.1	<0.1	<0.1	<0.1	<0.1	<0.1	<0.1	<0.1	<0.1
U	0.64	0.67	0.6	0.7	1.15	0.89	0.59	0.61	0.78	0.64	1.25	0.78	0.75	0.64
Zn	23	14	15	16	19	18	11.5	11.5	13	13	20.5	12	14.5	12.5

Table 4b.

11. Figure captions

Figure 1. Location diagram and general solid geology, Olary Domain. (adapted from Conor, 2000)

Figure 2. Relationship of Willyama Supergroup and contemporary igneous suites, Olary Domain (adapted from Connor, 2000a.)

Figure 3. Sample types and locations within the study area.

Figure 4. Spidergram plot for lithologies and channel sediments present in the study area.

Figure 5a Regolith profile at stream sample location 01.

Figure 5b Regolith profile near drill core 2

Figure 5c Regolith profile near drill core 3

Figure 6. Crude grain size distribution within units of the Luxemburg regolith profile.

Figure 7. Amphibolite Harker Plot for the major rock forming oxides, showing regression co-efficients (R^2).

Figure 8a Lithological discrimination plot for Na and K against Al oxides.

Figure 8b Lithological discrimination plot for Ca and Mg oxides.

Figure 9. Plot of Ti versus Zr for lithologies present within the study area. Solid lines denote boundaries between Mafic, Intermediate and Felsic fields. Open symbols represent average values, dashed oval indicates region where channel sediments fall. (adapted from Hallberg, 1983, p4)

Figure 10a Amphibolite and mining sensitive element concentrations with depth in regolith profile from drill hole 2 (major regolith units identified). Mining sensitive elements represented with dashed lines. Note logarithmic scale used for concentration values.

Figure 10b. Amphibolite and mining sensitive element concentrations with depth in regolith profile from drill hole 3 (major regolith units identified). Mining sensitive elements represented with dashed lines. Note logarithmic scale used for concentration values.

Figure 10c. Granite sensitive element concentrations with depth in regolith profile from drill hole 2. Major regolith units are marked. Note logarithmic scale used for concentration values.

Figure 10d. Granite sensitive element concentrations with depth in regolith profile from drill hole 3 Major regolith units are marked. Note logarithmic scale used for concentration values.

Figure 10e. MgO and CaO concentrations with depth in regolith profile from drill hole 2. Major regolith units are marked. Note logarithmic scale used for concentration values.

Figure 10f. MgO and CaO concentrations with depth in regolith profile from drill hole 3. Major regolith units are marked. Note logarithmic scale used for concentration values.

Figure 11a. Longitudinal profile of the Luxemburg channel, indicating the six zones of notable slope change.

Figure 11b. Crude grain size distribution along Luxemburg channel.

Figure 12a. Ca v Mg for channel sediments

Figure 12b. Ca/Mg v Si for channel sediments

Figure 12c. Ca/Mg v Al for channel sediments

Figure 12d. Ca/Mg v Fe for channel sediments

Figure 13a. V v Cr for channel sediments

Figure 13b. (Cr+V)/FeO for channel sediments

Figure 14a. Th v P203 for channel sediments

Figure 14b. K2O and NaO v Al2O3 for channel sediments

Figure 14c. oxides v Fe2O3T wt % for channel sediments

Figure 15a. Chrondrite normalized (La/Sc) versus Titanium (ppm) for lithologies and channel sediments. (normalized using Wood et al. 1979b). Open symbols indicate sample averages.

Figure 15b. Chrondrite normalized (La/Sc) versus Zirconium (ppm) for lithologies and channel sediments (normalized using Wood et al. 1979b). Open symbols indicate sample averages.

Figure 15c. Chrondrite normalized (La/Sc) versus Thorium (ppm) for lithologies and channel sediments (normalized using Wood et al. 1979b). Open symbols indicate sample averages.

Figure 16a. Copper, Gold and Zinc concentrations with distance along the channel, dashed lines represent detection limits. Primary axis represents detection limits and gold values, secondary axis represents copper and zinc values.

Figure 16b. Lead, Uranium and Cobalt concentrations with distance along the channel, dashed lines represent detection limits. Primary axis represents detection limits and lead and uranium values, secondary axis represents cobalt values.

Figure 17. Iron, Chromium and Vanadium concentrations with distance along the drainage channel. Primary axis represents iron and the sum of chromium and vanadium. Secondary axis represents the (Cr+V)/Fe index for elemental fractionation within heavy minerals along the drainage channel.

Figures 18a-h. Harker plots for major oxides within channel sediments, all showing linear relationships.

Figure 19. Simplified chronologies of late Quaternary wet and dry phases in Australia. Adapted from Thomas (1989, p327.

12. Figures

12. Figures

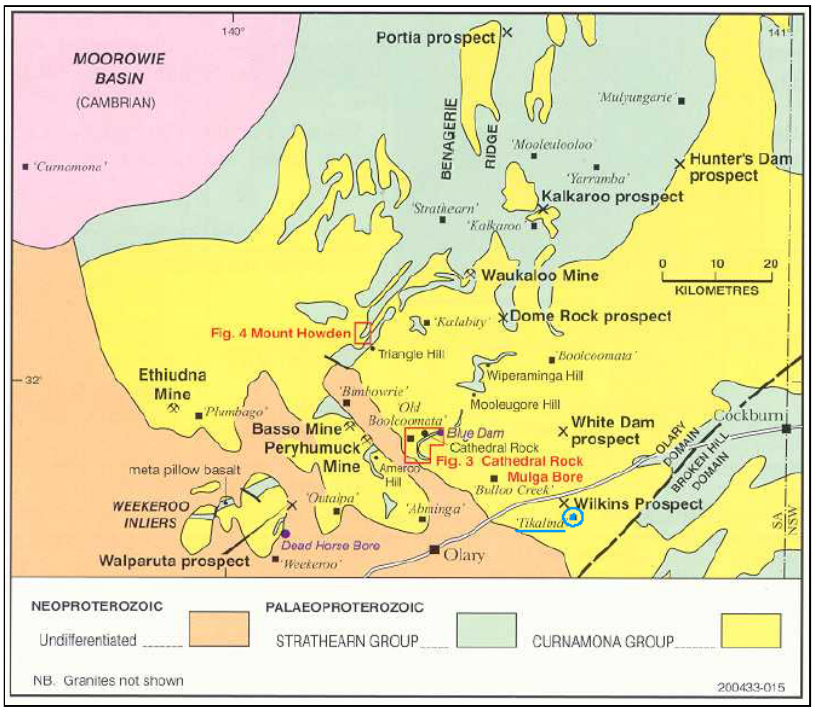

Figure 1a.

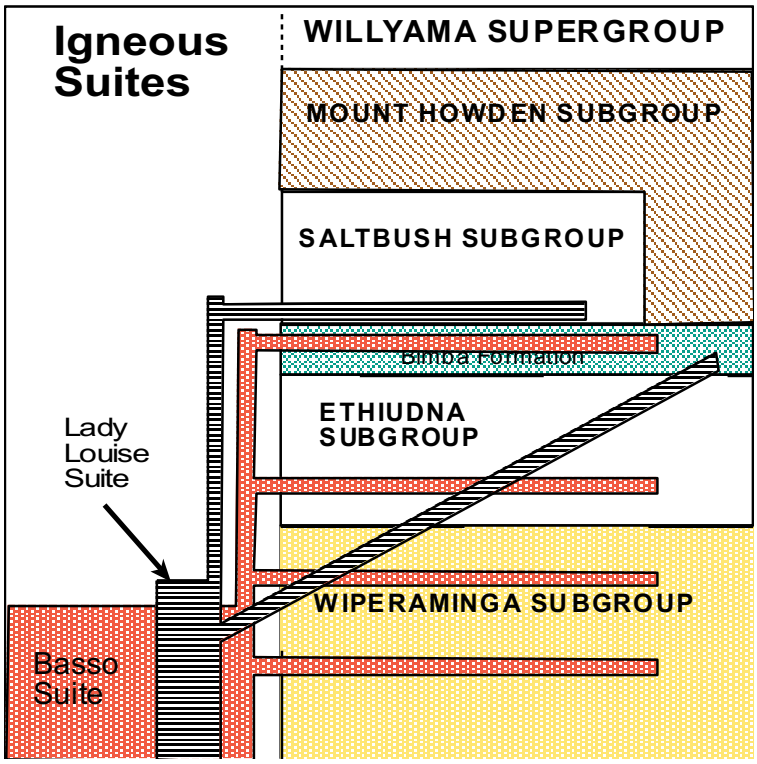

Figure 2a.

Point Sample Locations - Luxemburg Mine Site, Olary Domain, South Australia

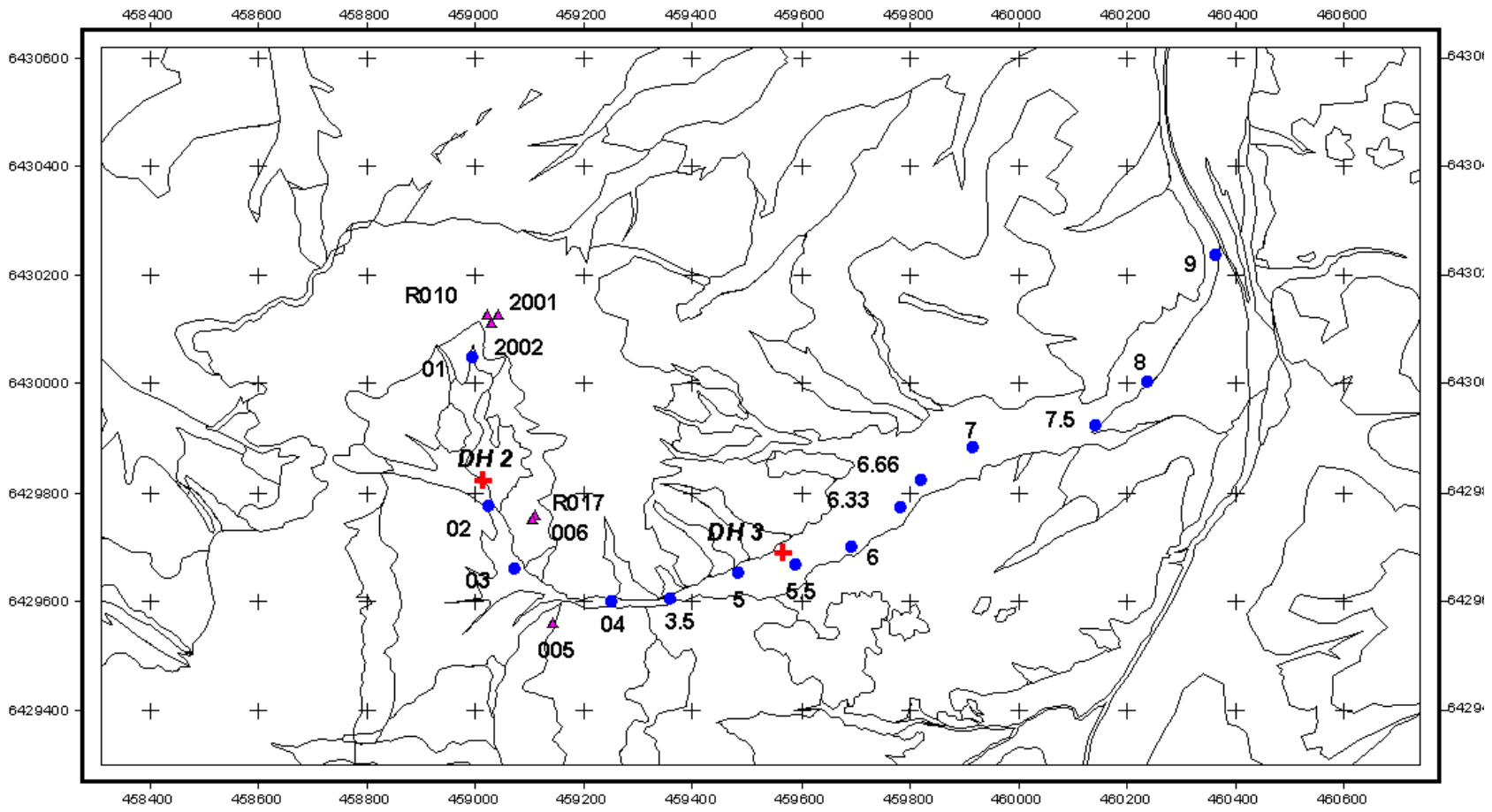

Mapped and Compiled By
Kernich, A and Brown, A
2002

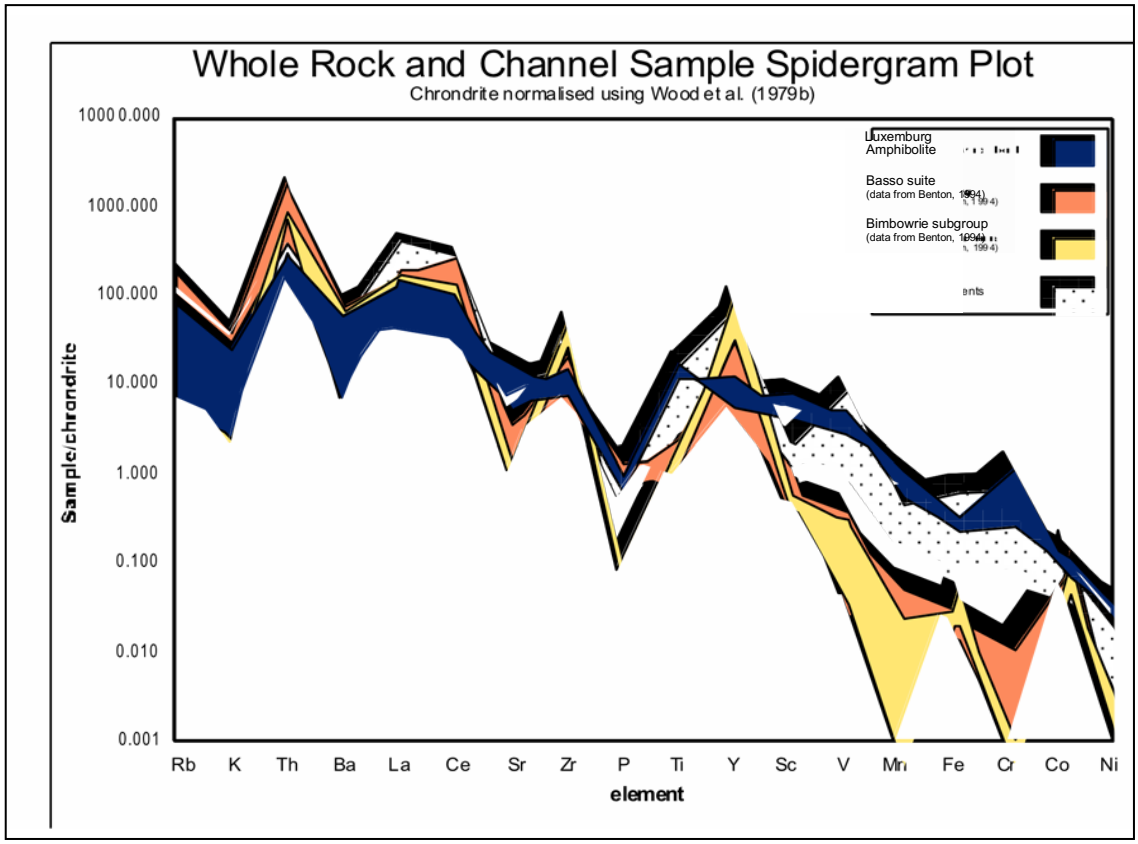

Figure 4a.

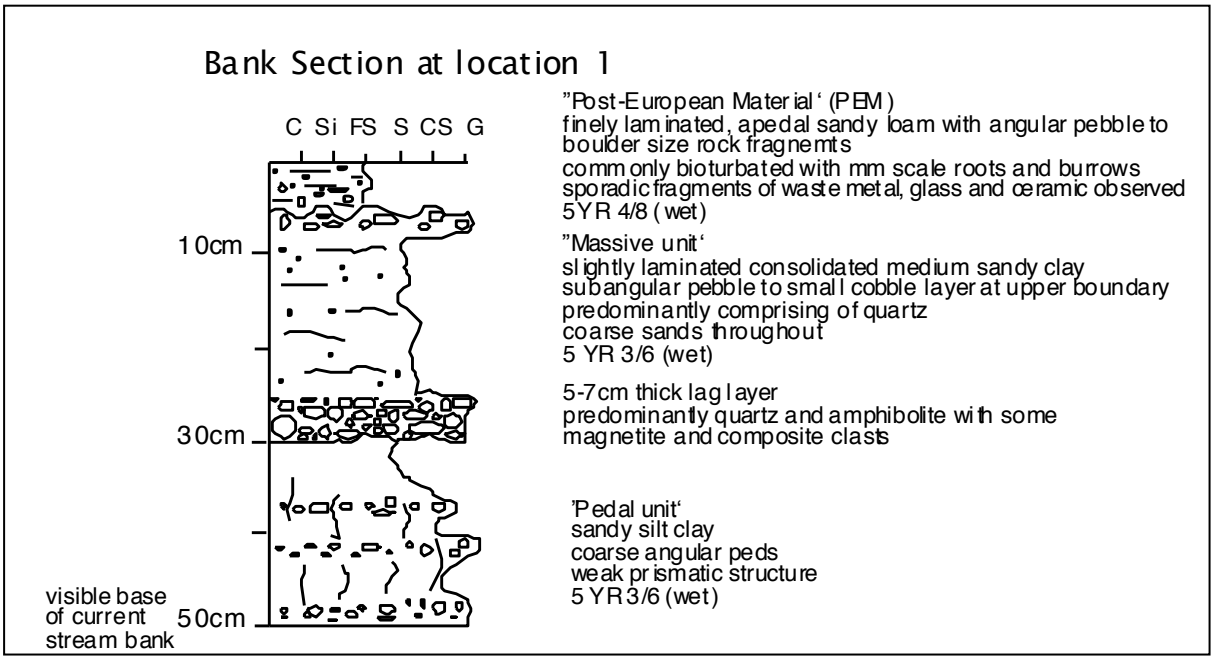

Figure 5a.

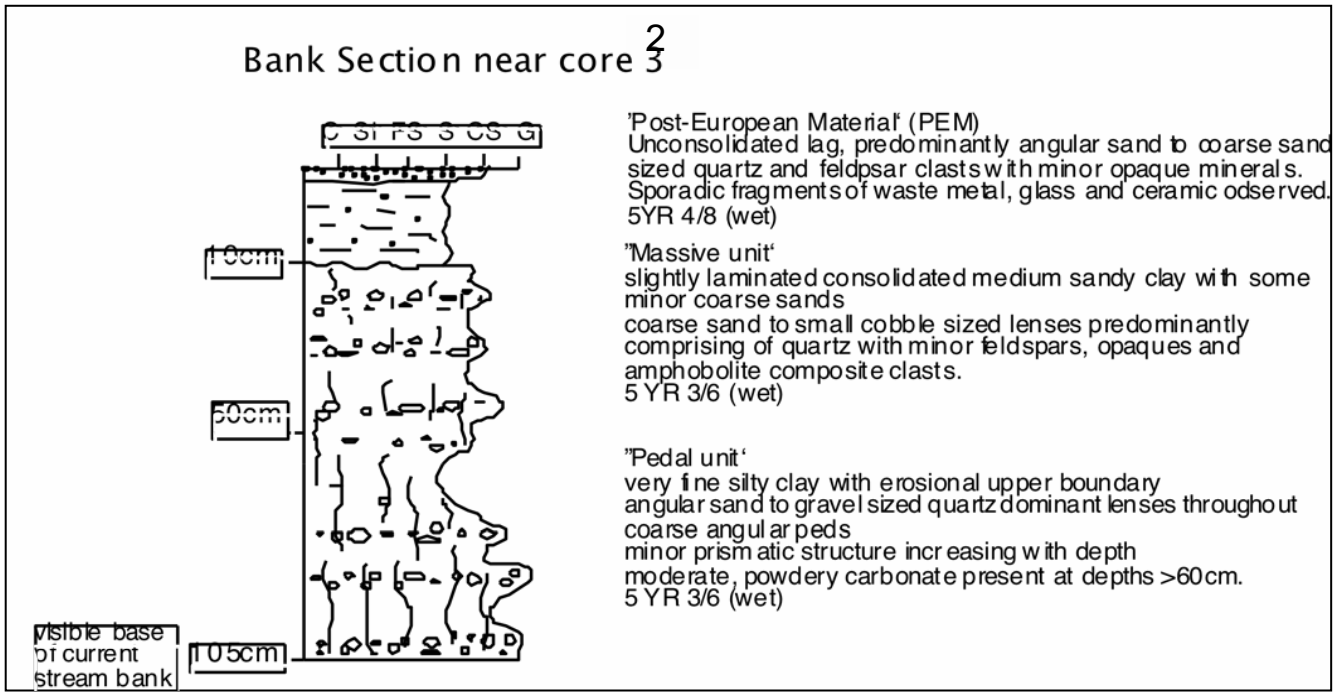
Bank Section near core 2
C Si Fs S CS G
100cm
50cm
105cm
visible base of current stream bank
'Post-European Material' (PEM)
Unconsolidated lag, predominantly angular sand to coarse sand sized quartz and feldpsar clasts with minor opaque minerals.
Sporadic fragments of waste metal, glass and ceramic odserved.
5YR 4/8 (wet)
'Massive unit'
slightly laminated consolidated medium sandy clay with some minor coarse sands
coarse sand to small cobble sized lenses predominantly comprising of quartz with minor feldspars, opaques and amphobolite composite clasts.
5 YR 3/6 (wet)
'Pedal unit'
very fine silty clay with erosional upper boundary
angular sand to gravel sized quartz dominant lenses throughout
coarse angular peds
minor prismatic structure increasing with depth
moderate, powdery carbonate present at depths >60cm.
5 YR 3/6 (wet)

Fi

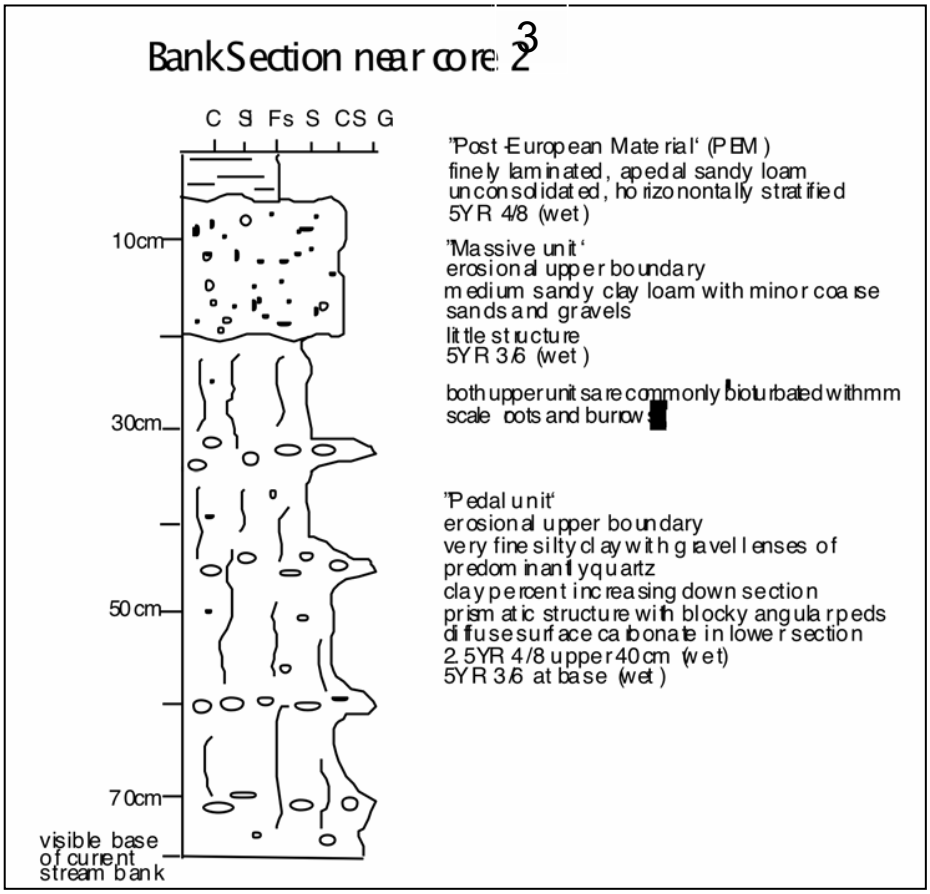
Bank Section near core 3
C Si Fs S CS G
10cm
30cm
50cm
70cm
visible base of current stream bank
'Post-European Material' (PEM)
finely laminated, apedal sandy loam
unconsolidated, horizonontally stratified
5YR 4/8 (wet)
'Massive unit'
erosional upper boundary
medium sandy clay loam with minor coarse sands and gravels
little structure
5YR 3/6 (wet)
both upper units are commonly bioturbated with mm scale roots and burrows
'Pedal unit'
erosional upper boundary
very fine silty clay with gravel lenses of predominantly quartz
clay percent increasing down section
prismatic structure with blocky angular peds
diffuse surface carbonate in lower section
2.5YR 4/8 upper 40cm (wet)
5YR 3/6 at base (wet)

Fi

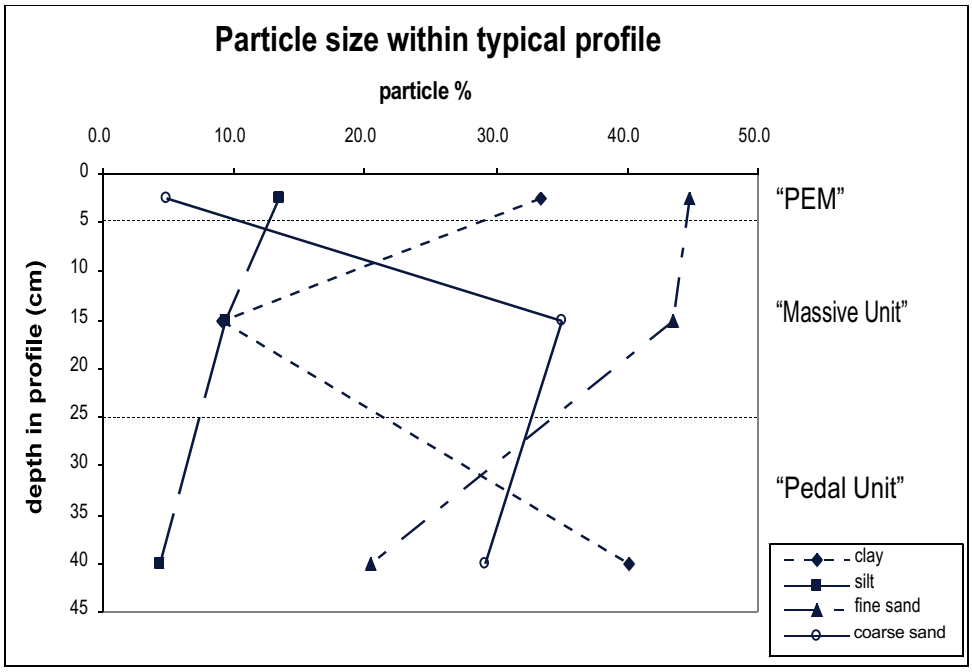

Figure 6a.

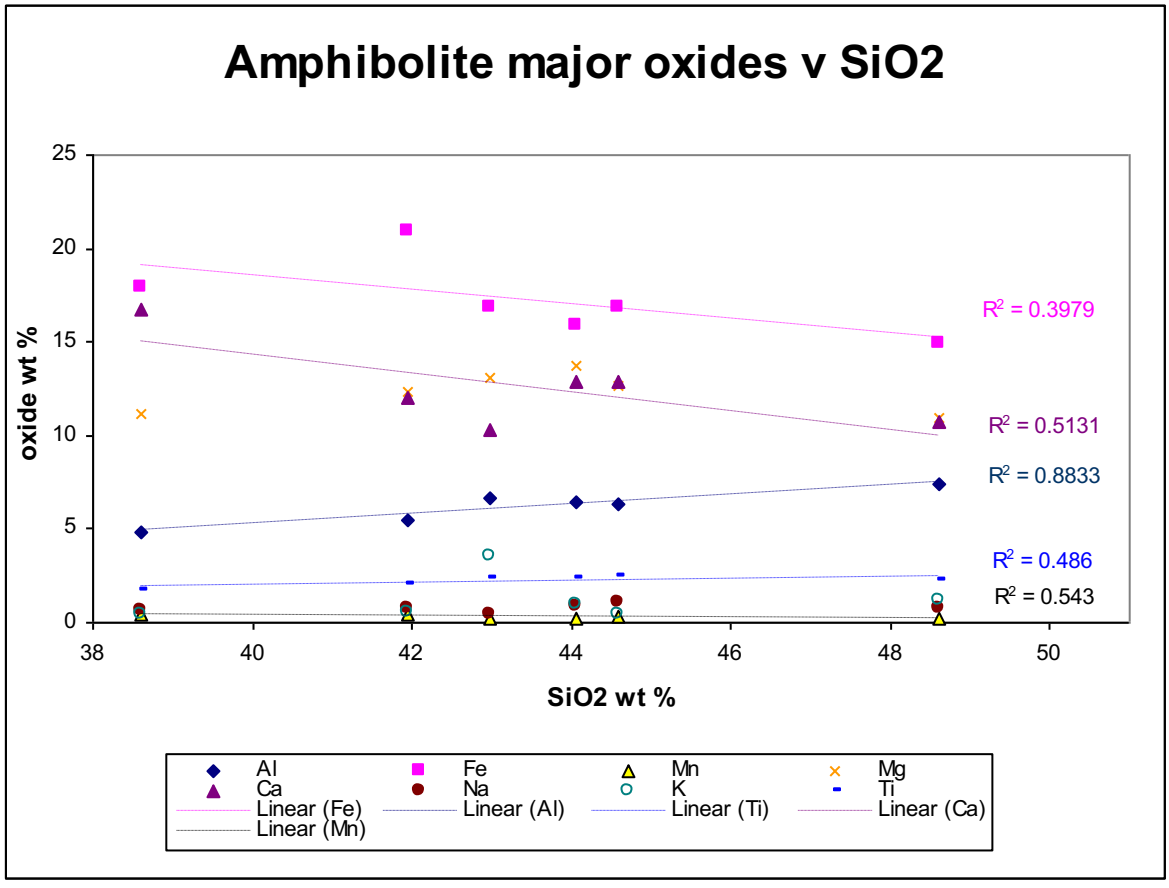

Figure 7a.

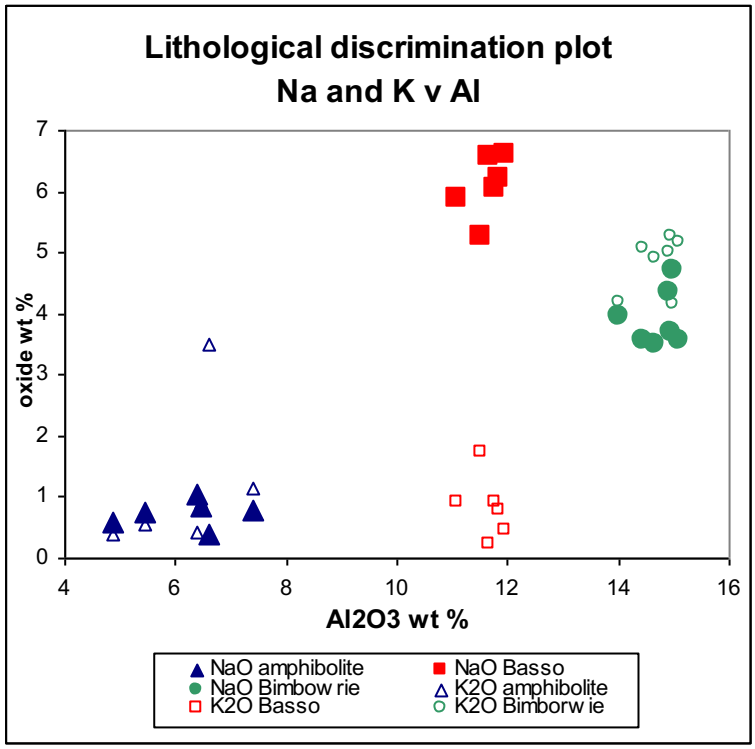
Lithological discrimination plot
Na and K v Al
oxide wt %
Al2O3 wt %
0
1
2
3
4
5
6
7
4
6
8
10
12
14
16
NaO amphibolite
NaO Basso
NaO Bimbow rie
K2O amphibolite
K2O Basso
K2O Bimborw ie

Figure 8a.

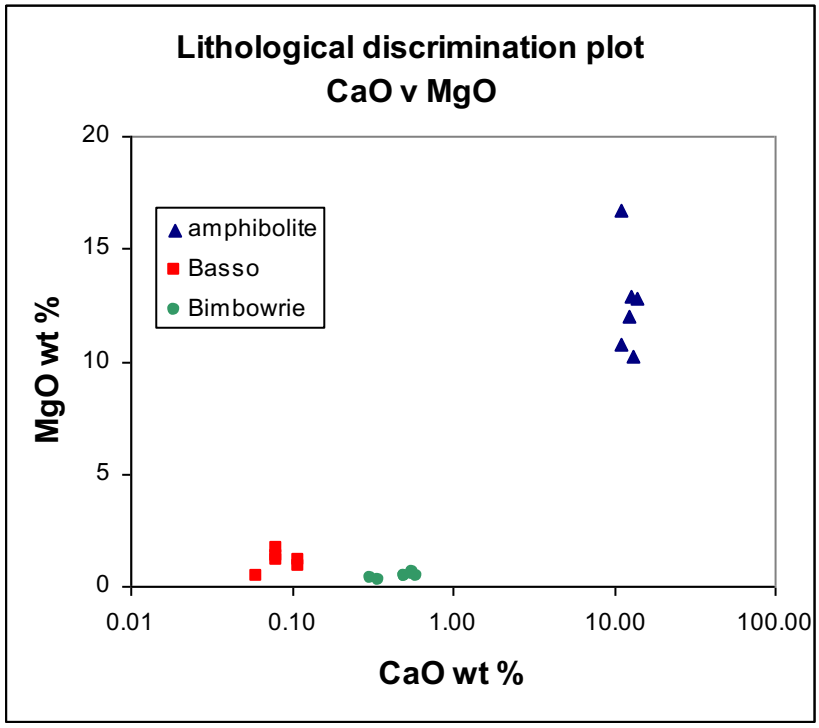
Lithological discrimination plot
CaO v MgO
MgO wt %
CaO wt %
0
5
10
15
20
0.01
0.10
1.00
10.00
100.00
amphibolite
Basso
Bimbowrie

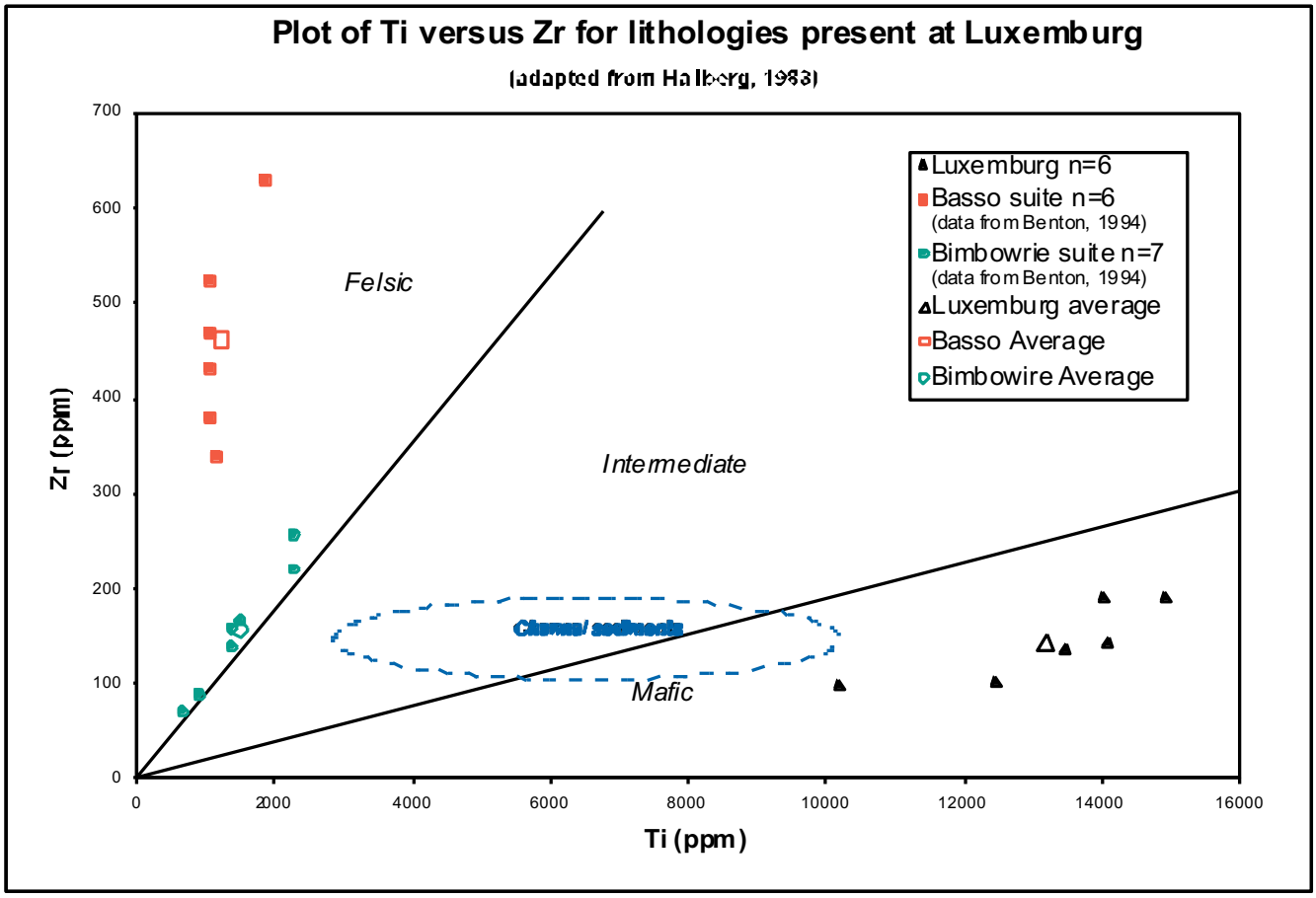
Plot of Ti versus Zr for lithologies present at Luxemburg
(adapted from Halberg, 1983)
Zr (ppm)
Ti (ppm)
Felsic
Intermediate
Mafic
Clasts/ sediments
Luxemburg n=6
Basso suite n=6
(data from Benton, 1994)
Bimbowrie suite n=7
(data from Benton, 1994)
Luxemburg average
Basso Average
Bimbowire Average

Fi

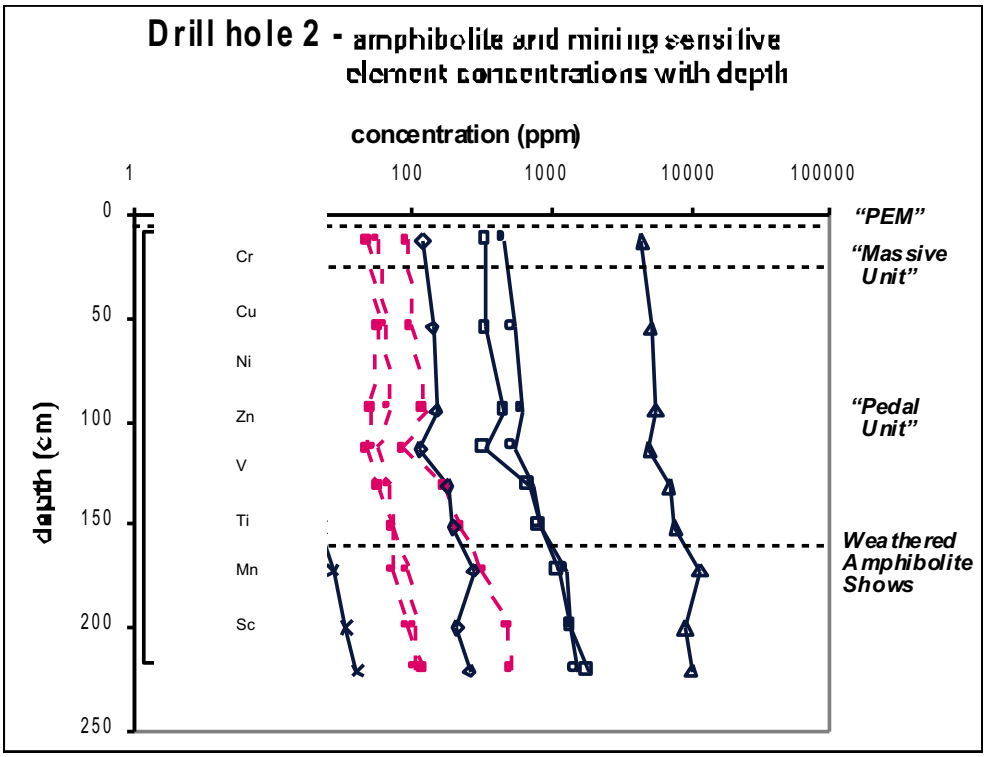
Drill hole 2 - amphibolite and mining sensitive element concentrations with depth
concentration (ppm)
depth (cm)
Cr
Cu
Ni
Zn
V
Ti
Mn
Sc
"PEM"
"Massive Unit"
"Pedal Unit"
Weathered Amphibolite Shows

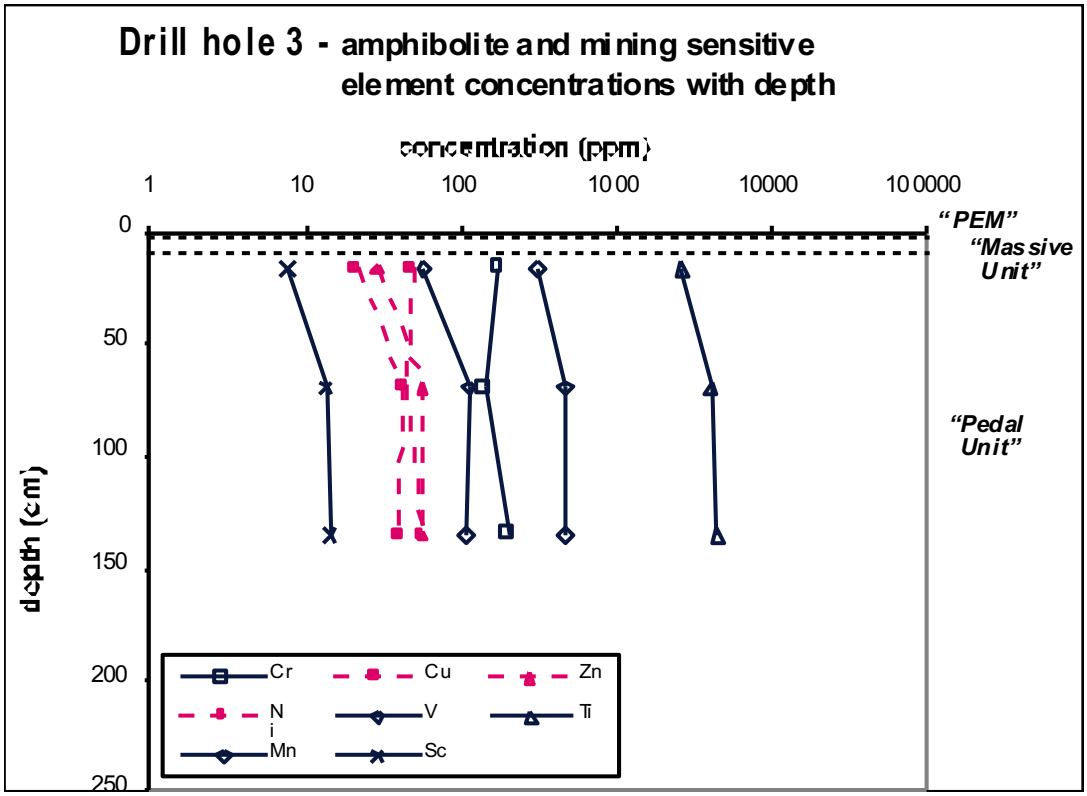
Drill hole 3 - amphibolite and mining sensitive element concentrations with depth
concentration (ppm)
1
10
100
1000
10000
100000
depth (cm)
0
50
100
150
200
250
"PEM"
"Massive Unit"
"Pedal Unit"
Cr
Cu
Zn
Ni
V
Ti
Mn
Sc

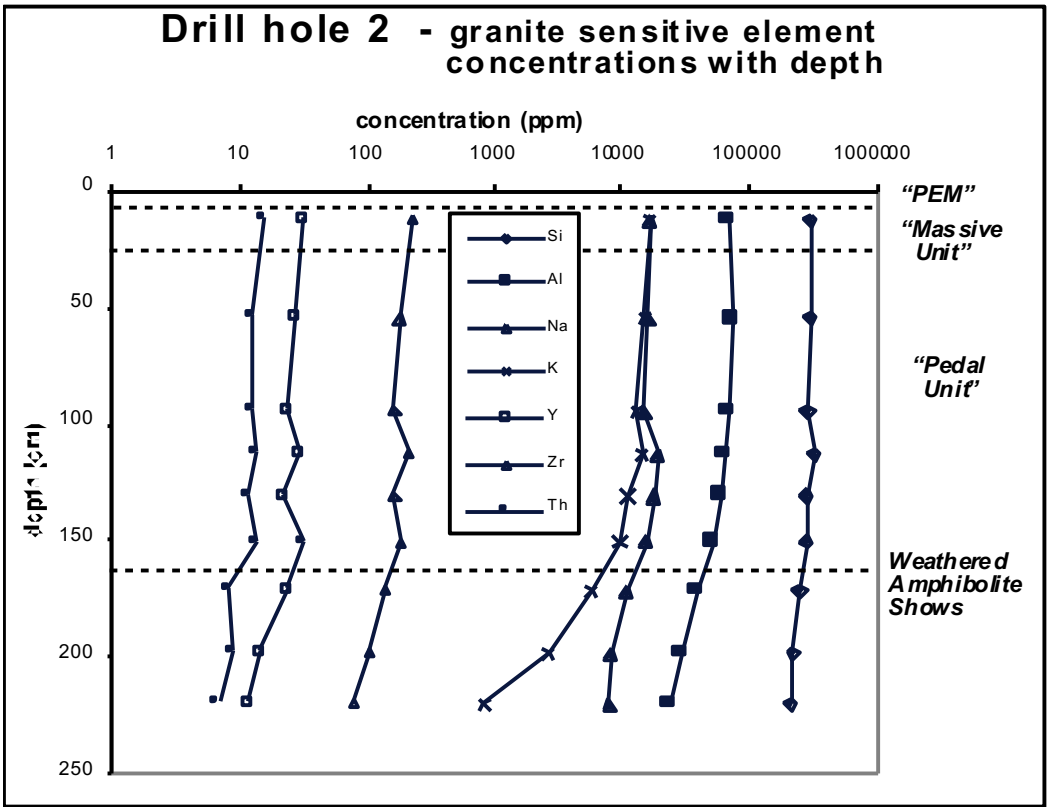
Drill hole 2 - granite sensitive element concentrations with depth
concentration (ppm)
1
10
100
1000
10000
100000
1000000
depth (cm)
0
50
100
150
200
250
"PEM"
"Massive Unit"
"Pedal Unit"
Weathered Amphibolite Shows
Si
Al
Na
K
Y
Zr
Th

Figure 10c.

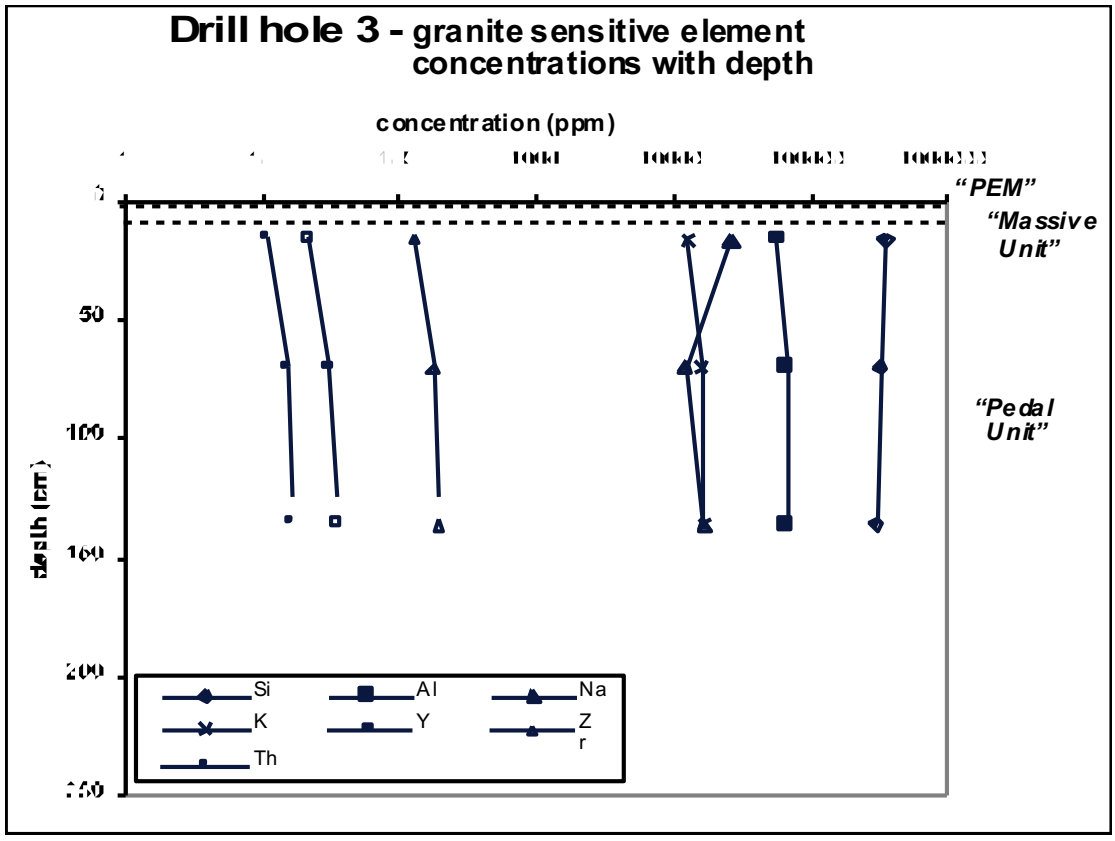
Drill hole 3 - granite sensitive element concentrations with depth
concentration (ppm)
depth (cm)
50
100
150
200
"PEM"
"Massive Unit"
"Pedal Unit"
Si
Al
Na
K
Y
Zr
Th

Figure 10d.

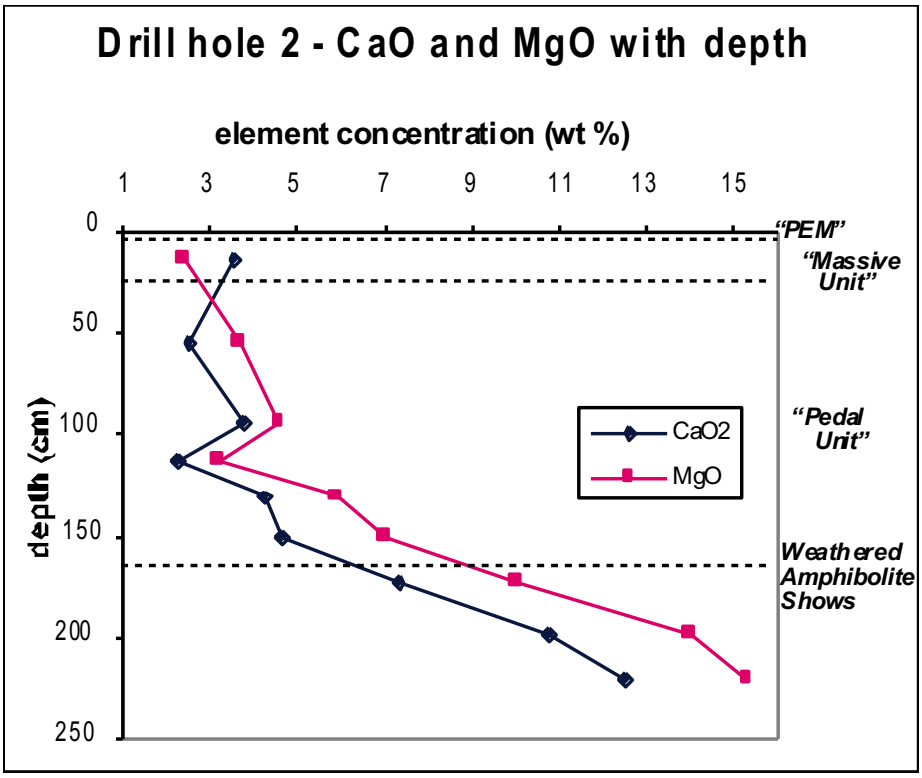
Drill hole 2 - CaO and MgO with depth
element concentration (wt %)
1
3
5
7
9
11
13
15
depth (cm)
0
50
100
150
200
250
"PEM"
"Massive Unit"
"Pedal Unit"
Weathered Amphibolite Shows
CaO2
MgO

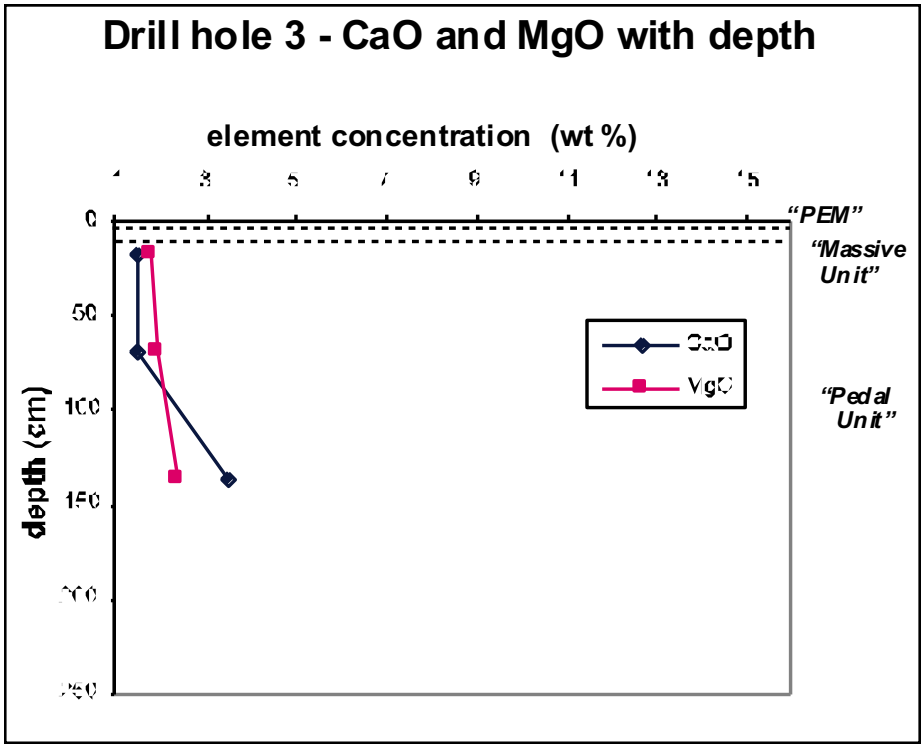

Figure 10f.

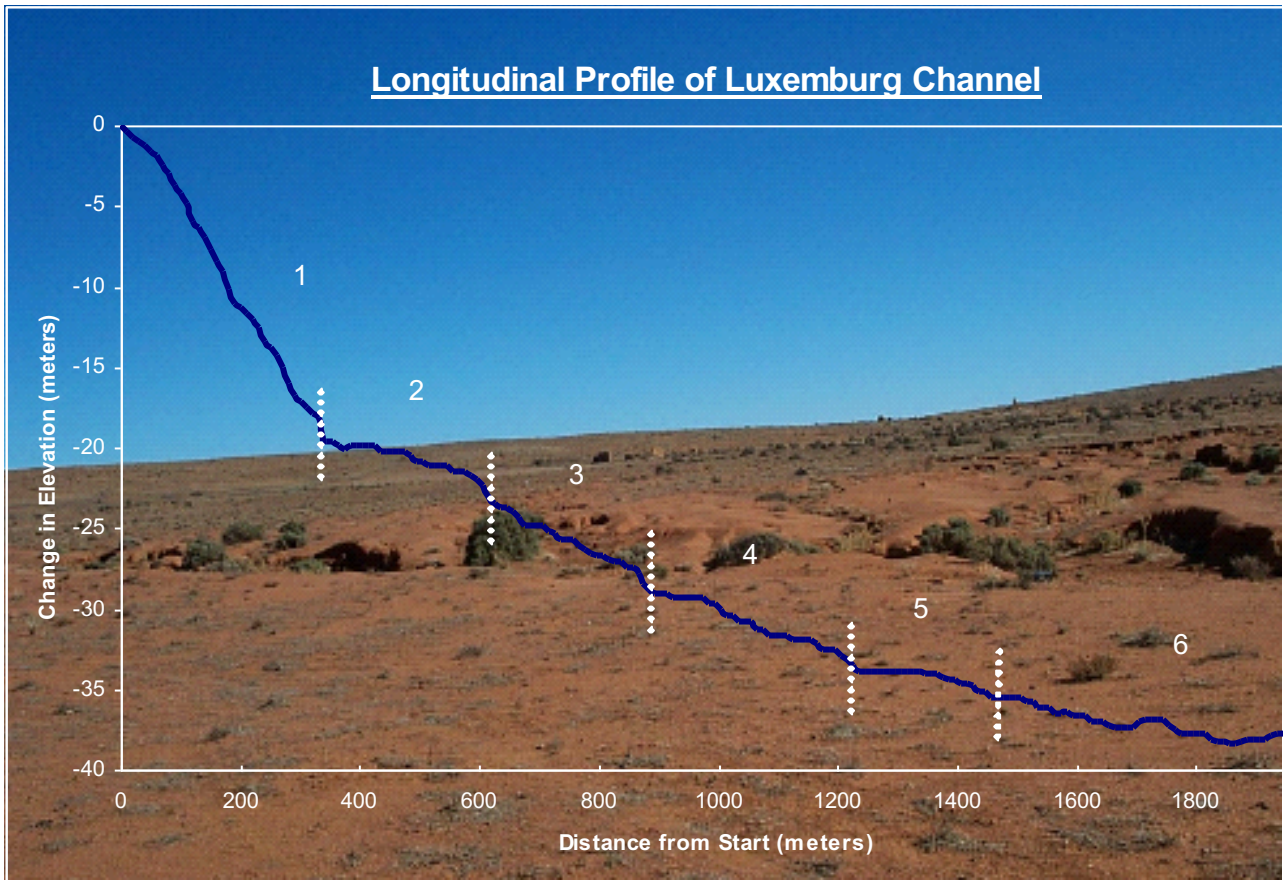

Figure 11a.

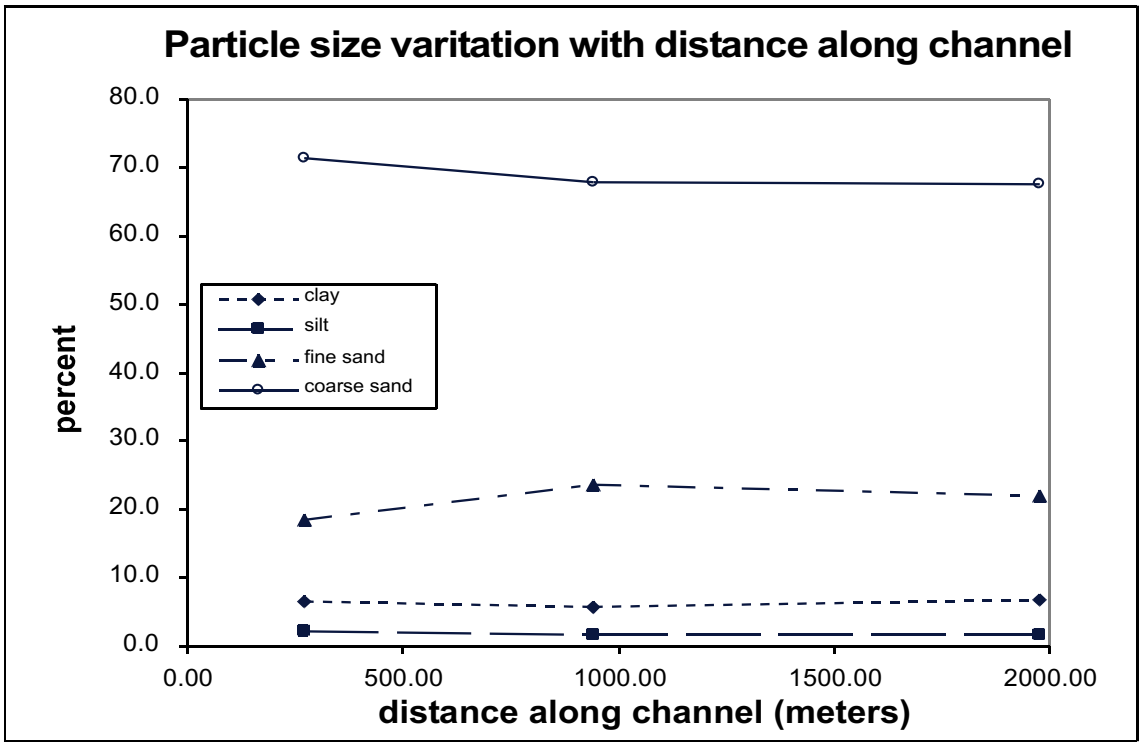
Particle size varitation with distance along channel
80.0
70.0
60.0
50.0
40.0
30.0
20.0
10.0
0.0
percent
clay
silt
fine sand
coarse sand
0.00
500.00
1000.00
1500.00
2000.00
distance along channel (meters)

Figure 11b.

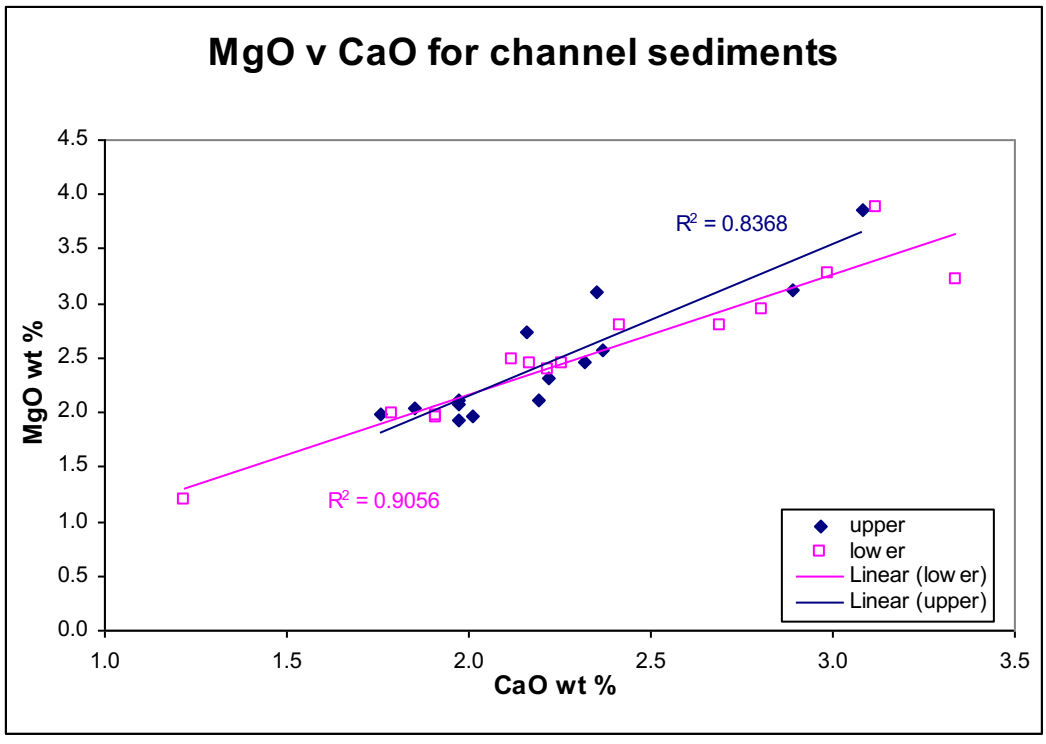
MgO v CaO for channel sediments
4.5
4.0
3.5
3.0
2.5
2.0
1.5
1.0
0.5
0.0
MgO wt %
R2 = 0.8368
R2 = 0.9056
upper
low er
Linear (low er)
Linear (upper)
1.0
1.5
2.0
2.5
3.0
3.5
CaO wt %

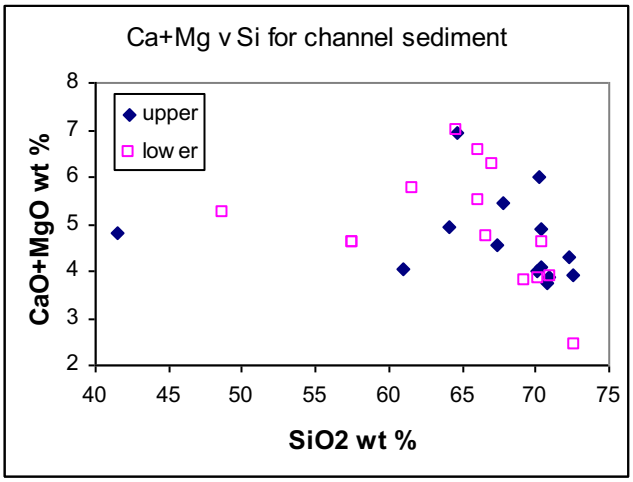

Figure 12b.

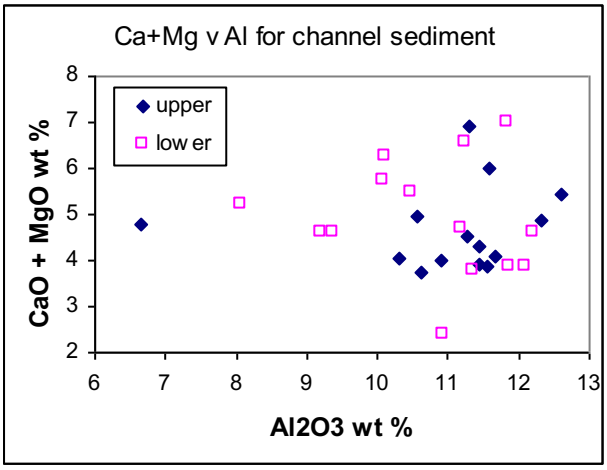

Figure 12c.

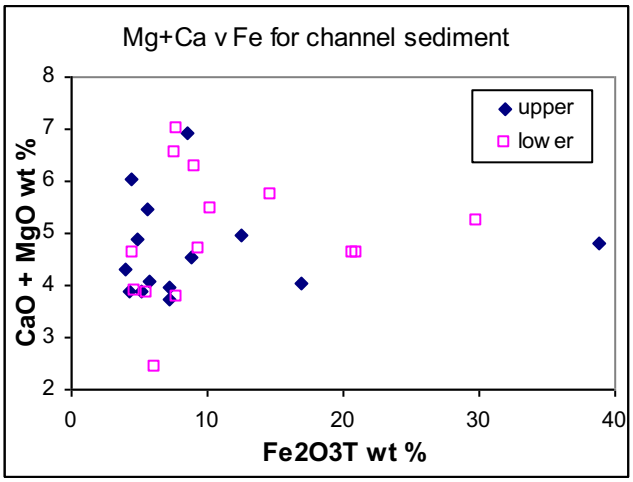

Fi

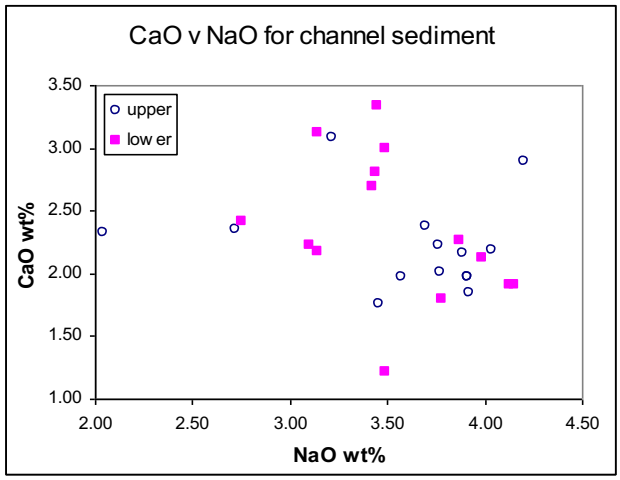

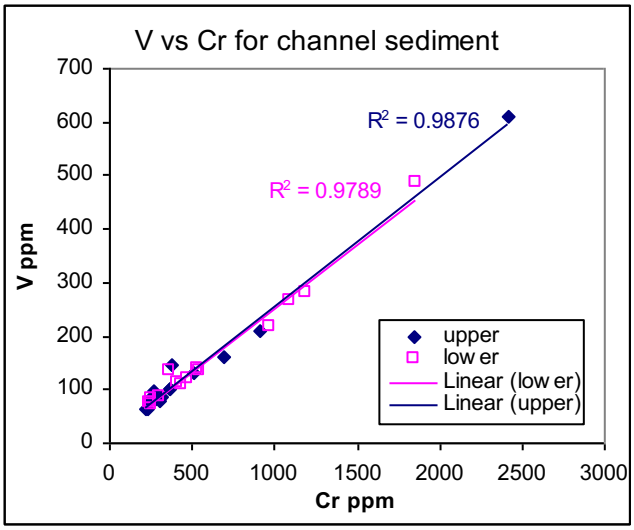

Fi

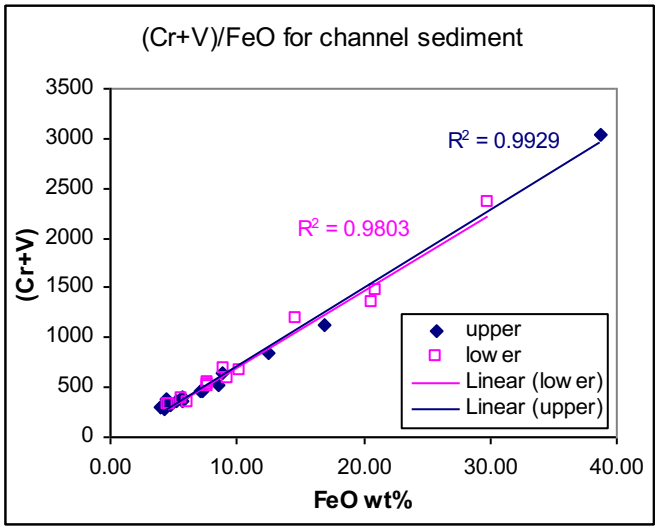

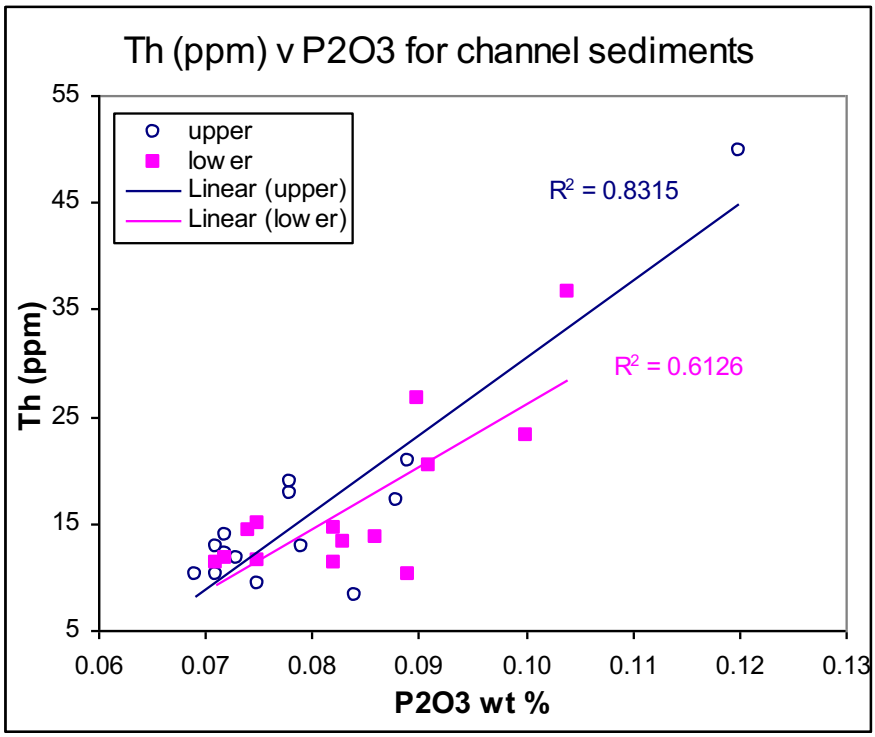

Figure 14a.

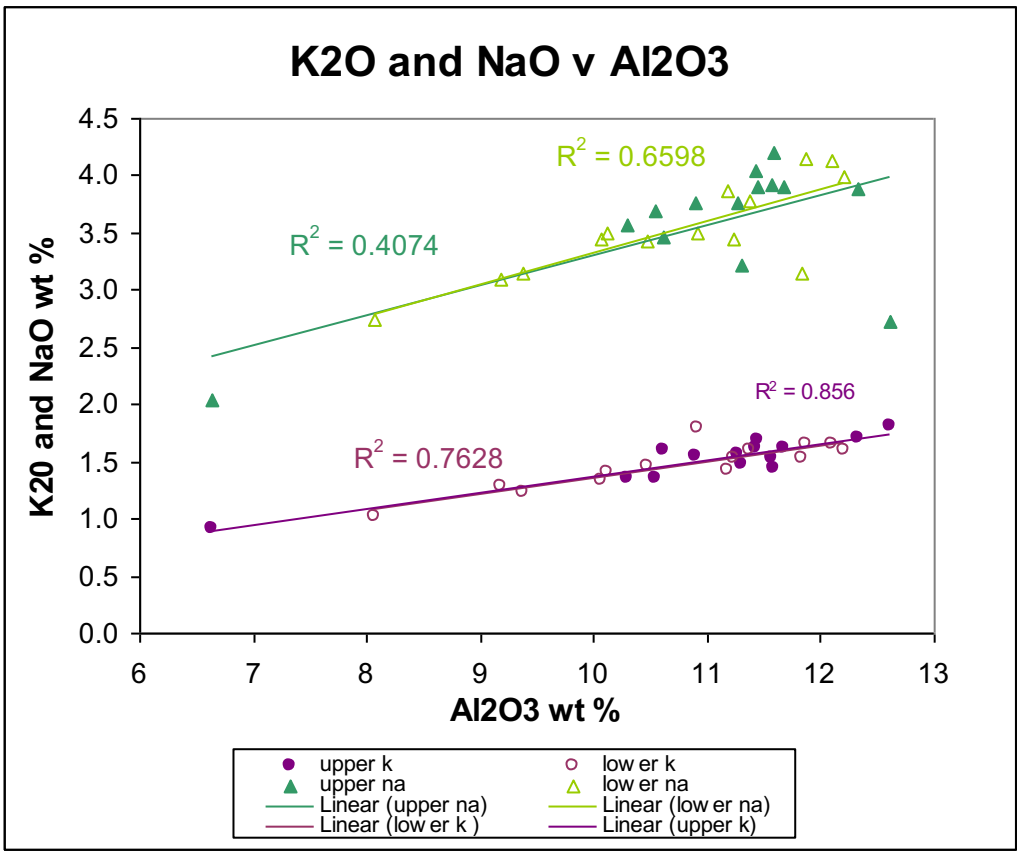

Figure 14b.

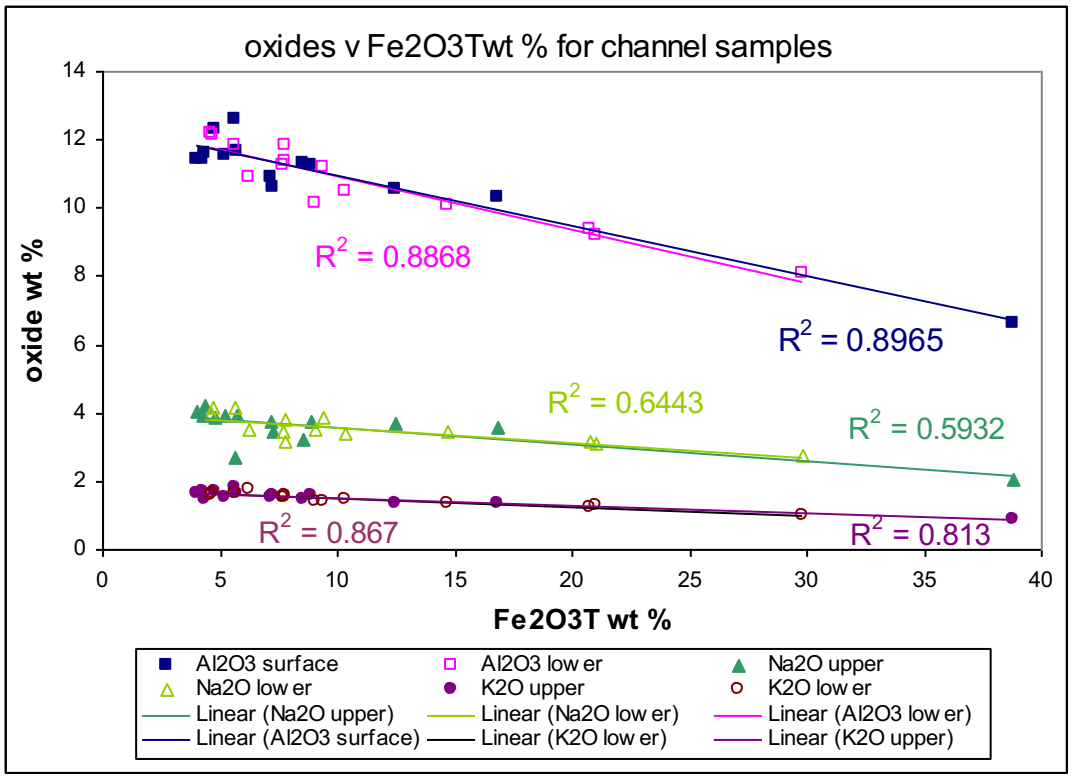

Figure 14c.

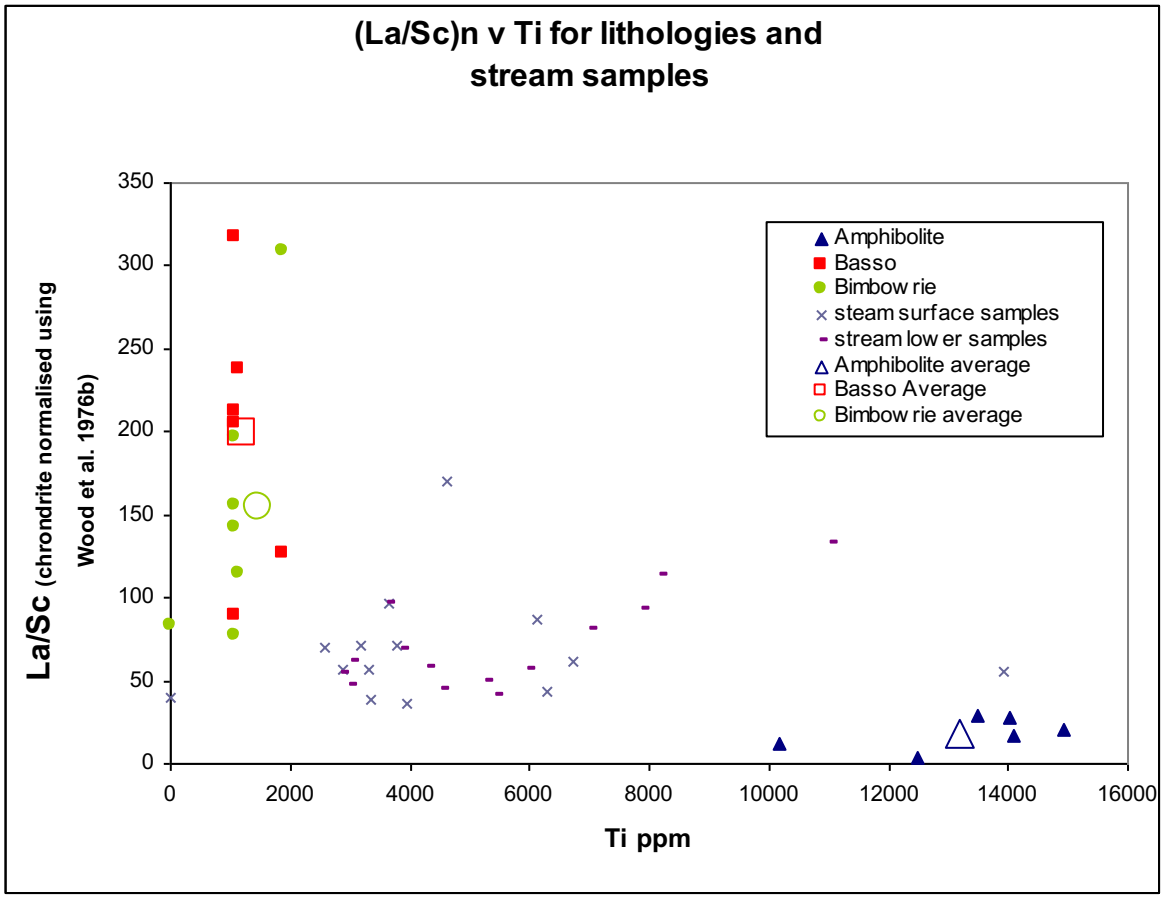

Figure 15a.

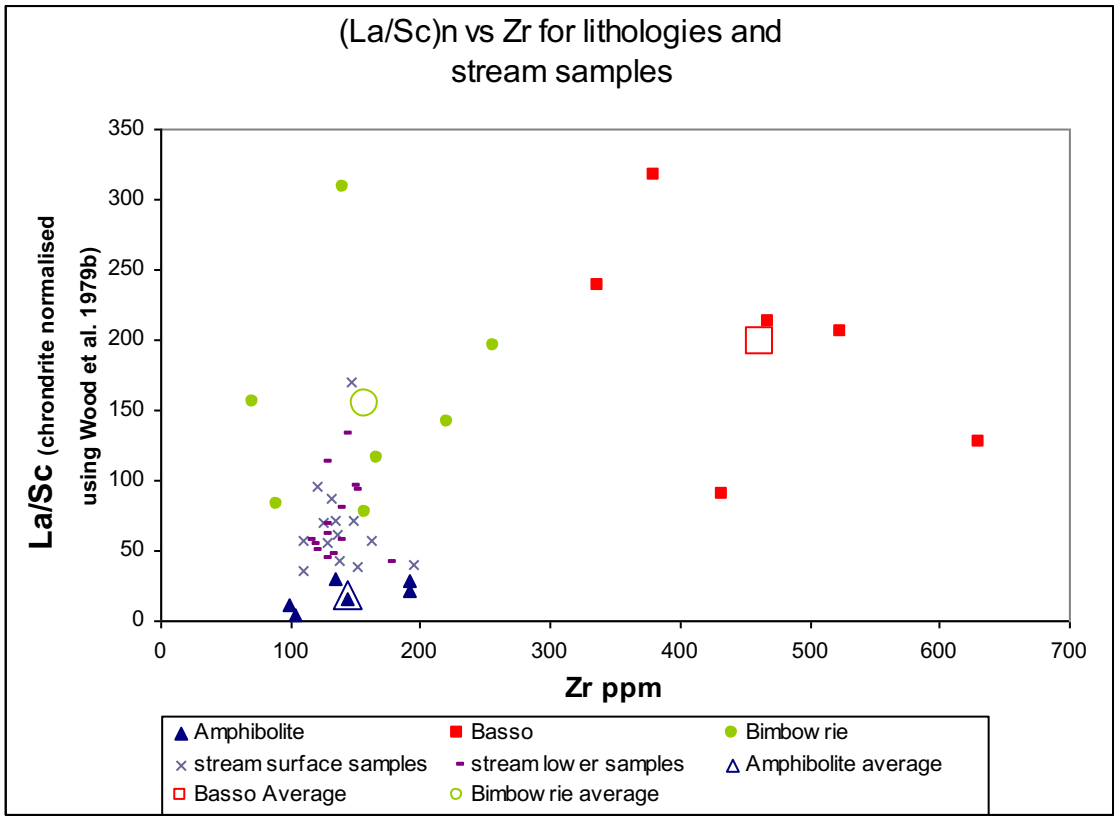

Figure 15b.

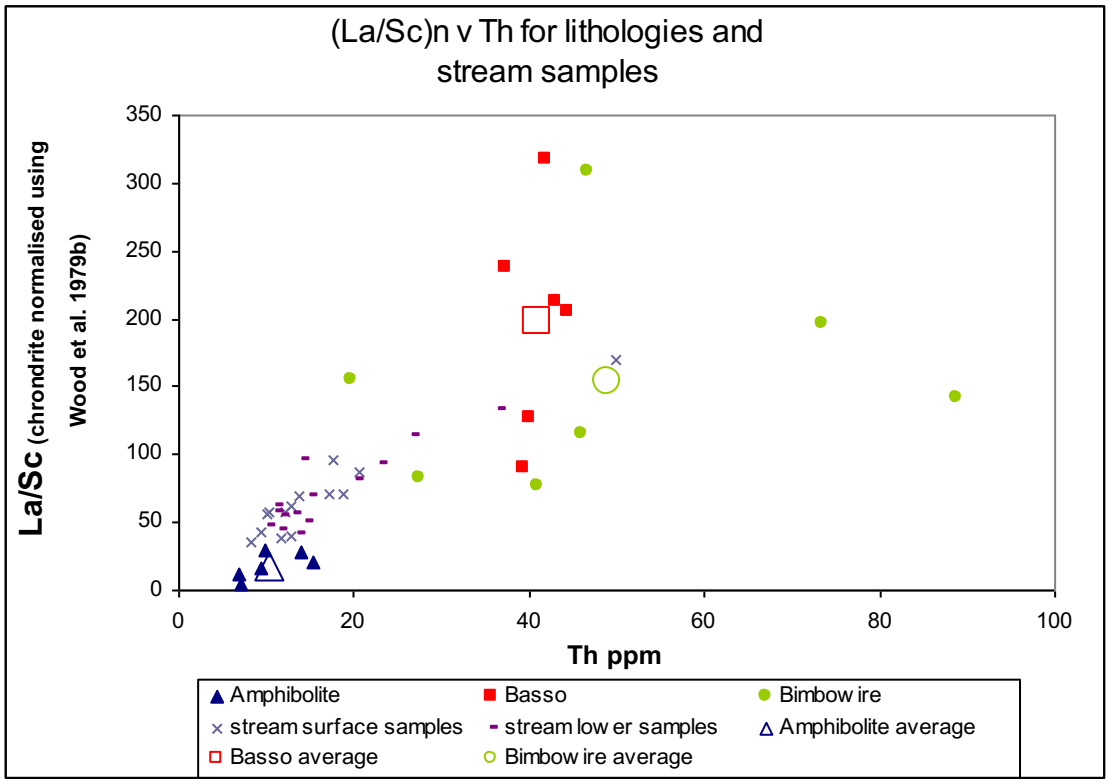

Figure 15c.

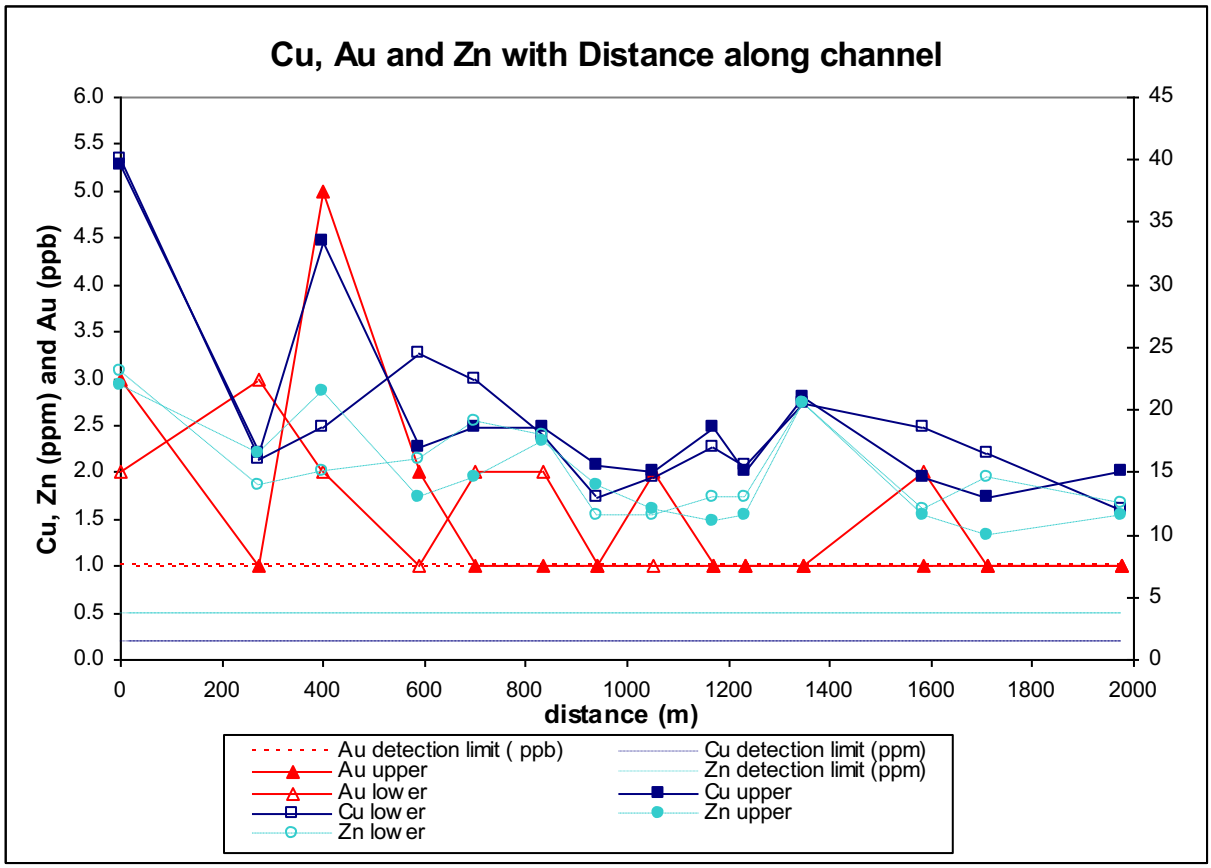

Figure 16a.

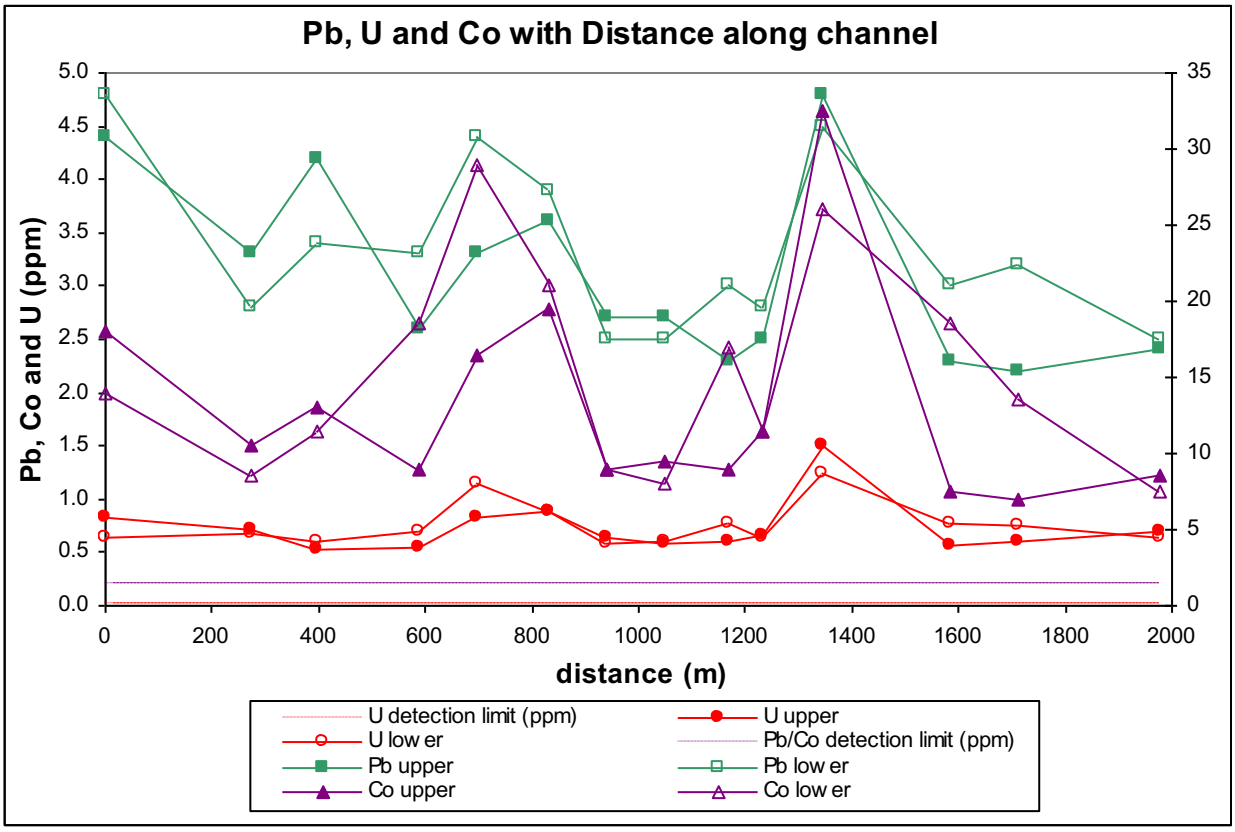

Figure 16b.

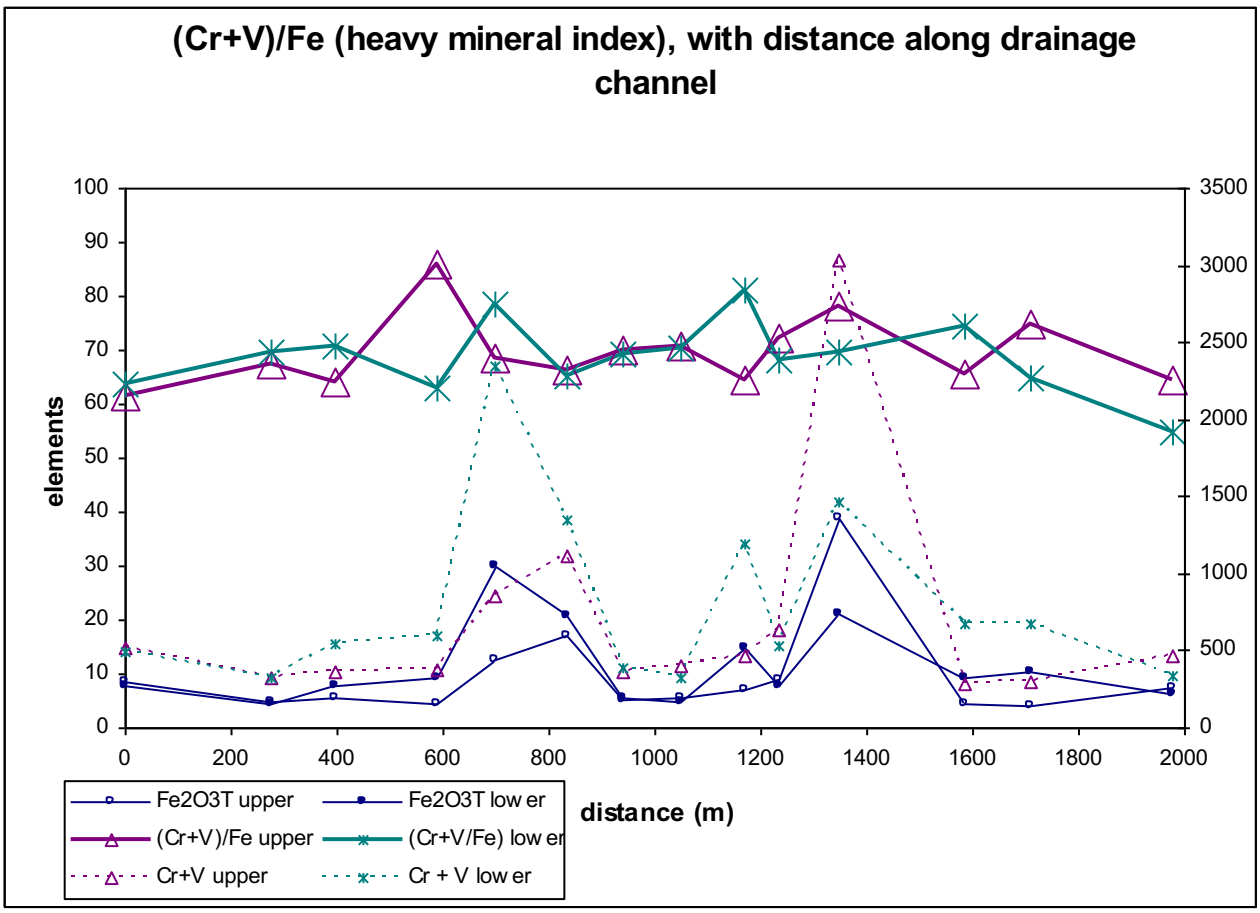

Figure 17a.

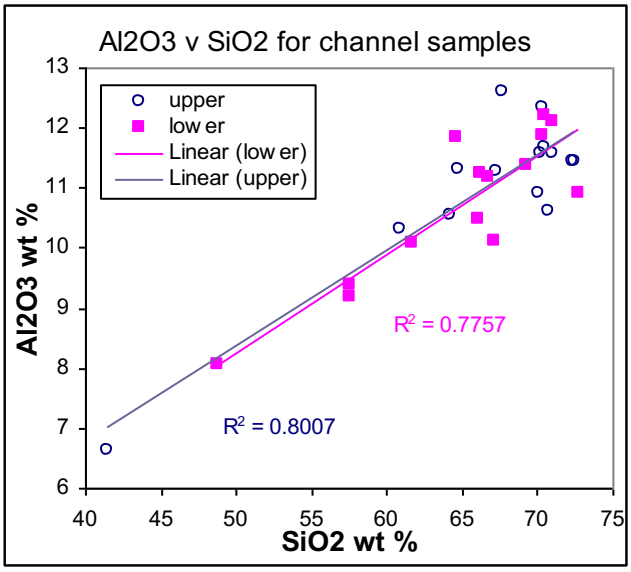

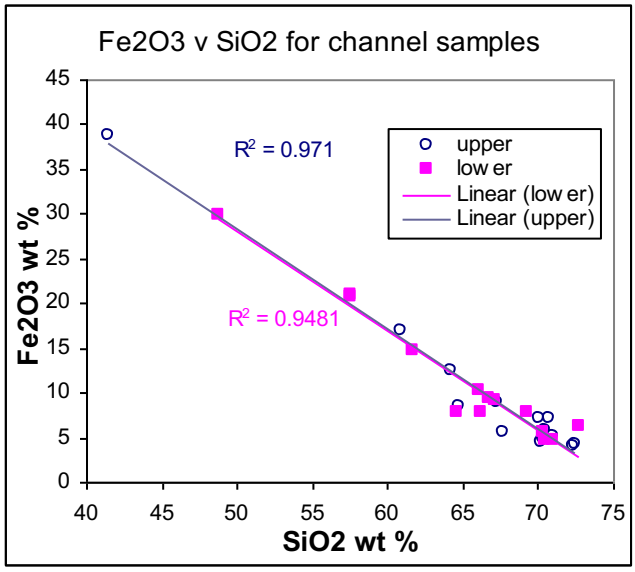

Fi

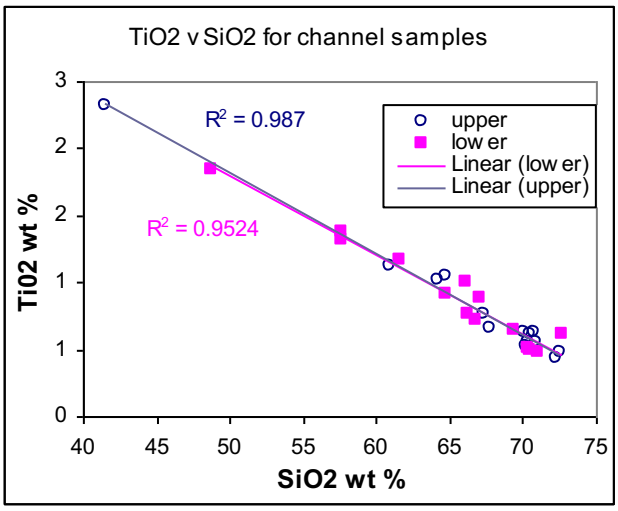

Figure 18c.

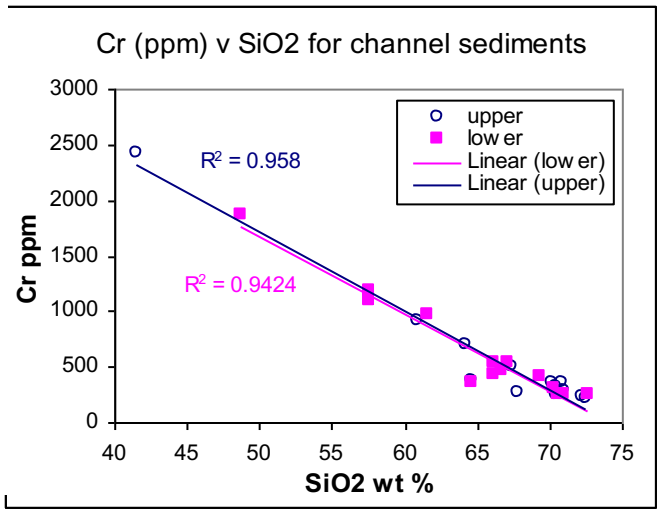

Figure 18d.

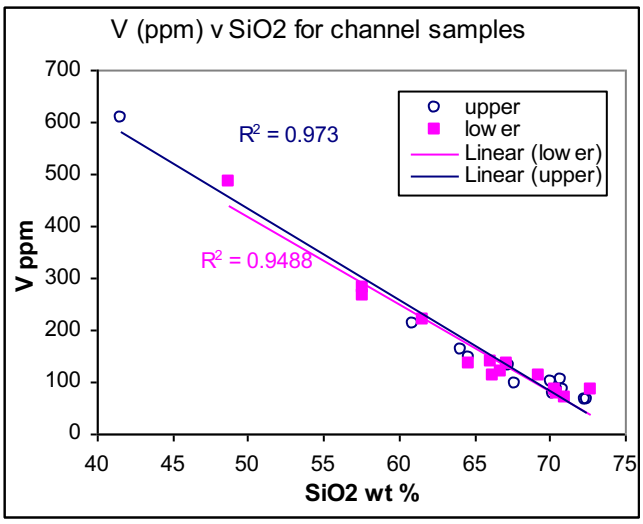

Fi

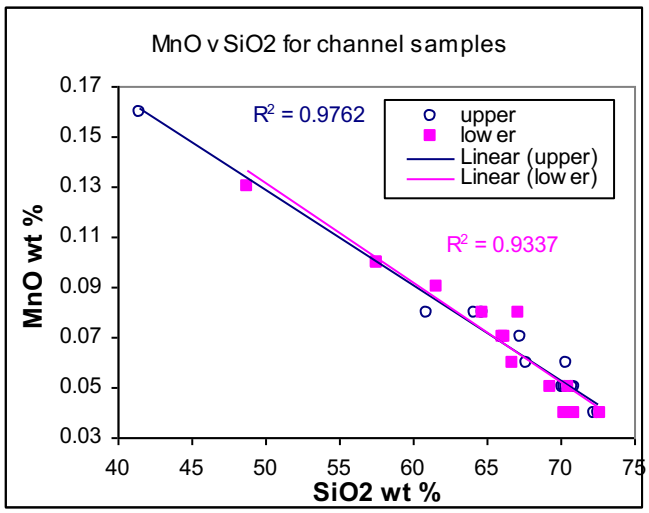

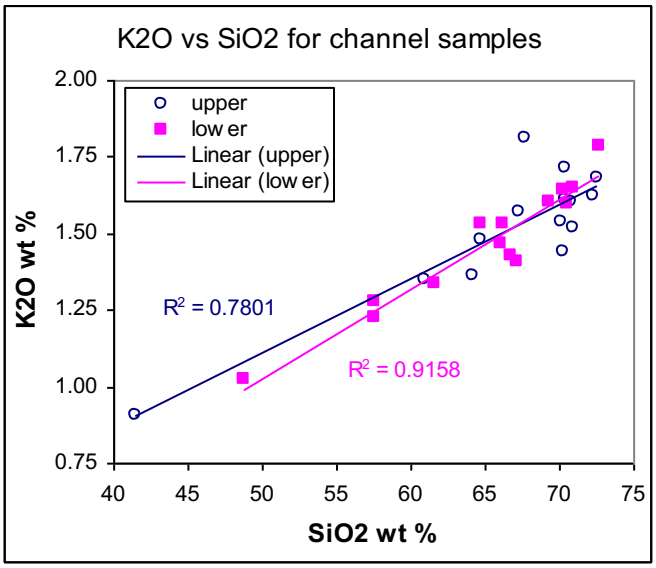

Fi

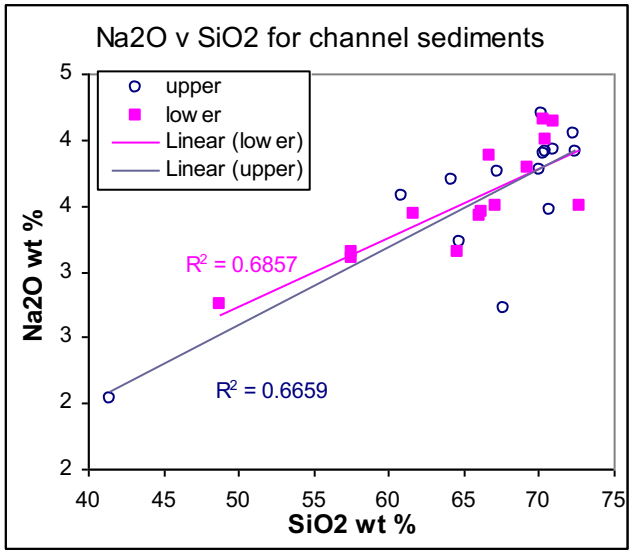

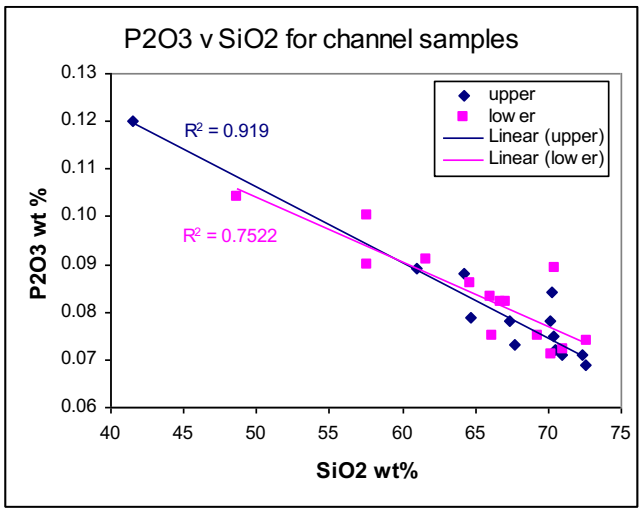
P2O3 v SiO2 for channel samples
upper
low er
Linear (upper)
Linear (low er)
R² = 0.919
R² = 0.7522
P2O3 wt %
SiO2 wt%
0.13
0.12
0.11
0.10
0.09
0.08
0.07
0.06
40
45
50
55
60
65
70
75

Figure 18i.

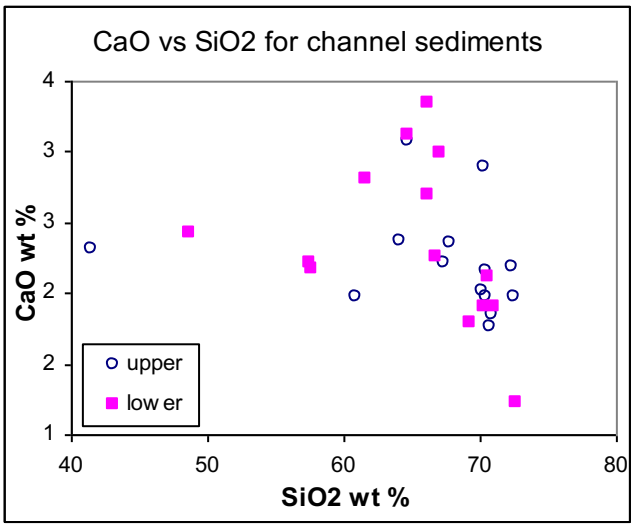
CaO vs SiO2 for channel sediments
upper
low er
CaO wt %
SiO2 wt %
4
3
3
2
2
1
40
50
60
70
80

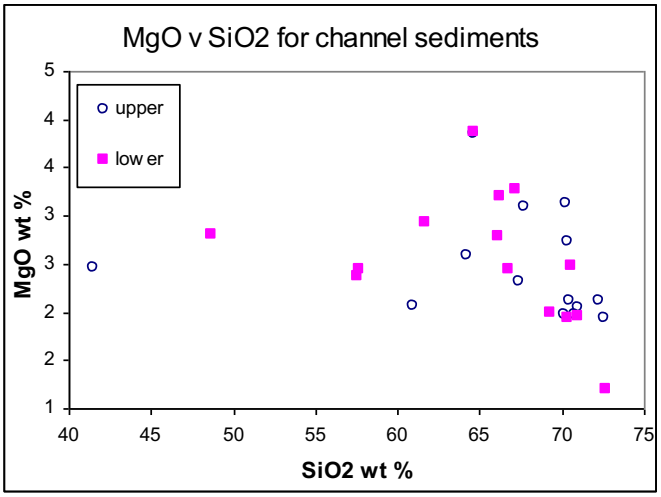
MgO v SiO2 for channel sediments
upper
low er
MgO wt %
SiO2 wt %
5
4
4
3
3
2
2
1
40
45
50
55
60
65
70
75

F

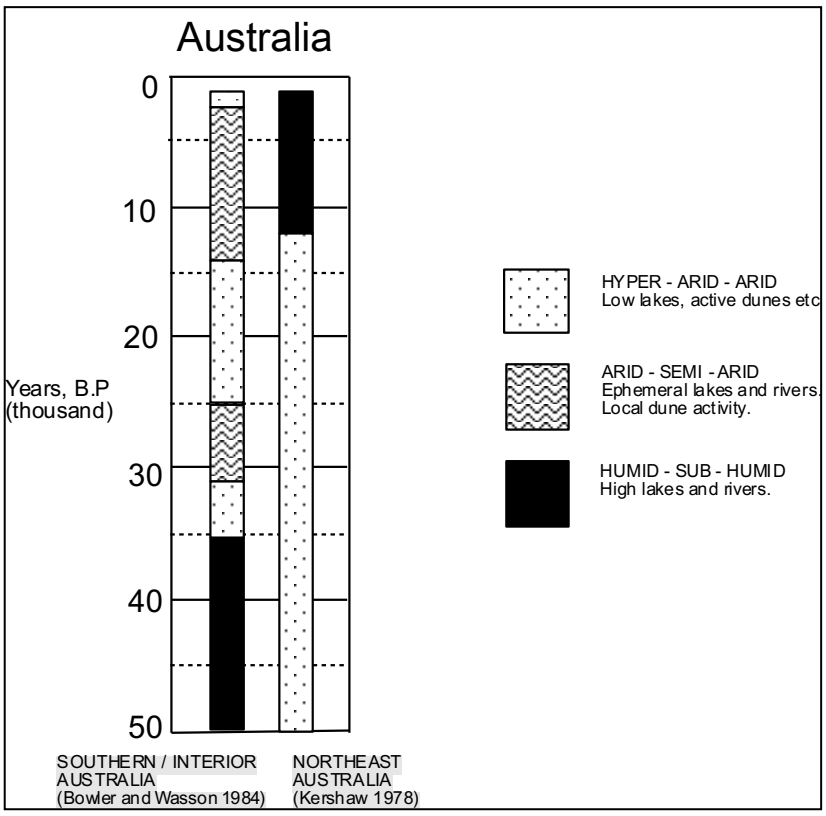
Australia
0
10
20
30
40
50
Years, B.P
(thousand)
HYPER - ARID - ARID
Low lakes, active dunes etc
ARID - SEMI - ARID
Ephemeral lakes and rivers.
Local dune activity.
HUMID - SUB - HUMID
High lakes and rivers.
SOUTHERN / INTERIOR
AUSTRALIA
(Bowler and Wasson 1984)
NORTHEAST
AUSTRALIA
(Kershaw 1978)

Figure 19a.